



MOSCOW CENTER  
FOR DIAGNOSTICS & TELEMEDICINE

ISSN 2712-8490 (Print)  
ISSN 2712-8962 (Online)

# DIGITAL DIAGNOSTICS

A peer-reviewed scientific medical journal

2 Volume 1 Issue



ECO • VECTOR

<https://journals.eco-vector.com/DD>

2021

## FOUNDERS

- Moscow Center for Diagnostics and Telemedicine
- Eco-Vector

## PUBLISHER

### Eco-Vector

Address: 3 liter A, 1H, Aptekarsky pereulok, 191186, Saint Petersburg Russian Federation  
E-mail: [info@eco-vector.com](mailto:info@eco-vector.com)  
WEB: <https://eco-vector.com>

## ADVERTISE

### Adv. department

Phone: +7 (495) 308 83 89

## EDITORIAL

### Executive editor

Elena A. Philippova

Email: [ddjournal@eco-vector.com](mailto:ddjournal@eco-vector.com)

Phone: +7(965)0127072

## SUBSCRIPTION

For print version:

[www.journals.eco-vector.com/](http://www.journals.eco-vector.com/)

## PUBLICATION ETHICS

Journal's ethic policies are based on:

- ICMJE
- COPE
- ORE
- CSE
- EASE

## OPEN ACCESS

Immediate Open Access is mandatory for all published articles

## INDEXATION

- Russian Science Citation Index
- Google Scholar
- Ulrich's International Periodicals Directory
- WorldCat

## TYPESET

complete in Eco-Vector

Copyeditor: *M.N. Shoshina*

Proofreader: *M.N. Shoshina*

Layout editor: *Ph. Ignashchenko*

Cover: *I. Feofanova*

ISSN 2712-8490 (Print)

ISSN 2712-8962 (Online)

# Digital Diagnostics

Volume 2 | Issue 1 | 2021

QUARTERLY PEER-REVIEW MEDICAL JOURNAL

## EDITOR-IN-CHIEF

Valentin E. Sinitsyn, MD, Dr.Sci. (Med), Professor (Moscow, Russia)

ORCID: 0000-0002-5649-2193

## DEPUTY EDITOR-IN-CHIEF

Sergey P. Morozov, MD, Dr.Sci. (Med), Professor (Moscow, Russia)

ORCID: 0000-0001-6545-6170

## EDITORIAL BOARD

Anna E. Andreychenko, PhD (Moscow, Russia) ORCID: 0000-0001-6359-0763

Leonard Berlin, Professor (Illinois, United States) ORCID: 0000-0002-0717-0307

Mikhail G. Belyaev, Cand.Sci. (Phys-Math), Assistant Professor, (Moscow, Russia)

ORCID: 0000-0001-9906-6453

Sotirios Bisdas, MBBS, MD, PhD (London, United Kingdom) ORCID: 0000-0001-9930-5549

Viktor A. Gombolevskiy, MD, Dr.Sci. (Med) (Moscow, Russia) ORCID: 0000-0003-1816-1315

Guy Frijia, Professor (Paris, France) ORCID: 0000-0003-0415-0586

Giuseppe Guglielmi, MD, Professor (Foggia, Italy) ORCID: 0000-0002-4325-8330

Andrei Holodny, MD (New-York, United States) ORCID: 0000-0002-1159-2705

Hongjun Li, MD, Professor (Beijing, China)

Nikolay S. Kul'berg, Cand.Sci. (Phys-Math) (Moscow, Russia) ORCID: 0000-0001-7046-7157

Lorenzo Mannelli, MD (New-York, United States) ORCID: 0000-0002-9102-4176

Olesya A. Mokienko, MD, Cand.Sci. (Med) (Moscow, Russia) ORCID: 0000-0002-7826-5135

Emanuele Neri, MD, Associate Professor (Pisa, Italy) ORCID: 0000-0001-7950-4559

Peter van Ooijen, PhD, Assoc. Professor (Groningen, Netherlands) ORCID: 0000-0002-8995-1210

Matthijs Oudkerk, Professor (Groningen, Netherlands) ORCID: 0000-0003-2800-4110

Pablo Riera Ros, MD, MPH, PhD, Professor (New-York, United States) ORCID: 0000-0003-3974-0797

Alex Rovira, Professor (Barcelona, Spain) ORCID: 0000-0002-2132-6750

Roman V. Reshetnikov, Cand.Sci. (Phys-Math) (Moscow, Russia) ORCID: 0000-0002-9661-0254

Pavel O. Rumyantsev, MD, Dr.Sci. (Med) (Moscow, Russia) ORCID: 0000-0002-7721-634X

## EDITORIAL COUNCIL

Aleksey A. Ansheles, MD, Dr.Sci. (Med) (Moscow, Russia) ORCID: 0000-0002-2675-3276

Andrey S. Belevskiy, MD, Dr.Sci. (Med), Professor (Moscow, Russia) ORCID: 0000-0001-6050-724X

Elena Y. Vasilieva, MD, Dr.Sci. (Med), Professor (Moscow, Russia) ORCID: 0000-0003-4111-0874

Alla B. Gekht, MD, Dr.Sci. (Med), Professor (Moscow, Russia) ORCID: 0000-0002-1170-6127

Elena I. Kremneva, MD, Cand.Sci. (Med) (Moscow, Russia) ORCID: 0000-0001-9396-6063

Sergey S. Petrikov, MD, Dr.Sci. (Med), Professor (Moscow, Russia) ORCID: 0000-0003-3292-8789

Denis N. Protsenko, MD, Cand.Sci. (Med) (Moscow, Russia) ORCID: 0000-0002-5166-3280

The editors are not responsible for the content of advertising materials. The point of view of the authors may not coincide with the opinion of the editors. Only articles prepared in accordance with the guidelines are accepted for publication. By sending the article to the editor, the authors accept the terms of the public offer agreement. The guidelines for authors and the public offer agreement can be found on the website: <https://journals.eco-vector.com/DD/>. Full or partial reproduction of materials published in the journal is allowed only with the written permission of the publisher — the Eco-Vector publishing house.



## УЧРЕДИТЕЛИ

- ГБУЗ «Научно-практический клинический центр диагностики и телемедицинских технологий ДЗМ»
- ООО «Эко-Вектор»

## ИЗДАТЕЛЬ

ООО «Эко-Вектор»

Адрес: 191186, г. Санкт-Петербург, Аптекарский переулочек, д. 3, литера А, помещение 1Н

E-mail: [info@eco-vector.com](mailto:info@eco-vector.com)

WEB: <https://eco-vector.com>

## РЕКЛАМА

Отдел рекламы

Тел.: +7 495 308 83 89

## РЕДАКЦИЯ

### Зав. редакцией

Елена Андреевна Филиппова

Email: [ddjournal@eco-vector.com](mailto:ddjournal@eco-vector.com)

Тел: +7 (965) 012 70 72

## ПОДПИСКА

Подписка на печатную версию через интернет:

[www.journals.eco-vector.com/](http://www.journals.eco-vector.com/)

[www.akc.ru](http://www.akc.ru)

[www.pressa-rf.ru](http://www.pressa-rf.ru)

## OPEN ACCESS

В электронном виде журнал распространяется бесплатно — в режиме немедленного открытого доступа

## ИНДЕКСАЦИЯ

- РИНЦ
- Google Scholar
- Ulrich's International Periodicals Directory
- WorldCat

## Оригинал-макет

подготовлен в издательстве «Эко-Вектор».

Литературный редактор: *М.Н. Шошина*

Корректор: *М.Н. Шошина*

Вёрстка: *Ф.А. Игнащенко*

Обложка: *И.С. Феофанова*

Сдано в набор 10.04.2021.

Подписано в печать 23.04.2021.

Формат 60 × 88%. Печать офсетная.

Печ. л. 11,5. Усл. печ. л. 10,7.

Уч.-изд. л. 6,3. Тираж 500 экз.

Отпечатано в ООО «Типография Михаила Фурсова».  
196105, Санкт-Петербург, ул. Благодатная, 69.  
Тел.: (812) 646-33-77

© ООО «Эко-Вектор», 2021

ISSN 2712-8490 (Print)

ISSN 2712-8962 (Online)

# Digital Diagnostics

Том 2 | Выпуск 1 | 2021

ЕЖЕКВАРТАЛЬНЫЙ РЕЦЕНЗИРУЕМЫЙ НАУЧНЫЙ  
МЕДИЦИНСКИЙ ЖУРНАЛ

## Главный редактор

Синицын Валентин Евгеньевич, д.м.н., профессор (Москва, Россия)

ORCID: 0000-0002-5649-2193

## Заместитель главного редактора

Морозов Сергей Павлович, д.м.н., профессор (Москва, Россия)

ORCID: 0000-0001-6545-6170

## Редакционная коллегия

Андрейченко Анна Евгеньевна, к.ф.-м.н. (Москва, Россия) ORCID: 0000-0001-6359-0763

Berlin Leonard, профессор (Иллинойс, США) ORCID: 0000-0002-0717-0307

Беляев Михаил Геннадьевич, к.ф.-м.н. (Москва, Россия) ORCID: 0000-0001-9906-6453

Bisdas Sotirios, MBBS, MD, PhD (Лондон, Великобритания) ORCID: 0000-0001-9930-5549

Гомболевский Виктор Александрович, к.м.н. (Москва, Россия) ORCID: 0000-0003-1816-1315

Grija Guy, профессор (Париж, Франция) ORCID: 0000-0003-0415-0586

Guglielmi Giuseppe, MD, профессор (Фоджа, Италия) ORCID: 0000-0002-4325-8330

Holodny Andrei, д.м.н. (Нью-Йорк, США) ORCID: 0000-0002-1159-2705

Li Hongjun, MD, профессор, (Пекин, КНР)

Кульберг Николай Сергеевич, к.ф.-м.н., (Москва, Россия) ORCID: 0000-0001-7046-7157

Mannelli Lorenzo, MD (Нью-Йорк, США) ORCID: 0000-0002-9102-4176

Мокиенко Олеся Александровна, к.м.н. (Москва, Россия) ORCID: 0000-0002-7826-5135

Neri Emanuele, д.м.н. (Пиза, Италия) ORCID: 0000-0001-7950-4559

van Ooijen Peter, к.м.н. (Гронинген, Нидерланды) ORCID: 0000-0002-8995-1210

Oudkerk Matthijs, профессор (Гронинген, Нидерланды) ORCID: 0000-0003-2800-4110

Ros Pablo Riera, MD, MPH, PhD, профессор (Нью-Йорк, США) ORCID: 0000-0003-3974-0797

Rovira Alex, профессор (Барселона, Испания) ORCID: 0000-0002-2132-6750

Решетников Роман Владимирович, к.ф.-м.н., (Москва, Россия) ORCID: 0000-0002-9661-0254

Румянцев Павел Олегович, д.м.н. (Москва, Россия) ORCID: 0000-0002-7721-634X

## Редакционный совет

Аншелес Алексей Аркадьевич, д.м.н. (Москва, Россия) ORCID: 0000-0002-2675-3276

Белевский Андрей Станиславович, д.м.н., профессор (Москва, Россия) ORCID: 0000-0001-6050-724X

Васильева Елена Юрьевна, д.м.н., профессор (Москва, Россия) ORCID: 0000-0003-4111-0874

Гехт Алла Борисовна, д.м.н., профессор (Москва, Россия) ORCID: 0000-0002-1170-6127

Кремнева Елена Игоревна, к.м.н. (Москва, Россия) ORCID: 0000-0001-9396-6063

Петриков Сергей Сергеевич, д.м.н., профессор (Москва, Россия) ORCID: 0000-0003-3292-8789

Проценко Денис Николаевич, к.м.н. (Москва, Россия) ORCID: 0000-0002-5166-3280

Редакция не несет ответственности за содержание рекламных материалов. Точка зрения авторов может не совпадать с мнением редакции. К публикации принимаются только статьи, подготовленные в соответствии с правилами для авторов. Направляя статью в редакцию, авторы принимают условия договора публичной оферты. С правилами для авторов и договором публичной оферты можно ознакомиться на сайте: <https://journals.eco-vector.com/DD/>. Полное или частичное воспроизведение материалов, опубликованных в журнале, допускается только с письменного разрешения издателя — издательства «Эко-Вектор».



# CONTENTS

---

## ORIGINAL STUDIES

*Morozov S.P., Reshetnikov R.V., Gombolevskiy V.A., Ledikhova N.V., Blokhin I.A., Mokienko O.A.*

Diagnostic accuracy of computed tomography for identifying hospitalizations for patients with COVID-19 ..... 5

*Neri E., Crocetti L., Lorenzoni G., Cioni R., Brady A., Caramella D.*

Students opinion about E-Learning in a Master course in Interventional Radiology:

a survey among participants ..... 17

*Morozov S.P., Chernina V.Yu., Andreychenko A.E., Vladzimirsky A.V., Mokienko O.A., Gombolevskiy V.A.*

How does artificial intelligence effect on the assessment of lung damage in COVID-19 on chest CT scan? ..... 27

## REVIEWS

*Girya E.N., Sinitsyn V.E., Tokarev A.S.*

Radiation diagnostics of cerebral cavernous malformations ..... 39

## TECHNICAL NOTES

*Pavlov N.A., Andreychenko A.E., Vladzimirsky A.V., Revazyan A.A., Kirpichev Y.S., Morozov S.P.*

Reference medical datasets (MosMedData) for independent external evaluation of algorithms

based on artificial intelligence in diagnostics ..... 49

## CASE REPORTS

*Dayneko Ya.A., Berezovskaya T.P., Myalina S.A., Orekhov I.A., Nevolskikh A.A.*

MRI evaluation of the neoadjuvant chemoradiation therapy result in a patient with rectal cancer,

supplemented with T2-WI texture analysis of the tumor: a clinical case. .... 67

*Gelezhe P.B., Bulanov D.V.*

Diagnosis of solitary eosinophilic granuloma by CT, MRI, and 18F-FDG PET/CT: two clinical cases. .... 75

## LETTERS TO THE EDITOR

*Rumyantsev P.O.*

Radiotheranostics: fresh impetus of personalized medicine ..... 83



# СОДЕРЖАНИЕ

---

## ОРИГИНАЛЬНЫЕ ИССЛЕДОВАНИЯ

*С.П. Морозов, Р.В. Решетников, В.А. Гомболевский, Н.В. Ледихова, И.А. Блохин, О.А. Мокиенко*

Диагностическая точность компьютерной томографии для определения необходимости госпитализации пациентов с COVID-19. .... 5

*E. Neri, L. Crocetti, G. Lorenzoni, R. Cioni, A. Brady, D. Caramella*

Мнение студентов магистратуры о дистанционном обучении по специальности «Интервенционная радиология» с помощью электронных технологий: опрос учащихся ..... 17

*С.П. Морозов, В.Ю. Чернина, А.Е. Андрейченко, А.В. Владимирский, О.А. Мокиенко, В.А. Гомболевский*

Как искусственный интеллект влияет на оценку поражения лёгких при COVID-19 по данным КТ грудной клетки? ..... 27

## ОБЗОР

*Е.Н. Гиря, В.Е. Синицын, А.С. Токарев*

Лучевая диагностика кавернозных мальформаций головного мозга ..... 39

## НАУЧНЫЕ ОТЧЁТЫ

*Н.А. Павлов, А.Е. Андрейченко, А.В. Владимирский, А.А. Реваян, Ю.С. Кирпичев, С.П. Морозов*

Эталонные медицинские датасеты (MosMedData) для независимой внешней оценки алгоритмов на основе искусственного интеллекта в диагностике. .... 49

## КЛИНИЧЕСКИЕ СЛУЧАИ

*Я.А. Дайнеко, Т.П. Березовская, С.А. Мялина, И.А. Орехов, А.А. Невольских*

МРТ-оценка результата неoadъювантной химиолучевой терапии у больной раком прямой кишки, дополненная текстурным анализом T2-ВИ опухоли (клинический случай) ..... 67

*П.Б. Гележе, Д.В. Буланов*

Два случая верифицированной солитарной эозинофильной гранулёмы: визуализация методами КТ, МРТ и 18f-ФДГ ПЭТ/КТ ..... 75

## ПИСЬМА В РЕДАКЦИЮ

*П.О. Румянцев*

Радиотераностика: новое дыхание персонализированной медицины ..... 83

DOI: <https://doi.org/10.17816/DD46818>

# Diagnostic accuracy of computed tomography for identifying hospitalizations for patients with COVID-19

© Sergey P. Morozov<sup>1</sup>, Roman V. Reshetnikov<sup>1,2</sup>, Victor A. Gomboleviskiy<sup>1</sup>, Natalya V. Ledikhova<sup>1</sup>, Ivan A. Blokhin<sup>1</sup>, Olesya A. Mokienko<sup>1</sup>

<sup>1</sup> Moscow Center for Diagnostics and Telemedicine, Moscow, Russian Federation

<sup>2</sup> I.M. Sechenov First Moscow State Medical University (Sechenov University), Moscow, Russian Federation

**BACKGROUND:** In Russia, a semi-quantitative CT 0–4 scoring system is used in the analysis of thoracic computed tomography (CT) scans of COVID-19 patients to grade the severity of lung lesions. Despite the widespread use of this approach, the scoring system's diagnostic accuracy for identification hospitalizations for patients with the disease is currently unknown.

**AIM:** To evaluate the sensitivity, specificity, positive (PPV) and negative (NPV) predictive value of the CT 0–4 system for the triage of COVID-19 patients.

**MATERIALS AND METHODS:** This retrospective study enrolled 575 patients of Moscow clinics with laboratory-verified COVID-19, aged  $57.2 \pm 13.9$  years, 55% females. All patients were examined with four consecutive chest CT scans, and the disease severity was assessed using the CT 0–4 scoring system. Sensitivity and specificity were calculated as conditional probabilities that a patient would experience clinical improvement or deterioration, depending on the preceding CT examination results. For the calculation of the NPV and PPV, we estimated the COVID-19 prevalence in Moscow. The data on total cases of COVID-19 from March 6 to November 28, 2020, were taken from the Rospotrebnadzor website. We used several ARIMA and EST models with different parameters to fit the data and forecast the incidence.

**RESULTS:** The median specificity of the CT 0–4 scoring system was 69% (95% CI 32%, 100%), and the sensitivity was 92% (95% CI 74%, 100%). The best statistical model describing the epidemiological situation in Moscow was ARIMA (0,2,1). According to our calculations, with the predicted point prevalence of 9.6%, the values of PPV and NPV were 56% and 97%, correspondingly.

**CONCLUSION:** The maximum Youden's index was observed for the period between the first and the second chest CT examinations when the majority of the included patients experienced clinical deterioration. The CT 0–4 scoring system makes it possible to safely exclude the development of pathological changes in patients with mild and moderate disease (categories CT-0 and CT-1), thereby optimizing the burden on hospitals in an unfavorable epidemic situation.

**Keywords:** COVID-19; computed tomography; sensitivity; specificity; triage.

## To cite this article

Morozov SP, Reshetnikov RV, Gomboleviskiy VA, Ledikhova NV, Blokhin IA, Mokienko OA. Diagnostic accuracy of computed tomography for identifying hospitalizations for patients with COVID-19. *Digital Diagnostics*. 2021;2(1):5–16. DOI: <https://doi.org/10.17816/DD46818>

Received: 19.01.2021

Accepted: 09.02.2021

Published: 30.03.2021

DOI: <https://doi.org/10.17816/DD46818>

# Диагностическая точность компьютерной томографии для определения необходимости госпитализации пациентов с COVID-19

© С.П. Морозов<sup>1</sup>, Р.В. Решетников<sup>1,2</sup>, В.А. Гомболевский<sup>1</sup>, Н.В. Ледихова<sup>1</sup>,  
И.А. Блохин<sup>1</sup>, О.А. Мокиенко<sup>1</sup>

<sup>1</sup> Научно-практический клинический центр диагностики и телемедицинских технологий Департамента здравоохранения города Москвы, Москва, Российская Федерация

<sup>2</sup> Первый Московский государственный медицинский университет имени И.М. Сеченова (Сеченовский Университет), Москва, Российская Федерация

**Обоснование.** Для выявления COVID-19-пневмоний, их осложнений и дифференциальной диагностики с другими заболеваниями лёгких, а также с целью сортировки пациентов в Российской Федерации применяют компьютерную томографию органов грудной клетки (КТ ОГК) с оценкой изменений по визуальной полуколичественной шкале КТ 0–4. Несмотря на широкое применение инструмента, численные показатели его диагностической точности в определении необходимости госпитализации пациентов с COVID-19 на настоящий момент неизвестны.

**Цель** — определение значений чувствительности, специфичности, положительной и отрицательной прогностической значимости шкалы.

**Материал и методы.** К участию в исследовании привлекли 575 пациентов (55% женщины) в возрасте  $57,2 \pm 13,9$  лет с лабораторно подтверждённым COVID-19. Для каждого пациента проводили по четыре последовательных исследования КТ ОГК с оценкой степени тяжести заболевания по шкале КТ 0–4. Чувствительность и специфичность рассчитывали как условную вероятность ухудшения или улучшения состояния пациента в зависимости от результатов предыдущего исследования КТ. Для расчёта положительной (PPV) и отрицательной (NPV) прогностической значимости проводили оценку распространённости COVID-19 в Москве. Данные обо всех случаях заболевания COVID-19 в период с 6 марта по 28 ноября 2020 г. взяты с сайта Роспотребнадзора. Использовали ряд моделей ARIMA и EST с различными параметрами для подбора наилучшего соответствия имеющимся данным и прогноза развития заболеваемости.

**Результаты.** Шкала оценки КТ 0–4 продемонстрировала медианные специфичность 69% и чувствительность 92%. Лучшей статистической моделью для описания эпидемиологической ситуации в Москве являлась ARIMA (0,2,1). Согласно проведённым подсчётам, при предсказанной годовой заболеваемости в 9,6% значения PPV и NPV составляют 56 и 97% соответственно.

**Заключение.** Максимальный индекс Юдена наблюдали на этапе между первым и вторым исследованием КТ ОГК, когда большинство пациентов в выборке демонстрировали тенденцию к ухудшению клинического состояния. Шкала КТ 0–4 позволяет безопасно исключить развитие патологических изменений у пациентов с лёгким и среднетяжёлым течением заболевания (категории КТ0 и КТ1), способствуя оптимизации нагрузки на стационары при неблагоприятной эпидемической обстановке.

**Ключевые слова:** COVID-19; компьютерная томография; чувствительность; специфичность; сортировка пациентов.

## Как цитировать

Морозов С.П., Решетников Р.В., Гомболевский В.А., Ледихова Н.В., Блохин И.А., Мокиенко О.А. Диагностическая точность компьютерной томографии для определения необходимости госпитализации пациентов с COVID-19 // *Digital Diagnostics*. 2021. Т. 2, № 1. С. 5–16. DOI: <https://doi.org/10.17816/DD46818>

DOI: <https://doi.org/10.17816/DD46818>

# CT诊断的准确率，以确定COVID-19患者的住院需求

© Sergey P. Morozov<sup>1</sup>, Roman V. Reshetnikov<sup>1,2</sup>, Victor A. Gomboleviskiy<sup>1</sup>,  
Natalya V. Ledikhova<sup>1</sup>, Ivan A. Blokhin<sup>1</sup>, Olesya A. Mokienko<sup>1</sup>

<sup>1</sup> Moscow Center for Diagnostics and Telemedicine, Moscow, Russian Federation

<sup>2</sup> I.M. Sechenov First Moscow State Medical University (Sechenov University), Moscow, Russian Federation

**论证：**在俄罗斯联邦，为了检测COVID-19肺炎及其并发症和与其他肺部疾病的鉴别诊断，以及对患者进行分类，使用了胸部CT，并在CT 0-4的半定量视觉尺度上评估变化。尽管胸部CT广泛使用，但其用于确定COVID-19患者住院需求的诊断准确性的数字指标目前尚不清楚。

**目的：**是确定该量表的敏感性、特异性、阳性预测值、阴性预测值。

**材料与方法：**研究涉及575名经实验室确诊的COVID-19患者（55%为女性），年龄为57.2±13.9岁。对于每个患者，进行了4次连续的胸部CT研究，并对疾病的严重程度进行了CT评分（0-4）。根据既往CT研究结果，将敏感性和特异性作为患者病情恶化或改善的条件概率进行计算。为计算阳性预测值（PPV）和阴性预测值（NPV），对COVID-19在莫斯科的流行情况进行了估计。2020年3月6日至11月28日期间所有COVID-19病例的数据来自俄国国家管理的保护消费者服务机构（Rospotrebnadzor）网站。使用了许多具有不同参数的ARIMA和EST模型来选择与现有数据最匹配的模型，并预测发病率的发展。

**结果：**0-4 CT分级的中位特异性为69%，敏感性为92%。描述莫斯科流行病学情况的最佳统计模型是ARIMA（0, 2, 1）。经计算，预测年发病率为9.6%，PPV值为56，NPV值为97%。

**结果：**Yuden指数最大的阶段出现在胸部CT第一次研究和第二次研究之间，此时样本中大多数患者表现出临床病情恶化的趋势。0-4 CT分级可以安全地排除轻、中度病程（CT0、CT1类）患者的病理变化发展，有助于优化患者在疫情不利的情况下住院。

**关键词：**COVID-19；计算机断层扫描；敏感性；特异性；病人排序。

## 引用本文：

Morozov SP, Reshetnikov RV, Gomboleviskiy VA, Ledikhova NV, Blokhin IA, Mokienko OA. CT诊断的准确率，以确定COVID-19患者的住院需求. *Digital Diagnostics*. 2021;2(1):5-16. DOI: <https://doi.org/10.17816/DD46818>

收到: 19.01.2021

接受: 09.02.2021

发布时间: 30.03.2021



## BACKGROUND

By January 14, 2021, the COVID-19 epidemic had caused approximately 92 million registered cases of infection worldwide, as well as approximately 2,000,000 lethal outcomes [1]. The SARS-CoV-2 virus disease can result in several scenarios. Symptoms may be completely absent or similar to flu-like symptoms (80%). In severe and critical cases, oxygen support or the use of an artificial lung ventilation apparatus (15% and 5%, respectively) is required [2]. Since a common manifestation of COVID-19 is viral damage to the lungs, methods of X-ray diagnostics represent one of the main tools for assessing disease severity and deciding whether hospitalization is required.

In accordance with the Temporary Methodological Recommendations of the Ministry of Health of the Russian Federation for the prevention, diagnosis, and treatment of new coronavirus infection COVID-19, for the assessment of changes in the lungs and differential diagnosis with other diseases, a visual semi-quantitative “empirical” scale of the degree of lung damage (computed tomography (CT) 0–4) should be used [3]. To this end, in their work, Morozov et al. [4] demonstrated not only the value of the scale as a predictor of lethal outcomes in COVID-19 patients but also its practical significance for routine patient management. However, despite the widespread use of the tool, as of this writing, an assessment of the numerical values of the indicators of its diagnostic accuracy has not been performed.

**The study aimed** to determine the diagnostic accuracy of the scale by four sequential CT studies to track the dynamics of the disease and make a decision on hospitalization of COVID-19 patients.

## MATERIALS AND METHODS

### Study design

Within this retrospective study, we used the database of the Unified Medical Information Analysis System (UMIAS) in Moscow to analyze a sequential sample of patients who were treated in medical organizations in Moscow from March 1 to August 1, 2020.

### Compliance criteria

**Inclusion criteria** were patients with a confirmed diagnosis of new coronavirus infection, aged 18 years or older, who underwent 4 consecutive CT examinations of the thoracic organs (TO). The diagnosis of COVID-19 in the enrolled patients was confirmed by detection of SARS-CoV-2 viral RNA in throat swabs by reverse transcription polymerase chain reaction (RT-PCR).

**Exclusion criteria** were age under 18 years, duplicate records, and records with incomplete data.

### Outcome registration methods

Studies of the chest organs were conducted using the recommended scanning parameters for patients with average anthropometric parameters (height 170 cm, weight 70 kg), voltage 120 kV, automatic adjustment of the current strength, scanning area 350 mm, and slice thickness 1.5 mm or thinner. The presentation was interpreted by roentgenologists who received special training in chest CT for COVID-19. Each medical description was sent to expert approbation at the Moscow Reference Center for Radiation Diagnostics.

For assessment of the results of CT studies, a semi-quantitative CT scale of 0–4 was used [5] in accordance with the Temporary Methodological Recommendations of the Ministry of Health of the Russian Federation for the prevention, diagnostics, and treatment of the new coronavirus infection COVID-19 [3]. According to the CT 0–4 scale, there are five degrees of lung tissue damage in COVID-19, namely normal (CT0), mild (CT1), moderate (CT2), severe (CT3), and critical (CT4). For patients with a mild to moderate course of the disease, medical care is allowed at home. Patients in severe and critical condition are subject to immediate hospitalization in a structural unit of a medical organization for the treatment of COVID-19.

If the radiologist, when interpreting medical descriptions, indicated the course of the disease as moderate (CT1–CT2) or severe (CT3–CT4), the patient was assigned the more severe of the two categories. If the doctor did not indicate the category on the CT scale of 0–4, but noted a positive or negative tendency, then in the presence of data on the previous CT study, the category was lowered or raised by one level, respectively.

To assess the duration of the convalescence period from COVID-19 pneumonia, the difference between the date of laboratory confirmation of the diagnosis and the date of the first of four CT examinations was determined, and according to the results, the patient was assigned to the CT0 category, provided that the category did not change in subsequent studies. Patients who had not recovered by August 1, 2020 were not included in the convalescence time analysis. Missing values were processed by excluding a specific indication from the corresponding analysis.

### Statistical analysis

When assessing the sensitivity and specificity of the CT scale 0–4 to identify the need for hospitalization, the disease dynamics were studied according to the results of repeated CT studies in a sequential sample of patients.

In diagnostic tests, *sensitivity* is defined as the conditional probability that the test results will be positive in the presence of the condition under study. *Specificity* is the conditional probability that test results will be negative if the condition under study is not noted. In the present study, a positive test result corresponded to worsening of the patient’s condition, and based on the results of a repeated CT scan, the patient was assigned to category CT3 or CT4 (the

result is “worse”). The test result was recognized as negative if, based on the results of the repeated study, the patient was assigned to categories CT 0–2, in other words, if their condition did not worsen and they were not subject to hospitalization (the result is “better”).

In the model presented, the need for hospitalization of the patient due to belonging to the CT3 or CT4 category (the condition “hospital”) was taken as the condition under study. The absence of the condition under study included all cases when treatment at home was prescribed for patients of CT categories 0–2 (condition “home”).

Thus, in the model presented, the sensitivity ( $Se$ ) was estimated as the conditional probability  $P_{worse/hospital}$ :

$$P_{worse/hospital} = \frac{\text{Number of 'hospital' patients after second CT study}}{\text{Total number of 'hospital' patients}} \quad (1).$$

The specificity ( $Sp$ ) of the model corresponded to the conditional probability  $P_{better/home}$ :

$$P_{better/home} = \frac{\text{Number of 'home' patients after second CT study}}{\text{Total number of 'home' patients}} \quad (2).$$

The Youden index  $J$  was calculated from the values of sensitivity and specificity:

$$J = Se + Sp - 1 \quad (3).$$

The positive predictive value (PPV) and negative predictive value (NPV) of the test depend on the disease prevalence. The Exponential Smoothing (ETS [6]) and Auto-Regressive Integrated Moving Average (ARIMA [7]) models were used to predict the incidence of COVID-19 in Moscow. Daily information on all cases of COVID-19 infection in the period from March 6 to November 28, 2020 was obtained from the Russian Agency for Health and Consumer Rights website [8]. Time series analysis was performed using R 3.6.3 [9] with the use of the forecast [10] and ggplot2 [11] packages. The

development of the disease prevalence was assessed for a period of 120 days. For accuracy of assessment, the model was trained on morbidity data from March 6 to November 15, 2020, after which the predicted and actual values for the period from November 15 to November 28, 2020 were compared using the metrics of mean absolute percentage error (MAPE) and mean absolute scaled error (MASE).

Using the prevalence value, PPV was calculated as follows:

$$PPV = \frac{\text{Sensitivity} \times \text{prevalence}}{(\text{sensitivity} \times \text{prevalence}) + (1 - \text{specificity}) \times (1 - \text{prevalence})} \quad (4).$$

The test NPV was calculated in the same way:

$$NPV = \frac{\text{Specificity} \times (1 - \text{prevalence})}{\text{Specificity} \times (1 - \text{prevalence}) + (1 - \text{sensitivity}) \times \text{prevalence}} \quad (5).$$

## RESULTS

### Objects (participants) of the study

Records of 139,592 patients of medical organizations in Moscow for the period from March 1 to August 1, 2020 were assessed for compliance with the criteria for inclusion in the study. After exclusion of 139,017 participants for various reasons, for statistical analysis, data from 575 patients with confirmed COVID-19 was used, each of whom underwent four consecutive TCT (thoracic computed tomography) scans (Fig. 1).

### Main research findings

The mean age of patients in the final sample was  $57.2 \pm 13.9$  (range 2292) years; the sample included 314 women (54.6%). During the study, 49 lethal outcomes were registered. CT scanning 1 revealed no signs of viral pneumonia in 70 patients; 223 participants had a mild degree of lung tissue changes (CT1), a moderate degree (CT2) was

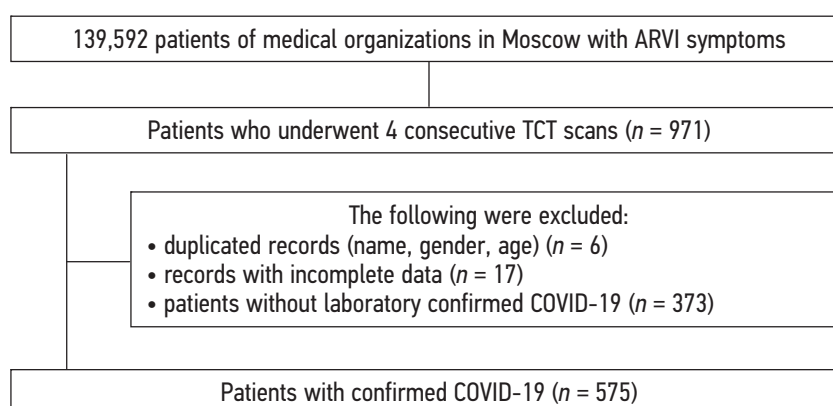


**Fig. 1.** Scheme of the examination of the study participants.

ARVI — acute respiratory viral infections; TCT — thoracic computed tomography.

noted in 163 patients, severe degree (CT3) was registered in 84 cases, and critical (CT4) was revealed in 16 patients. For 19 patients, the severity level was not indicated due to other pulmonological diseases ( $n = 13$ ), or the study was conducted earlier than March 1, 2020 ( $n = 6$ ). The average time period between TCT 1 and 2 was  $9.4 \pm 8.3$ , that between TCT 2 and 3 was  $10.2 \pm 8.1$ , and the period between TCT 3 and 4 was  $22.6 \pm 17.5$  days.

The dynamics of the distribution of disease cases in the sample according to the degree of severity followed a clear pattern. In the interval between TCT studies 1 and 2, the number of patients in categories CT0 and CT1 decreased with an increase in the number of patients of categories CT2, CT3, and CT4. In the interval between studies 2 and 3, the number of patients in categories CT0, CT3, and CT4 stabilized, and relative stability in the number of patients with mild and moderate changes was noted in the presence of an increase in the number of CT1 cases and a decrease in the number of CT2 cases. Finally, at stage 3, the tendencies of stage 1 were reversed, as there was a significant increase in the number of patients in the categories CT0 and CT1, with an equally noticeable decrease in the number of patients in the categories CT2, CT3, and CT4 (Fig. 2).

### Convalescence time

To assess the convalescence time, the sample ( $n = 124$ ) was divided into three cohorts:

- 1) patients of the categories CT1–CT4 according to the results of CT scan 1 of the T0, who had resolution of COVID-19 pneumonia after study 2 (CT0) without further deterioration of the clinical condition. This cohort included four patients with an average convalescence time of  $23.5 \pm 4.9$  days, all patients of the CT1 category according to the results of CT scan 1. Note that two patients from this cohort had positive RT-PCR tests for COVID-19 5 and

21 days later, respectively, after elimination of the characteristic manifestations of the disease;

- 2) patients of the categories CT1–CT4 according to the results of TCT study 2, who changed the category to CT0 according to the results of study 3 without further deterioration of the clinical condition. The cohort consisted of 12 patients, including 11 patients with CT1 based on study 2, and one patient had CT2. The mean convalescence time in the cohort was  $36.3 \pm 21.3$  days. Five patients also had positive test results  $11.0 \pm 13.1$  days after being assigned to category CT0;
- 3) patients of categories CT1–CT4 according to TCT study 3, who changed the category to CT0 according to the results of study 4. The cohort included 108 patients, one of whom died due to pathological changes not associated with COVID-19. According to the results of study 3, 81 patients from the cohort had category CT1, 16 patients had category CT2, 9 patients had category CT3, and two patients had category CT4. The average convalescence time was  $36.0 \pm 24.3$  days; four patients tested positive for COVID-19  $16.0 \pm 17.1$  days after being assigned to category CT0.

### Assessment of diagnostic accuracy

When assessing the diagnostic accuracy of TCT and the semi-quantitative CT scale 0–4 to determine the need for hospitalization of COVID-19 patients, three stages of the study were considered separately (Fig. 2). According to the results of TCT study 2, the greatest specific changes in the clinical condition occurred among patients of the CT0 category, 53% of which changed category to CT1, 19% changed to CT2, and 6% had a severe disease course (Table 1).

To calculate the values of specificity and sensitivity at stage 1 of the study from the data presented in Table 1, a  $2 \times 2$  cross-classification table can be drawn up (Table 2).

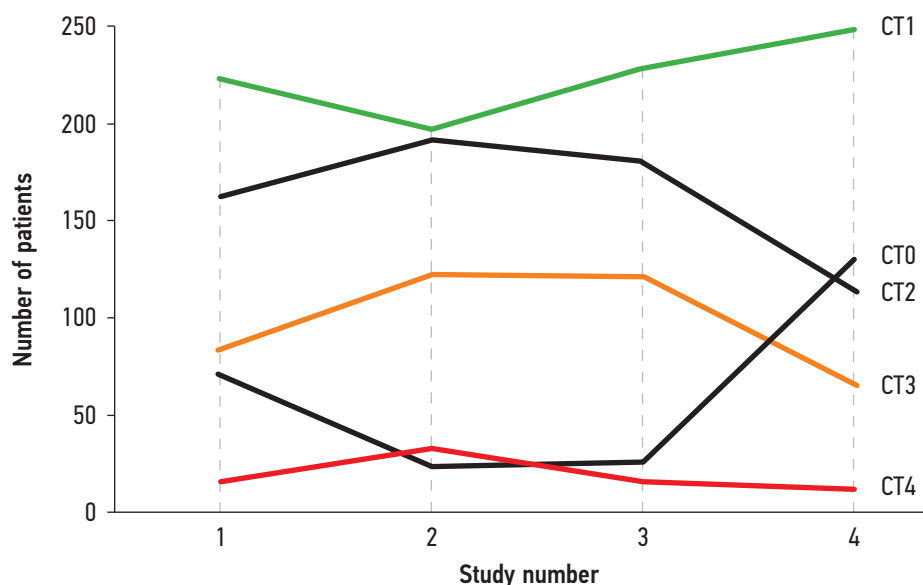


Fig. 2. Dynamics of the distribution of the number of patients according to the degree of changes in the lung tissue.

According to Table 2, from equations (1) and (2), the specificity and sensitivity of TCT when using the CT scale 0–4 to determine the need for hospitalization of COVID-19 patients were 84.3% and 83%, respectively.

When comparing the results of TCT studies 2 and 3, the greatest specific changes occurred in patients of the CT4 category, the clinical condition of 64% of whom improved (Table 3).

The specificity and sensitivity of TCT and the CT scale 0–4 for the stage 2 of the study were 92.9 and 69.5%, respectively [equations (1) and (2); Table 4].

Finally, at the stage 3, the greatest specific changes in the clinical condition of patients were registered in the categories CT2 (the condition improved in 54% of patients and worsened in 3% of cases) and CT3 (the condition improved in 49% of patients and worsened in 3% of cases); Table 5.

At stage 3 of the study, the specificity of TCT and the CT scale 0–4 to determine the need for hospitalization of COVID-19 patients was 98.8%, and sensitivity was 53.7% [equations (1) and (2); Table 6].

If we consider all stages of the study as a single block, the approach sensitivity was 91.8% (95% CI 83.7–100), and the specificity was 68.7% (95% CI 52.1–85.3).

### Assessment of NPV and PPV values

#### Prediction of the prevalence of COVID-19 in Moscow

According to the Russian Agency for Health and Consumer Rights website [8], the infection curve demonstrated exponential growth until July 1, 2020. After that, the number of daily new cases reached a constant level of  $658 \pm 42$  (Fig. 3).

Phase II of exponential growth started between September 15 and 23, 2020 (Fig. 3). To select a predictive model, the data on the incidence of COVID-19 were divided into groups for training and testing, followed by training for various models of EST and ARIMA. According to the MAPE and MASE values, the ARIMA (0,2,1) and ETS ZZZ (autoselectable parameters) models were the best predictors of the test data (Table 7).

The ARIMA (0,2,1) and ETS ZZZ models predicted an almost linear increase in new COVID-19 cases after the end of

**Table 1.** Categorization of participants between thoracic computed tomography scanning 1 and 2

Indicator	CT	Total*	Category according to the study 2 results				
			CT0	CT1	CT2	CT3	CT4
Category according to the study 1 results	CT0	70	16	37	13	3	1
	CT1	223	7	122	71	18	4
	CT2	163	1	29	85	40	5
	CT3	84	0	1	15	56	12
	CT4	16	0	0	1	4	11

**Note.** \*Here and in Tables 3 and 5, the discrepancy in the total number of patients according to the results of the adjacent TCT scan is associated with the missing results of the numerical study for some participants. Such cases were not excluded, since such data were available for other studies of these patients.

**Table 2.** 2 × 2 table for stage 1 of the study

Indicator	Improvement	Deterioration	Total
Home	381	71	452
Hospital	17	83	100
Total	398	154	552

**Table 3.** Categorization of participants between thoracic computed tomography scanning 2 and 3

Indicator	CT	Total*	Category according to the study 3 results				
			CT0	CT1	CT2	CT3	CT4
Category according to the study 2 results	CT0	24	11	5	7	1	0
	CT1	197	13	158	20	6	0
	CT2	192	1	59	110	21	1
	CT3	122	0	4	39	75	3
	CT4	33	0	1	3	17	12



**Table 4.** 2 × 2 table for stage 2 of the study

Indicator	Improvement	Deterioration	Total
Home	384	29	413
Hospital	47	107	154
Total	431	136	567

**Table 5.** Categorization of participants between thoracic computed tomography scanning 3 and 4

Indicator	CT	Total*	Category according to the study 4 results				
			CT0	CT1	CT2	CT3	CT4
Category according to the study 3 results	CT0	26	22	4	0	0	0
	CT1	229	81	144	3	1	0
	CT2	181	16	81	77	4	1
	CT3	121	9	17	33	57	4
	CT4	16	2	1	1	5	7

**Table 6.** 2 × 2 table for stage 3 of the study

Indicator	Improvement	Deterioration	Total
Home	428	5	433
Hospital	63	73	136
Total	491	78	569

phase II of exponential growth (Figure 3). The most optimistic scenario offered by the ETS MMM model did not prove true already on the testing sample (Fig. 3, Table 7). As a result, the incidence curve is not likely to flatten over the estimated

time period. The curve corresponding to the predictions of the ARIMA (0,2,1) and ETS ZZZ models is not asymptotic, which complicates the estimation of the limit value for the total number of COVID-19 cases in Moscow (Fig. 3).

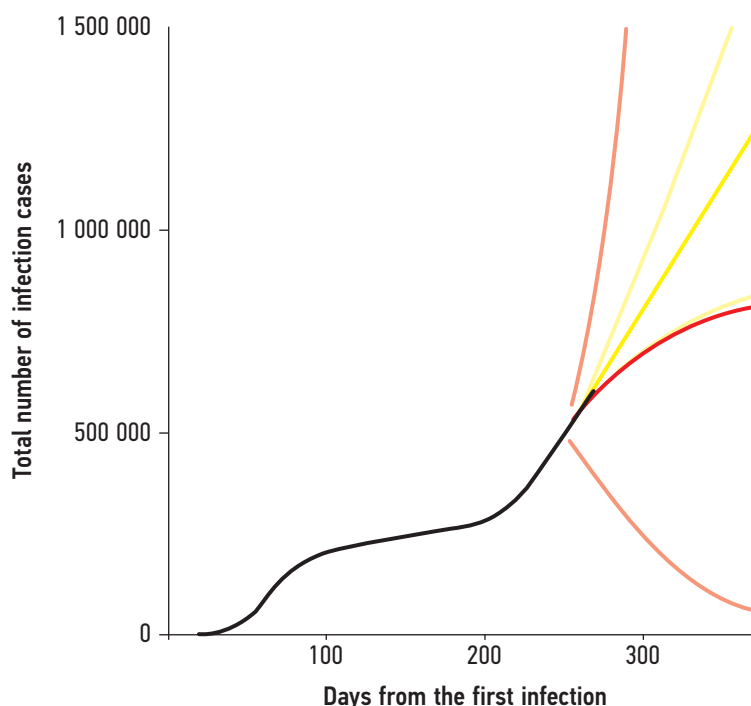


**Fig. 3.** Prediction of the prevalence of COVID-19 in Moscow: actual data (black curve); ETS MMM model (yellow curve); ARIMA model (0,2,1) (red curve). The prognosis of the ETS ZZZ model is not displayed as it coincides with ARIMA (0,2,1). For each of the models, the 95% confidence intervals are shown in the corresponding dimmed color.

**Table 7.** Accuracy statistics for different predictive models

Model	MAPE	MASE
ARIMA (0,2,1)	0.233	0.634
ETS ZZZ	0.233	0.634
ETS MMM	1.436	4.063

**Table 8.** PPV and NPV values for different stages of the study

Stage	1	2	3	General value (95% CI)
PPV, %	35.9	50.9	82.6	56.5 (29.5–83.4)
NPV, %	97.9	96.6	95.2	96.6 (95.0–98.1)

Since the infection curve has not flattened, only the annual number of cases of COVID-19 infection can be estimated. According to the ARIMA (0,2,1) and ETS ZZZ models, this figure will reach 1,220,500 cases per year, provided the current tendency continues. It should be noted that this prognostic estimate is approximate, and there may be effects of seasonal fluctuations and expected mass vaccination, which cannot be predicted due to the available data. According to Rosstat data as of January 1, 2020, the population of Moscow was 12,678,079 people<sup>1</sup>. Based on this information, the Moscow instantaneous prevalence of COVID-19, characterized as the percentage of cases in the urban population at risk of the disease, will amount to 9.63% by March 6, 2021.

#### Predictive value

Considering the value of the instantaneous prevalence of COVID-19 in Moscow, as well as the values of sensitivity and specificity presented in Tables 2, 4, and 6, the PPV and NPV can be calculated using equations (3) and (4) (Table 8).

Thus, the results of a retrospective follow-up of 575 patients with laboratory confirmed COVID-19 demonstrated 69% specificity, 92% sensitivity, 56% PPV, and 97% NPV of CT for making a decision on hospitalization of the patients.

## DISCUSSION

This work aimed to evaluate the numerical indicators of the diagnostic accuracy of TCT and the CT scale 0–4 for making a decision on hospitalization of COVID-19 patients. According to the results obtained, the scale showed average values of specificity and PPV with high sensitivity and NPV.

The role and importance of CT for the detection of COVID-19 pneumonia, their complications, and differential diagnostics with other lung diseases have caused an onslaught of discussion in the medical community [12, 13].

TCT scan has low rates of underdiagnosis [14]. In addition, a positive correlation of the CT scale 0–4 with mortality rates among patients with coronavirus pneumonia COVID-19 [4] has been demonstrated. However, the severity of the patient's condition, as well as its dynamics, do not always correlate with the quantitative assessment of the volume of indurated lung tissue [15].

In the present work, we used the results of four consecutive TCT studies in patients with confirmed COVID-19. This enabled us to divide the study into three stages with pronounced trends in the change in the clinical condition of patients in the sample. At stage 1, corresponding to the period between CT examinations 1 and 2, deterioration in the clinical condition of the majority of patients was registered (Fig. 2). This stage was characterized by maximum sensitivity of the CT scale 0–4 (83.0%), the maximum Youden's index (0.673), and the lowest PPV value (35.9%).

At stage 2, no significant changes in the number of categories of patients of different severity were registered (Fig. 2). This situation was accompanied by a decrease in sensitivity (–13.5%) and an increase in specificity (+8.6%) and PPV (+15%) of the CT scale 0–4, and Youden's index was 0.624.

Finally, at the stage 3, corresponding to the period between CT studies 3 and 4, the majority of patients showed an improvement in their clinical condition (Fig. 2). At the same time, a further decrease in the method's sensitivity (–29.3%) and an increase in specificity (+14.5%) and PPV (+46.7%) were noted. Youden's index at this stage reached a minimum value of 0.525. All changes are given relative to the values of stage 1.

#### Study limitations

This study has limitations. The resulting convalescence times are higher than previously published values for cohorts 2 and 3 of participants (about 36 days). According to Bi et al. [16], the median convalescence time from COVID-19 is estimated at 20.8 days, while for patients aged 50–70 years and older, the period is increased to 22.6 days, and up to 28.3 days for patients with severe symptoms. This may be

<sup>1</sup> Department of the Federal State Statistics Service for Moscow and the Moscow Region. Estimation of the resident population of Moscow as of January 1, 2020. Access mode: [https://mosstat.gks.ru/storage/mediabank/Оценка\\_численности\\_населения\\_2020\\_383215.xls..](https://mosstat.gks.ru/storage/mediabank/Оценка_численности_населения_2020_383215.xls..) Date of reference: 01/15/2021.

due to the methodology for assessing the indicator used in this work. The moment of convalescence was identified with the date of the CT scan, according to which the patient was transferred to category CT0, which is not always the proper approach [15].

Another study limitation was that, when the diagnostic value indicators were calculated, all patients with mild and moderate lung tissue changes were included in the “home” group, whereas, according to the Temporary Methodological Recommendations of the Ministry of Health of the Russian Federation for the prevention, diagnostics and treatment of new coronavirus infection COVID-19, such patients should be hospitalized, and treatment at home is allowed only under certain conditions.

## CONCLUSION

The CT scale 0–4 demonstrated the maximum diagnostic value under conditions of a high probability of deterioration in the condition of study participants, which confirms its practical significance for triage of patients in an unfavorable epidemic situation. The scale enables the development of

pathological changes in patients of the CT0–CT1 categories to be ruled out with high confidence, thereby optimizing the workload on in-patient hospitals.

## ADDITIONAL INFORMATION

**Funding source.** This study was not supported by any external sources of funding.

**Competing interests.** The authors declare that they have no competing interests.

**Author contribution.** S.P. Morozov — conceptualization and funding of the study, editing of the text of the article; R.V. Reshetnikov — collection and analysis of literary sources, statistical analysis, preparation and writing of the text of the article; V.A. Gombolevsky — conceptualization of the study, data preparation; N.V. Ledikhova — collection and preparation of data; I.A. Blokhin — writing and editing the text of the article; O.A. Mokienko — conceptualization of the study, editing of the text of the article. All authors made a substantial contribution to the conception of the work, acquisition, analysis, interpretation of data for the work, drafting and revising the work, final approval of the version to be published and agree to be accountable for all aspects of the work».

## REFERENCES

1. Coronavirus update (live) [cited 2002 Oct 20]. Available from: <https://www.worldometers.info/coronavirus>
2. World Health Organization. Coronavirus disease 2019 (COVID-19): situation report, 46 [cited 2002 March 06]. World Health Organization, Geneva; 2020. Available from: [https://www.who.int/docs/default-source/coronaviruse/situation-reports/20200306-sitrep-46-covid-19.pdf?sfvrsn=96b04adf\\_4](https://www.who.int/docs/default-source/coronaviruse/situation-reports/20200306-sitrep-46-covid-19.pdf?sfvrsn=96b04adf_4)
3. Temporary guidelines «Prevention, diagnosis and treatment of new coronavirus infection (COVID-19). Version 9 (26.10.2020)» (approved by the Ministry of Health of the Russian Federation) [Internet]. (In Russ.). Available from: [http://disuria.ru/\\_ld/8/846\\_mrC19p-dl261020.pdf](http://disuria.ru/_ld/8/846_mrC19p-dl261020.pdf)
4. Morozov SP, Gombolevskiy VA, Chernina VYu, et al. Prediction of lethal outcomes in COVID-19 cases based on the results chest computed tomography. *Tuberculosis and Lung Diseases*. 2020;98(6):7–14. (In Russ.) doi: 10.21292/2075-1230-2020-98-6-7-14
5. Morozov SP, Andreychenko AE, Pavlov NA, et al. MosMedData: chest CT scans with COVID-19 related findings dataset. *medRxiv*. 2020. doi: 10.1101/2020.05.20.20100362
6. Hyndman RJ, Khandakar Y. Automatic time series forecasting: the forecast package for R. *J Stat Softw*. 2008;27(3). doi: 10.18637/jss.v027.i03
7. Box GE, Jenkins GM, Reinsel GC, Ljung GM. Time series analysis: forecasting and control. John Wiley & Sons, Hoboken; 2015.
8. Rospotrebnadzor. The epidemiological situation and the spread of COVID-19 in the world as of 8.00 Moscow Time on 28.11.2020. Available from: [https://www.rospotrebnadzor.ru/region/korono\\_virus/epid.php](https://www.rospotrebnadzor.ru/region/korono_virus/epid.php)
9. R Core Team. R: A language and environment for statistical computing. R foundation for statistical computing. Vienna, Austria; 2020.
10. Hyndman RJ, Athanasopoulos G, Bergmeir C, et al. forecast: Forecasting functions for time series and linear models. Semantic Scholar; 2020.
11. Wickham H. ggplot2: elegant Graphics for Data Analysis. Springer-Verlag New York; 2016. doi: 10.1007/978-3-319-24277-4
12. Hamilton MC, Lyen S, Manghat NE. Controversy in coronaViral Imaging and Diagnostics (COVID). *Clin Radiol*. 2020;75(7):557–558. doi: 10.1016/j.crad.2020.04.011
13. Morozov S, Ledikhova N, Panina E, et al. Re: Controversy in coronaViral Imaging and Diagnostics (COVID). *Clin Radiol*. 2020;75(11):871–872. doi: 10.1016/j.crad.2020.07.023
14. Li Y, Xia L. Coronavirus Disease 2019 (COVID-19): Role of Chest CT in Diagnosis and Management. *AJR Am J Roentgenol*. 2020;214(6):1280–1286. doi: 10.2214/AJR.20.22954
15. Feng Z, Yu Q, Yao S, et al. Early prediction of disease progression in COVID-19 pneumonia patients with chest CT and clinical characteristics. *Nat Commun*. 2020;11(1):4968. doi: 10.1038/s41467-020-18786-x
16. Bi Q, Wu Y, Mei S, et al. Epidemiology and transmission of COVID-19 in 391 cases and 1286 of their close contacts in Shenzhen, China: a retrospective cohort study. *Lancet Infect Dis*. 2020;20(8):911–919. doi: 10.1016/S1473-3099(20)30287-5

## СПИСОК ЛИТЕРАТУРЫ

1. Coronavirus update (live) [cited 2020 Oct 20]. Available from: <https://www.worldometers.info/coronavirus>
2. World Health Organization. Coronavirus disease 2019 (COVID-19): situation report, 46 [cited 2020 March 06]. WHO, Geneva; 2020. Available from: [https://www.who.int/docs/default-source/coronaviruse/situation-reports/20200306-sitrep-46-covid-19.pdf?sfvrsn=96b04adf\\_4](https://www.who.int/docs/default-source/coronaviruse/situation-reports/20200306-sitrep-46-covid-19.pdf?sfvrsn=96b04adf_4)
3. Временные методические рекомендации «Профилактика, диагностика и лечение новой коронавирусной инфекции (COVID-19). Версия 9 (26.10.2020)» (утв. Министерством здравоохранения Российской Федерации) [интернет]. Режим доступа: [http://disuria.ru/\\_ld/8/846\\_mrC19pdl261020.pdf](http://disuria.ru/_ld/8/846_mrC19pdl261020.pdf). Дата обращения: 15.01.2021.
4. Морозов С.П., Гомболевский В.А., Чернина В.Ю. и др. Прогнозирование летальных исходов при COVID-19 по данным компьютерной томографии органов грудной клетки // Туберкулез и болезни легких. 2020. Т. 98, № 6. С. 7–14. doi: 10.21292/2075-1230-2020-98-6-7-14
5. Morozov S.P., Andreychenko A.E., Pavlov N.A., et al. MosMed-Data: chest CT scans with COVID-19 related findings dataset // medRxiv. 2020. doi: 10.1101/2020.05.20.20100362
6. Hyndman R.J., Khandakar Y. Automatic time series forecasting: the forecast package for R // J Stat Softw. 2008. Vol. 27, N 3. doi: 10.18637/jss.v027.i03
7. Box G.E., Jenkins G.M., Reinsel G.C., Ljung G.M. Time series analysis: forecasting and control. John Wiley & Sons, Hoboken; 2015.
8. Роспотребнадзор. Эпидемиологическая обстановка и распространение COVID-19 в мире по состоянию на 8.00 по МСК от 28.11.2020. Режим доступа: [https://www.rosпотребнадзор.ru/region/korono\\_virus/epid.php](https://www.rosпотребнадзор.ru/region/korono_virus/epid.php). Дата обращения: 15.01.2021.
9. R Core Team. R: A language and environment for statistical computing. R foundation for statistical computing. Vienna, Austria; 2020.
10. Hyndman R.J., Athanasopoulos G., Bergmeir C., et al. forecast: Forecasting functions for time series and linear models. Semantic Scholar; 2020.
11. Wickham H. ggplot2: elegant Graphics for Data Analysis. Springer-Verlag New York; 2016. doi: 10.1007/978-3-319-24277-4
12. Hamilton M.C., Lyen S., Manghat N.E. Controversy in coronaViral Imaging and Diagnostics (COVID) // Clin Radiol. 2020. Vol. 75, N 7. P. 557–558. doi: 10.1016/j.crad.2020.04.011
13. Morozov S., Ledikhova N., Panina E., et al. Re: Controversy in coronaViral Imaging and Diagnostics (COVID) // Clin Radiol. 2020. Vol. 75, N 11. P. 871–872. doi: 10.1016/j.crad.2020.07.023
14. Li Y., Xia L. Coronavirus Disease 2019 (COVID-19): Role of Chest CT in Diagnosis and Management // AJR Am J Roentgenol. 2020. Vol. 214, N 6. P. 1280–1286. doi: 10.2214/AJR.20.22954
15. Feng Z., Yu Q., Yao S., et al. Early prediction of disease progression in COVID-19 pneumonia patients with chest CT and clinical characteristics // Nat Commun. 2020. Vol. 11, N 1. P. 4968. doi: 10.1038/s41467-020-18786-x
16. Bi Q., Wu Y., Mei S., et al. Epidemiology and transmission of COVID-19 in 391 cases and 1286 of their close contacts in Shenzhen, China: a retrospective cohort study // Lancet Infect Dis. 2020. Vol. 20, N 8. P. 911–919. doi: 10.1016/S1473-3099(20)30287-5

## AUTHORS' INFO

\* **Roman V. Reshetnikov**, Cand.Sci. (Phys-Math);  
address: Petrovka str., 24, 127051, Moscow, Russia;  
ORCID: <https://orcid.org/0000-0002-9661-0254>;  
eLibrary SPIN: 8592-0558; e-mail: reshetnikov@fbb.msu.ru

**Sergey P. Morozov**, MD, Dr.Sci. (Med), Professor;  
ORCID: <https://orcid.org/0000-0001-6545-6170>;  
eLibrary SPIN: 8542-1720; e-mail: morozov@npcmr.ru

**Victor A. Gombolevskiy**, MD, Cand.Sci. (Med);  
ORCID: <https://orcid.org/0000-0003-1816-1315>;  
eLibrary SPIN: 6810-3279; e-mail: g\_victor@mail.ru

**Natalya V. Ledikhova**, MD; eLibrary SPIN: 6907-5936; e-mail: n.ledikhova@npcmr.ru

**Ivan A. Blokhin**, MD;  
ORCID: <https://orcid.org/0000-0002-2681-9378>;  
eLibrary SPIN: 3306-1387; e-mail: i.blokhin@npcmr.ru

**Olesya A. Mokienko**, MD, Cand.Sci. (Med);  
ORCID: <https://orcid.org/0000-0002-7826-5135>;  
eLibrary SPIN: 8088-9921; e-mail: Lesya.md@yandex.ru

## ОБ АВТОРАХ

\* **Решетников Роман Владимирович**, к.ф.-м.н.;  
адрес: 127051, Москва, ул. Петровка, д. 24  
ORCID: <https://orcid.org/0000-0002-9661-0254>;  
eLibrary SPIN: 8592-0558; e-mail: reshetnikov@fbb.msu.ru

**Морозов Сергей Павлович**, д.м.н., профессор;  
ORCID: <https://orcid.org/0000-0001-6545-6170>;  
eLibrary SPIN: 8542-1720; e-mail: morozov@npcmr.ru

**Гомболевский Виктор Александрович**, к.м.н.;  
ORCID: <https://orcid.org/0000-0003-1816-1315>;  
eLibrary SPIN: 6810-3279; e-mail: g\_victor@mail.ru

**Ледихова Наталья Владимировна**; eLibrary SPIN: 6907-5936;  
e-mail: n.ledikhova@npcmr.ru

**Блохин Иван Андреевич**;  
ORCID: <https://orcid.org/0000-0002-2681-9378>;  
eLibrary SPIN: 3306-1387; e-mail: i.blokhin@npcmr.ru

**Мокиенко Олеся Александровна**, к.м.н.;  
ORCID: <https://orcid.org/0000-0002-7826-5135>;  
eLibrary SPIN: 8088-9921; e-mail: Lesya.md@yandex.ru





DOI: <https://doi.org/10.17816/DD53701>

# Students opinion about E-Learning in a Master course in Interventional Radiology: a survey among participants

© Emanuele Neri<sup>1</sup>, Laura Crocetti<sup>2</sup>, Giulia Lorenzoni<sup>2</sup>, Roberto Cioni<sup>2</sup>, Adrian Brady<sup>3</sup>, Davide Caramella<sup>1</sup>

<sup>1</sup> University of Pisa, Pisa, Italy

<sup>2</sup> Pisa University Hospital, Pisa, Italy

<sup>3</sup> Mercy University Hospital, Cork & University College, Cork, Ireland.

**AIM:** To evaluate the opinion of students about Tele-education in a post-graduate University Master in Interventional Radiology.

**METHODS:** The core curriculum of the Master is divided into 3 e-Learning modules and 2 e-Learning plus Hands-on Training modules. E-Learning is delivered through a webinar platform that allows to perform a synchronous training providing real-time lectures that are recorded for streaming on a dedicated website. The Hands-on Training is provided on site, assisting interventional radiologists in interventional procedures on patients. An online survey of 12 questions has been prepared to determine the quality of training. Students indicated their level of agreement regarding the impact of eLearning and Hands on Training using a 5-point scale. The mean score of the level of agreement was calculated.

**RESULTS:** The series include 16 participants. The 62.5% work in a public non-academic Hospital and 80% have already performed >300 interventional procedures as primary operator.

The main advantage of the eLearning module was considered the capability to facilitate the attendance to lectures (68.8%) followed by the low cost training (18.8%), with a good agreement between participants. No students scored the statements as less than 3. The Master fulfilled the learning expectations in 81.3% of cases with a good agreement between participants.

**CONCLUSIONS:** The participants were highly satisfied and would recommend the Master to other colleagues. The blended type of education of our Master received high appreciation and could be a model to be follow in the future, also in IR.

**Keywords:** Interventional Radiology; Education; Surveys and Questionnaires; Learning; Informatics.

## To cite this article

Neri E, Crocetti L, Lorenzoni G, Cioni R, Brady A, Caramella D. Students opinion about E-Learning in a Master course in Interventional Radiology: a survey among participants. *Digital Diagnostics*. 2021;2(1):17–26. DOI: <https://doi.org/10.17816/DD53701>

DOI: <https://doi.org/10.17816/DD53701>

# Мнение студентов магистратуры о дистанционном обучении по специальности «Интервенционная радиология» с помощью электронных технологий: опрос учащихся

© Emanuele Neri<sup>1</sup>, Laura Crocetti<sup>2</sup>, Giulia Lorenzoni<sup>2</sup>, Roberto Cioni<sup>2</sup>,  
Adrian Brady<sup>3</sup>, Davide Caramella<sup>1</sup>

<sup>1</sup> University of Pisa, Пиза, Италия

<sup>2</sup> Pisa University Hospital, Пиза, Италия

<sup>3</sup> Mercy University Hospital, Cork & University College, Корк, Ирландия

**Обоснование.** Программа магистратуры «Интервенционная радиология» — первый учебный курс смешанного типа, предложенный нашим университетом по данному направлению. Программа включает практические занятия, очные лекции в отделении «Интервенционная радиология» в сочетании с онлайн-обучением.

**Цель** — оценить мнение студентов о дистанционном обучении по программе магистратуры «Интервенционная радиология» (ИР) с помощью электронных технологий.

**Методы.** Основная учебная программа включает в себя 3 модуля дистанционного обучения и 2 смешанных модуля (дистанционное обучение + практические занятия). Электронное обучение осуществляется через специальную платформу для синхронного проведения практических и теоретических занятий в форме вебинаров и онлайн-лекций, которые записываются и загружаются на специальный веб-сайт для прямой трансляции. Практическое обучение проводится в лечебном учреждении, что позволяет студентам проводить интервенционные процедуры непосредственно с пациентами. Для оценки качества обучения подготовлен онлайн-опрос из 12 пунктов. Студенты оценивали степень согласия с предложенными утверждениями об эффективности электронного и практического обучения по пятибалльной шкале. По полученным ответам рассчитывали средний балл.

**Результаты.** В опросе принимали участие 16 человек: часть из них работает в государственных (неакадемических) лечебных учреждениях (62,5%), большинство участников на момент проведения опроса выполнили более 300 интервенционных процедур в качестве ведущих операторов (80%). Участники согласились с тем, что основные преимущества электронного модуля обучения — возможность удалённого прослушивания лекций (68,8%) и относительно низкая стоимость обучения (18,8%). Все студенты оценили указанные преимущества не менее чем в 3 балла. В целом программа оправдала ожидания студентов в 81,3% случаев, что позволяет говорить об эффективности предложенной формы обучения.

**Заключение.** Участники остались довольны и выразили готовность рекомендовать учебный курс своим коллегам. Смешанная форма обучения получила высокую оценку и, как ожидается, станет полезной моделью изучения интервенционной радиологии.

**Ключевые слова:** интервенционная радиология; образование; опросы и опросники; обучение; информатика.

## Как цитировать

Neri E., Crocetti L., Lorenzoni G., Cioni R., Brady A., Caramella D. Мнение студентов магистратуры о дистанционном обучении по специальности «Интервенционная радиология» с помощью электронных технологий: опрос учащихся // *Digital Diagnostics*. 2021. Т. 2, №1. С.17–26.  
DOI: <https://doi.org/10.17816/DD53701>

DOI: <https://doi.org/10.17816/DD53701>

# 学生对介入放射学硕士课程电子学习的看法：一项学员调查

© Emanuele Neri<sup>1</sup>, Laura Crocetti<sup>2</sup>, Giulia Lorenzoni<sup>2</sup>, Roberto Cioni<sup>2</sup>,  
Adrian Brady<sup>3</sup>, Davide Caramella<sup>1</sup>

<sup>1</sup> University of Pisa, Pisa, Italy

<sup>2</sup> Pisa University Hospital, Pisa, Italy

<sup>3</sup> Mercy University Hospital, Cork & University College, Cork, Ireland.

**目的：**探讨介入放射学硕士研究生对远程教育的看法。

**方法：**硕士的核心课程分为3个电子学习模块和2个电子学习+实践培训模块。电子学习通过一个在线会议平台开展，该平台可实现同步培训，提供实时授课，并在专门的网站上录制播放。提供实地操作培训，可帮助介入放射科医生对患者执行介入手术治疗。目前已准备了包括12个问题的在线调查，用以确定培训质量。学生通过5分制量表说明其对电子学习和实践培训影响的认同程度，并计算认同程度的平均分数。

**结果：**本系列研究有16名学员参加。62.5%的学员在公立非学术性医院工作，80%的学员已经以主刀身份执行超过300次介入手术。

学员一致认为，电子学习模块的主要优势是能够方便讲座出勤（68.8%），其次是培训成本低（18.8%）。没有学生对陈述的评分低于3分。81.3%的学员一致认为，该硕士课程达到了学习预期。

**讨论：**学员非常满意，并愿意向其他同事推荐该硕士课程。该复合型硕士课程教育获高度评价，并且可能成为未来介入放射学（IR）可以采用的模式。

**关键词：**介入放射学；教育；调研和问卷调查；学习；信息学。

## 引用本文：

Neri E, Crocetti L, Lorenzoni G, Cioni R, Brady A, Caramella D. 学生对介入放射学硕士课程电子学习的看法：一项学员调查. *Digital Diagnostics*. 2021;2(1):17–26. DOI: <https://doi.org/10.17816/DD53701>

收到: 07.12.2020

接受: 09.02.2021

发布时间: 12.02.2021



## Abbreviations and acronyms:

**IR:** Interventional Radiology

**UEMS:** Union of European Medical Specialists

**CIRSE:** Cardiovascular and Interventional Radiological Society of Europe

**EBIR:** European Board of Interventional Radiology

**SIRM:** Società Italiana di Radiologia Medica e Interventistica

**CME:** Continuing Medical Education

## INTRODUCTION

The clinical importance and contribution of Interventional Radiology (IR) has grown substantially in recent decades, with ever-expanding applications and image-guided therapies, especially in the vascular and oncologic fields. Correspondingly, the demand for interventional radiologists is growing.

In 2009 the Union of European Medical Specialists (UEMS) recognized IR as a distinct specialty of radiology [1]. A particular objective of the “UEMS Specialist Division—Interventional Radiology” has been to establish standards for the required knowledge and training of interventional radiologists [2]. However, the processes and requirements for accreditation and certification of IR training vary from country to country. To assist in the unification and standardization of international IR training and certification in Europe, the “Cardiovascular and Interventional Radiological Society of Europe” (CIRSE) created a comprehensive examination for professional interventional radiologists in 2010 (The European Board of Interventional Radiology, EBIR) and a “European Curriculum and Syllabus for Interventional Radiology” in 2013 [3]. Appropriate provision and certification of training, and clinical practice are now important requirements for IR in order to ensure a certain standard which will enhance patient care and safety [4]. For these reasons, it is imperative that radiologists in training acquire a minimum skill set and knowledge base during their basic radiology (Levels 1 & 2) training, which can be integrated with an advanced training fellowship to achieve good interventional competence [5].

Training in IR relies on a traditional and practical apprenticeship to gain technical skills in minimally invasive interventional procedures. However, in combination with traditional face to face teaching, the continuous evolution of information technology offers new e-learning tools that have been already successfully adopted in medical education for distance learning courses [6]. Such learning technology is aimed at delivering training or educational content quickly, effectively and economically, integrating learning materials, tools, and services into a single solution. Perhaps the most obvious advantage of e-learning is that it overcomes physical distances, with the possibility to learn at any time from any location without having to travel or spend time away from work [7]. Distance learning is important particularly for teaching settings in which faculty expertise varies across sites, and for post-certification further training, catering for

radiologists with limited time and opportunities for travel to teaching centers. Added to this is the possibility of making the course format homogeneous for all participants with a standard format, both in teaching and in learning assessment.

A typical e-learning technology is the asynchronous web-based system (allowing the student access teaching resources at any time of their choosing) which allows great flexibility in timing of participation. Such technology allows rapid access to material suitable for radiological education, allows students to skip information they already know and move on to less familiar issues, and has the capacity to be easily and quickly updated. However, it is a one-way process with no interaction, unlike face-on-face learning.

On the other hand, synchronous learning is based on a real-time education with the simultaneous communication between multiple users. The main advantage of this model is the ability to improve communication and interaction between students and teachers, promoting online collaborative learning and discussions.

In interventional radiology, electronic communication provides great potential for education by disseminating new techniques and procedures and by creation of an opportunity for spreading knowledge about this ever-growing specialty around the globe. Up to now this learning method has not yet been widely used in IR training programs.

At our University a Master in Interventional Radiology course was started in 2017, with the aim of providing interventional postgraduate training to radiologists. The Master is focused on body endovascular interventions. Accredited direct hands-on training is provided on site in the interventional suite. Lectures are provided through webinars with video conferencing software. The purpose of the study was to evaluate the opinion of students about Tele-education in Interventional Radiology.

## MATERIALS AND METHODS

### Master curriculum and training format

At present in Italy the radiology residency program consists of 4 years' training, which includes some participation in interventional radiological procedures. However, it is acknowledged by the Italian Society of Diagnostic and Interventional Radiology (SIRM) that the training in interventional

procedures is not adequate to achieve core interventional skills. Therefore, SIRM has promoted among its members the development of post-graduate academic training courses in interventional radiology, which could integrate with already-existing radiology training programs. Since the 4 year Training program is not enough to provide even a complete interventional radiology training, the Master is foreseen as a complementary training to fulfill the gap caused by this rules. In view of this goal, in September 2016 our University launched the post-graduate Master in Interventional Radiology course. The access to the Master is limited to Board certified radiologists.

The Master course lasts one year, at the end of which all trainees must produce a thesis in order to receive certification of training. The maximum number of course participants is 40, with a minimum of 8.

The core curriculum of the course is divided into 3 e-learning modules:

1. Theory of Interventional Radiology (which includes the basic on "how to perform" the procedure, the clinical indication, the expected outcomes, etc.)
2. Radiation Protection in Interventional Radiology
3. CT and MR planning of interventional procedures

There are also 2 e-learning and Hands-on Training modules:

1. Endovascular interventions (vascular applications excluding Neuro interventions)
2. Interventions in Oncology

The Endovascular interventions module focuses on puncture technique, closure devices and different endovascular procedures such as aortic aneurysm repair, limb revascularization, uro-gynecologic and venous interventions and IR in emergency care.

The Oncology module includes embolization (including chemo- and radio-embolization) and ablation techniques, with a special focus on liver tumours.

Each module is weighted in CME (where 1 CME = 6 hours of training).

E-learning is delivered through 26 CME (156 hours) of teaching via a webinar platform (<https://www.gotomeeting.com/>) during a period of 7 months from November to May.

Each lesson is taught by different trainers from the local University, on one day per week, with a specific program delivered to all participants at the beginning of the course.

The e-learning platform facilitates synchronous training, providing real-time lectures at a defined time-slot (3 hours per day).

Each delegate connects through a PC client to the webinar server. The teacher is able to share the screen of his/her desktop, and interact with the delegates through audio-video tools. Each delegate can interact with the teacher via the same facilities. All lectures are recorded and made available for asynchronous streaming on a dedicated website, with restricted access for the trainees.

The participation of the students at the webinars is verified by checking the time of their entrance to and exit from the chatroom of the webinar.

Each student is asked by the teacher to interact during the webinar, but no tests need be completed at the end of each session. The software allows a 2-ways interaction with the teacher asking the students to participate and answer questions. Frequency and quality of interaction was valued as prove of attendance and understanding of the teaching content.

A moderator (the Master Chair) regularly attends the session in order to regulate the interaction between teachers and students, stimulate questions and answers, and verify attendance.

The Hands-on Training is provided with 7 CME (42 hours), on site, in the Interventional Radiology Unit of the University Hospital.

All physicians in training take part in the daily activity in the Interventional suite for at least one week. During this time they can actively participate in all procedures performed on live patients, not only as observers but also with the opportunity to perform the procedure with support from and teaching by skilled Radiologists.

The Interventional Radiology Unit has 2 fluoroscopy suites; therefore no more than 4 students per week can participate simultaneously and they must agree the timing of their specific week of training with the Master Chair. Beyond this week, additional hands-on training can be provided upon request by the students.

At the end of the course each student produces a thesis on a chosen topic of interventional radiology, that is discussed during a dedicated session of thesis defense.

## Survey among participants

To determine the quality of this training, an online survey among Master course participants was prepared, using open access Google Form software and structured in 12 questions about the student's professional background in IR, personal motivations for participation in the course, and their level of agreement with regard to the impact of e-learning and hands-on training on their clinical practice (Table 1).

The survey was launched through the mailing list of Master course participants and respondents were able to access the online Google form for responses for 1 week.

Students indicated independently their level of agreement with questions about the impact of e-learning and Hands-on Training, using a 5-point Likert scale, as follows:

1. Strongly disagree with the statement;
2. Disagree somewhat with the statement;
3. Undecided;
4. Agree somewhat with the statement;
5. Strongly agree with the statement.

The mean score of the level of agreement was calculated. A mean score of 4 was considered to represent "good" agreement between respondents, a score of 5 "complete" agreement.

**Table 1:** Online Survey to determinate the quality of Training of the IR Master course.

The level of agreement in questions 5 to 11 was indicated using a 5-point scale, as follows: 1, strongly disagree with the statement; 2, disagree somewhat with the statement; 3, undecided; 4, agree somewhat with the statement; 5, strongly agree with the statement.

**QUESTIONNAIRE**

Which is your role in the Imaging Department?	Chair Staff Radiologist
Interventional procedures performed as primary operator before attending the Master course	None Less than 50 50-300 300-1000 More than 1000
Reasons for attending the Master course (more than 1 answer possible)	Personal motivation only (to acquire or improve interventional competences) Personal motivation and need for interventional radiologists in the Imaging Department No specific personal motivation but forced by the need for interventional radiologists in the Imaging Department No opportunity or inadequate interventional training during Radiology Residency Other
Which of the following statements do you agree with regard to the e-learning module of the Master?	It facilitates attendance during lectures It is low-cost since the student does not move to the learning center It facilitates teacher-student interaction Other
The e-learning module of the Master course facilitates attendance during lectures	Score 1 to 5
The e-learning module of the Master course is low-cost, as the student does not move to the learning center	Score 1 to 5
The e-learning module of the Master course facilitates teacher-student interaction	Score 1 to 5
The hands-on training in the Department of Interventional Radiology increased your interventional skills	Score 1 to 5
The Master course has enhanced your job opportunities	Score 1 to 5
The Master course attendance has changed your local interventional practice	Score 1 to 5
In summary, did the Master course fulfil your learning expectations?	Score 1 to 5
Would you suggest that your colleagues should apply for the Master course?	Yes No Maybe

All responses were automatically processed by the form and presented as charts on a Google spreadsheet.

## RESULTS

Sixteen out of 16 (100%) students of the University Master in Interventional Radiology course who had provided their names and affiliation addresses were invited to complete the survey. Not all of 16 answered every question; hence, the number in each table may not total 16 responses.

The attendees came from different Italian regions and only one participant was a local Radiologist. The majority of them (62.5%) work in public non-academic Hospitals, all as Staff Radiologist.

Before attending the Master course, all participants were already members of CIRSE and 80% of them had already performed a substantial number of interventional procedures (>300) as primary operator.

The most common motivation for participating in the Master course was a personal desire to acquire or improve the individual's interventional competence (75% of students); 25% were motivated also by the need for a trained Interventional Radiologist in their Imaging Department. In 12.5% of cases, students attended the Master course because of a belief that the interventional skills acquired during their Radiology Residency were inadequate.

Regarding the e-learning module of the Master course, the majority of participants (68.8%) considered the main advantage to be the capability to facilitate remote lecture attendance; 18.8% chose the low-cost system and 12.5% the facilitation of teacher-student interaction as the principal benefit.

The level of agreement (on a Likert scale) with the statements regarding the e-learning module of the Master course and the Interventional skills and practice is summarised in Table 2. No trainees scored the statements as less than 3 on the 5-point rating scale, indicating that all of them agreed to some extent with all statements, but the level of support differed. In particular, facilitation of off-site attendance of lectures and the low-cost system of the e-learning module of the Master course were scored particularly highly in terms of agreement.

The Master course fulfilled the learning expectations in 81.3% of cases with a good agreement between participants (mean score  $4.25\pm0.775$ ), and 93.8% of participants would recommend the Master course to other colleagues.

## DISCUSSION

Over the years, there has been a worldwide growth in IR post-graduate courses to ensure the provision of more trained IR practitioners with competent knowledge and practical skills. Some of these take the form of one or more years of full-time Fellowship training, working exclusively in IR. Others involve shorter periods of training, with variable opportunities for hands-on work and varying amounts of formal didactic teaching. Accreditation and certification for IR training varies from country to country, with different learning methods and tools used to develop advanced interventional competencies.

In 2001, Rösch [8] stated that tele-education was becoming an essential part of interventional education to help “the growing number of interventionalists around the world to expand and improve standards of their treatment”.

Our post-graduate Master course is the first blended course in Interventional radiology education in which hands-on training with face-to-face time in the Interventional suite is enhanced by online learning. It is designed to offer a feasible middle ground between e-learning (which can teach theory but cannot provide direct training in the manual skills required in IR) and full-time practical IR Fellowship-level training (which cannot be accessed by already-qualified radiologists with existing work commitments, who want to upgrade and expand their skills).

A recent large meta-analysis by the United States Department of Education [9] concluded that blended learning was significantly more effective than fully face-to-face or online courses and is an important emerging mode of instruction in specialist education.

One of the reasons we decided to adopt this type of education method was to promote students' participation with real-time distance learning.

**Table 2.** the mean score of the level of agreement of the statements regarding the e-learning module of the Master and the Interventional skill and practice

Questions	Mean Scores	Std dev
The e-learning module of the Master course facilitates attendance during lectures	<b>4,56</b>	0,629
The e-learning module of the Master is low-cost, as the student does not move to the learning center	<b>4,88</b>	0,342
The e-learning module of the Master course facilitates teacher-student interaction	3,81	1,424
The hands-on training in the Department of Interventional Radiology increased your interventional skills	3,56	1,209
The Master course has enhanced your job opportunities	3,69	1,401
The Master course attendance has changed your local interventional practice	3,4	0,828

All participants were already staff radiologists in their own hospitals at the time of the course, with on-going work commitments. The use of an e-learning method was one way in which course participation by these already-employed radiologists could be facilitated in a timely and cost-effective manner [10, 11].

All participating radiologists could learn from any location without having to travel or spend time away from their base hospital. The majority of course participants considered the main advantage of the course structure to be the capability to facilitate lecture attendance from their home base, followed by the low cost of the course resulting from its e-learning structure.

The deployment of digital imaging networks, teleradiology, and Internet services strongly suggests that e-learning will become an important method of education in radiology, particularly for young physicians and students who are comfortable using these new technologies and require to be easily and quickly updated [7].

However, the tele-education method is not without its disadvantages.

In 2007, Cook [12] analyzed the pros and cons of this new type of learning, pointing out that the main disadvantages are related to social isolation and the de-individualized instructions due to an absence of face-to-face contact between teachers and students. This is particularly true in case of an asynchronous system, which offers flexibility in the timing of participation to the detriment of the direct interaction between teacher and student that is still seen as a necessary component of education.

The platform of our Master course was explicitly designed to overcome these limitations.

Several studies [9, 13–14] report that online instruction cannot completely replace traditional education, while a combination of e-learning and face-to-face lectures is the preferred type of education, at the best convenience of the students.

Our platform provides a synchronous tele-education system in which all participants are connected in real-time, and can interact directly with the academic staff online if they have questions or doubts. Teachers take on the role of facilitators, monitoring and guiding the discussion as needed and providing or helping students to find additional resources, as in a traditional classroom.

All lectures are recorded, facilitating the repetition and temporal spacing required for enduring learning, giving the students the opportunity to learn or revise the subject in their own time and at their own speed.

In our survey, participants rated this type of e-learning module positively with quite good agreement between respondents regarding the benefit of facilitated teacher-student interaction.

However, personal contact between the course participants and teachers is still an important ingredient in the learning situation; online courses are not universally

accepted, with a percentage of students preferring traditional lecture-based courses.

This is a limitation of the tele-education module, which could be overcoming with some modifications.

Not all e-learning approaches are equally efficient, and e-learning success depends also on the provided content. For this reason, teachers must learn the necessary technological skills and teaching strategies to create effective educational online environments and they must prepare proper material to obtain the desired e-learning results [15].

Moreover, personal contact between teachers and students can be provided by hands-on training with face-to-face contact. To ensure this element is provided for, our Master course combines online learning with traditional hands-on training in the Angio suite with the opportunity to watch expert interventionalists in action in their own suites, working with their own teams, and with the possibility to interact with them and participate actively in performance of procedures.

Regarding the hands-on training in the Department of Interventional Radiology, not all participants agreed that it increases their interventional skills. This is probably due to the limited number of hours of the hands-on training module of the Master course at present; this time availability may need to be increased as the course develops, bearing in mind that practical hands-on training is a key component of IR teaching.

Overall, the participants who took part in the survey were highly satisfied with the course and would recommend the Master to other colleagues.

## CONCLUSION

Distance learning represents an educational technique which occupies a significant place in real-life medical teaching, especially in postgraduate and continuing medical education. Our Master course has shown that this type of education can be implemented in the Interventional Radiology scenario, providing an opportunity for spreading knowledge about this ever-growing subspecialty around the globe.

Overall, the study suggests that the blended type of education of our Master course is a feasible contribution to IR training, received high appreciation among participants and could be a model to be followed in the future.

## ADDITIONAL INFORMATION

**Funding source.** This study was not supported by any external sources of funding.

**Competing interests.** The authors declare that they have no competing interests.

**Authors contribution.** All authors made a substantial contribution to the conception of the work, acquisition, analysis, interpretation of data for the work, drafting and revising the work, final approval of the version to be published and agree to be accountable for all aspects of the work.



## REFERENCES

1. Union Européenne des Médecins Spécialistes. Medical Specialties. UEMS; 2009. Accessed 24 Jan 2017. Available from: <https://www.uems.eu/about-us/medical-specialties>.
2. Mahnken AH, Bücker A, Hohl C, Berlis A. White Paper: curriculum in interventional radiology. *Fortschr Röntgenstr.* 2017;189(4):309–311. doi: 10.1055/s-0043-104773
3. Tsetis D, Uberoi R, Fanelli F, et al. The Provision of Interventional Radiology Services in Europe: CIRSE Recommendations. *Cardiovasc Intervent Radiol.* 2016;39(4):500–506. doi: 10.1007/s00270-016-1299-0
4. Lee MJ, Belli AM, Brountzos E, et al. Specialty status for interventional radiology: the time is now. *Cardiovasc Intervent Radiol.* 2014;37(4):862. doi: 10.1007/s00270-014-0903-4
5. Siragusa DA, Cardella JF, Hieb RA, et al. Requirements for Training in Interventional Radiology. *J Vasc Interv Radiol.* 2013;24(11):1609–1612. doi: 10.1016/j.jvir.2013.08.002
6. Xiberta P, Boada I. A new e-learning platform for radiology education (RadEd). *Comput Methods Programs Biomed.* 2016;126:63–75. doi: 10.1016/j.cmpb.2015.12.022
7. Pinto A, Brunese L, Pinto F, et al. E-learning and education in radiology. *Eur J Radiol.* 2011;78(3):368–371. doi: 10.1016/j.ejrad.2010.12.029
8. Rösch J. Tele-education in Interventional Radiology. *Cardio-Vascular and Interventional Radiology.* 2001;24(5):295–296. doi: 10.1007/s00270-001-0020-z
9. U.S. Department of Education. Evaluation of Evidence-Based Practices in online learning: a meta-analysis and review of online learning studies. U.S. Department of Education, Washington DC; 2010. Accessed 3 Jan 2017. Available from: <https://www2.ed.gov/rschstat/eval/tech/evidence-based-practices/finalreport.pdf>
10. Sparacia G, Cannizzaro F, D'Alessandro DM, et al. Initial experiences in radiology e-learning. *Radiographics.* 2007;27(2):573–581. doi: 10.1148/rg.272065077
11. Ruiz JG, Mintzer MJ, Leipzig RM. The impact of e-learning in medical education. *Acad Med.* 2006;81(3):207–212. doi: 10.1097/00001888-200603000-00002
12. Cook DA. Web-based learning: pros, cons and controversies. *Clin Med.* 2007;7(1):37–42. doi: 10.7861/clinmedicine.7-1-37
13. Nkenke E, Vairaktaris E, Bauersachs A, et al. Acceptance of technology-enhanced learning for a theoretical radiological science course: a randomized controlled trial. *BMC Med Educ.* 2012;12:18. doi: 10.1186/1472-6920-12-18
14. Santos GN, Leite AF, Figueiredo PT, et al. Effectiveness of e-learning in oral radiology education: a systematic review. *J Dent Educ.* 2016;80(9):1126–1139.
15. Ellaway R. E-learning: Is the revolution over? *Medical Teacher.* 2011;33(4):297–302. doi: 10.3109/0142159X.2011.550968

## СПИСОК ЛИТЕРАТУРЫ

1. Union Européenne des Médecins Spécialistes. Medical Specialties. UEMS; 2009. Accessed 24 Jan 2017. Available from: <https://www.uems.eu/about-us/medical-specialties>.
2. Mahnken A.H., Bücker A., Hohl C., Berlis A. White Paper: curriculum in interventional radiology // *Fortschr Röntgenstr.* 2017. Vol. 189, N 4. P. 309–311. doi: 10.1055/s-0043-104773
3. Tsetis D., Uberoi R., Fanelli F., et al. The Provision of Interventional Radiology Services in Europe: CIRSE Recommendations // *Cardiovasc Intervent Radiol.* 2016. Vol. 39, N 4. P. 500–506. doi: 10.1007/s00270-016-1299-0
4. Lee M.J., Belli A.M., Brountzos E., et al. Specialty status for interventional radiology: the time is now // *Cardiovasc Intervent Radiol.* 2014. Vol. 37, N 4. P. 862. doi: 10.1007/s00270-014-0903-4
5. Siragusa D.A., Cardella J.F., Hieb R.A., et al. Requirements for Training in Interventional Radiology // *J Vasc Interv Radiol.* 2013. Vol. 24, N 11. P. 1609–1612. doi: 10.1016/j.jvir.2013.08.002
6. Xiberta P., Boada I. A new e-learning platform for radiology education (RadEd) // *Comput Methods Programs Biomed.* 2016. Vol. 126. P. 63–75. doi: 10.1016/j.cmpb.2015.12.022
7. Pinto A., Brunese L., Pinto F., et al. E-learning and education in radiology // *Eur J Radiol.* 2011. Vol. 78, N 3. P. 368–371. doi: 10.1016/j.ejrad.2010.12.029
8. Rösch J. Tele-education in Interventional Radiology // *Cardio-Vascular and Interventional Radiology.* 2001. Vol. 24, N 5. P. 295–296. doi: 10.1007/s00270-001-0020-z
9. U.S. Department of Education. Evaluation of Evidence-Based Practices in online learning: a meta-analysis and review of online learning studies. U.S. Department of Education, Washington DC; 2010. Accessed 3 Jan 2017. Available from: <https://www2.ed.gov/rschstat/eval/tech/evidence-based-practices/finalreport.pdf>
10. Sparacia G., Cannizzaro F., D'Alessandro D.M., et al. Initial experiences in radiology e-learning // *Radiographics.* 2007. Vol. 27, N 2. P. 573–581. doi: 10.1148/rg.272065077
11. Ruiz J.G., Mintzer M.J., Leipzig R.M. The impact of e-learning in medical education // *Acad Med.* 2006. Vol. 81, N 3. P. 207–212. doi: 10.1097/00001888-200603000-00002
12. Cook D.A. Web-based learning: pros, cons and controversies // *Clinical Medicine.* 2007. Vol. 7, N 1. P. 37–42. doi: 10.7861/clinmedicine.7-1-37
13. Nkenke E., Vairaktaris E., Bauersachs A., et al. Acceptance of technology-enhanced learning for a theoretical radiological science course: a randomized controlled trial // *BMC Med Educ.* 2012. Vol. 12. P. 18. doi: 10.1186/1472-6920-12-18
14. Santos G.N., Leite A.F., Figueiredo P.T., et al. Effectiveness of e-learning in oral radiology education: a systematic review // *J Dent Educ.* 2016. Vol. 80, N 9. P. 1126–1139.
15. Ellaway R. E-learning: Is the revolution over? *Medical Teacher.* 2011. Vol. 33, N 4. P. 297–302. doi: 10.3109/0142159X.2011.550968

## AUTHORS' INFO

**Emanuele Neri**, MD, Dr. Sci. (Med), Associate Professor; address: Lungarno Pacinotti, 43, 56126, Pisa, PI, Italy; e-mail: [emanuele.neri@med.unipi.it](mailto:emanuele.neri@med.unipi.it); ORCID: <https://orcid.org/0000-0001-7950-4559>

**Laura Crocetti**, MD, Associate professor; e-mail: [laura.crocetti@med.unipi.it](mailto:laura.crocetti@med.unipi.it); ORCID: <https://orcid.org/0000-0002-8160-0483>

**Giulia Lorenzoni**, PhD Student; e-mail: [giulia.lorenzoni@unipd.it](mailto:giulia.lorenzoni@unipd.it); ORCID: <https://orcid.org/0000-0003-1771-4686>

**Roberto Cioni**, MD; e-mail: [c.cioni@ao-pisa.toscana.it](mailto:c.cioni@ao-pisa.toscana.it); ORCID: <https://orcid.org/0000-0001-9425-0286>

**Adrian P. Brady**, MD, Clinical Senior Lecturer; e-mail: [adrianbrady@me.com](mailto:adrianbrady@me.com); ORCID: <https://orcid.org/0000-0003-3473-0282>

**Davide Caramella**, MD, Professor; e-mail: [davide.caramella@unipi.it](mailto:davide.caramella@unipi.it); ORCID: <https://orcid.org/0000-0002-9951-2916>

DOI: <https://doi.org/10.17816/DD60040>

# How does artificial intelligence effect on the assessment of lung damage in COVID-19 on chest CT scan?

© Sergey P. Morozov, Valeria Yu. Chernina, Anna E. Andreychenko, Anton V. Vladzimirskiy, Olesya A. Mokienko, Victor A. Gomboleviskiy

Moscow Center for Diagnostics and Telemedicine, Moscow, Russian Federation

**BACKGROUND:** During the pandemic, computed tomography (CT) was one of the most important tools for assessing COVID-19-related lung changes. In COVID-19 patients, radiologists in Moscow used the adapted CT0-4 scale to visually assess the dependence of the severity of the general condition on the nature and severity of radiological signs of changes in the lungs based on computed tomography. In a large stream of scans, the doctor may miss findings and make errors in assessing the volume of lung damage, so the use of AI services in outpatient healthcare during a pandemic can be beneficial.

**AIM:** The goal of this study is to compare the distribution of CT0-4 categories designed by radiologists with the results of AI services processing and categories formed without AI services.

**METHODS:** We used retrospective study design, full study protocol is registered on ClinicalTrials.gov (NCT04489992). The results of primary CT scans with the CT0-4 categories were analyzed in outpatient medical institutions of the Health Department from April 08, 2020, to December 01, 2020, and separately for November (from November 01, 2020, to December 01, 2020). CT was performed on 48 computed tomographs in accordance with standard protocols, and the data was processed by the single radiology information systems. CTs in the test group received AI services, while CTs in the control group did not. The analysis includes five AI services: RADLogics COVID-19 (RADLogics, USA), COVID-IRA (IRA labs, Russia), Care Mentor AI, COVID (Care Mentor AI, Russia), Third Opinion. CT-COVID-19 (Third Opinion, Russia), and COVID-MULTIVOX (Gammamed, Russia). Moreover, AI services are encoded at random.

**RESULTS:** The CT scan results of 260,594 patients were examined (m/f % = 44/56, mean age = 49.5). The test group consisted of 115,618 CT scans, while the control group consisted of 144,976 CT scans. Depending on the specific AI service, CT0 was established by 2.3–18.5% less than the control group for different subgroups of categories. The categories CT3-4 were established by 4.7–27.6% less than without AI, and the categories CT4 by 40–60% less than without AI ( $p < 0.0001$ ). For November (from November 01, 2020, to December 01, 2020), the CT scan results of 41,386 patients were analyzed (m/f % = 44/56, average age = 53.2 years). The test group consisted of 28,881 CT scans, while the control group included 12,505 CT scans. Depending on the specific AI service, CT0 was established by 1–2.6% less than the control group for different subgroups of categories. Further, the categories CT3–CT4 were established by 0.2–15.7% less than without AI, and the categories CT4 were established by 25% less than without AI ( $p = 0.001$ ).

**CONCLUSION:** The use of AI services for primary CT scans on an outpatient basis reduces the number of CT0 and CT3–CT4 results, which can influence the therapeutic approach for COVID-19 patients.

**Keywords:** COVID-19; community-acquired pneumonia; computed tomography; artificial intelligence.

## To cite this article

Morozov SP, Chernina VYu, Andreychenko AE, Vladzimirskiy AV, Mokienko OA, Gomboleviskiy VA. How does artificial intelligence effect on the assessment of lung damage in COVID-19 on chest CT scan? *Digital Diagnostics*. 2020;2(1):27–38. DOI: <https://doi.org/10.17816/DD60040>

DOI: <https://doi.org/10.17816/DD60040>

# Как искусственный интеллект влияет на оценку поражения лёгких при COVID-19 по данным КТ грудной клетки?

© С.П. Морозов, В.Ю. Чернина, А.Е. Андрейченко, А.В. Владзимирский,  
О.А. Мокиенко, В.А. Гомболевский

Научно-практический клинический центр диагностики и телемедицинских технологий Департамента здравоохранения города Москвы, Москва, Российская Федерация

**Обоснование.** В период пандемии компьютерная томография (КТ) является одним из ключевых инструментов оценки изменений в лёгких, связанных с COVID-19. Рентгенологи Москвы используют адаптированную шкалу КТ 0–4 для визуальной оценки зависимости тяжести общего состояния от характера и выраженности рентгенологических признаков изменений в лёгких при COVID-19 по данным КТ. В большом потоке исследований врач может пропустить находку и ошибиться в оценке объёма поражения лёгких, поэтому применение сервисов искусственного интеллекта (ИИ) обосновано в амбулаторном здравоохранении в период пандемии.

**Цель** — сравнить распределение категорий КТ 0–4 в заключениях, сформированных рентгенологами с использованием ИИ-сервисов и без них.

**Материал и методы.** Ретроспективное исследование, протокол исследования зарегистрирован в ClinicalTrials.gov (NCT04489992). Проанализированы результаты первичных КТ с категориями КТ 0–4 в период с 08.04.2020 по 01.12.2020 и отдельно за ноябрь 2020 года (с 01.11.2020 по 01.12.2020) в амбулаторных медицинских организациях Департамента здравоохранения. КТ проводились на 48 компьютерных томографах по стандартным протоколам, результаты обрабатывались через Единый радиологический информационный сервис. В тестовую группу включены КТ, обработанные ИИ-сервисами, в контрольную — без обработки ИИ. В анализ включены 5 ИИ-сервисов: RADlogics COVID-19 (RADLogics, США); COVID-IRA (IRA labs, Россия); Care Mentor AI, COVID (CareMentor AI, Россия); Третье Мнение. КТ-COVID-19 (Третье мнение, Россия); COVID-MULTIVOX (Гаммамед, Россия). ИИ-сервисы кодированы случайным образом.

**Результаты.** Проанализированы результаты КТ 260 594 пациентов (соотношение мужчины/женщины — 44/56%, средний возраст 49,5 года). В тестовую группу включены 115 618 КТ, в контрольную — 144 976. В зависимости от конкретного ИИ-сервиса для разных подгрупп категорий КТ-0 выставлено от 2,3 до 18,5% меньше, категорий КТ 3–4 — от 4,7 до 27,6% меньше, КТ-4 — от 40 до 60% меньше, чем в контрольной группе ( $p < 0,0001$ ). За ноябрь (с 01.11.2020 по 01.12.2020) проанализированы результаты КТ 41 386 пациентов (соотношение мужчины/женщины — 44/56%, средний возраст 53,2 года). В тестовую группу включено 28 881 КТ, в контрольную — 12 505. В зависимости от конкретного ИИ-сервиса для разных подгрупп категорий КТ-0, КТ 3–4 и КТ-4 выставлено соответственно от 1 до 2,6, от 0,2 до 15,7 и на 25% меньше, чем в контрольной группе ( $p = 0,001$ ).

**Заключение.** Применение ИИ-сервисов для первичных КТ в амбулаторных условиях приводит к уменьшению количества выставляемых категорий КТ-0 и КТ 3–4, способных влиять на тактику ведения пациентов с COVID-19.

**Ключевые слова:** COVID-19; внебольничная пневмония; компьютерная томография; искусственный интеллект.

## Как цитировать

Морозов С.П., Чернина В.Ю., Андрейченко А.Е., Владзимирский А.В., Мокиенко О.А., Гомболевский В.А. Как искусственный интеллект влияет на оценку поражения лёгких при COVID-19 по данным КТ грудной клетки? // *Digital Diagnostics*. 2021. Т. 2, №1. С. 27–38. DOI: <https://doi.org/10.17816/DD60040>

DOI: <https://doi.org/10.17816/DD60040>

# 人工智能如何影响胸部CT扫描对COVID-19中肺损伤的评估？

© Sergey P. Morozov, Valeria Yu. Chernina, Anna E. Andreychenko,  
Anton V. Vladzimirsky, Olesya A. Mokienko, Victor A. Gombolevskiy

Moscow Center for Diagnostics and Telemedicine, Moscow, Russian Federation

**理由：**在大流行期间，计算机断层扫描（CT）是评估与COVID-19相关的肺部变化的主要工具之一。莫斯科的放射学家使用了经过调整的KT0-4量表，根据计算机断层扫描技术，通过视觉评估了一般病情严重程度对COVID-19中肺部改变的放射学征象的性质和严重程度的依赖性。大量的研究中，医生可能会遗漏发现结果并在评估肺损伤量方面犯错误，因此在大流行期间，在门诊医疗中使用AI服务可能很有用。

**目的：**比较放射科医生形成的CT0-4类别的分布与AI服务处理的结果以及没有AI服务形成的类别的比较。

**方法：**回顾性研究，ClinicalTrials.gov (NCT04489992)。DZM的门诊医疗组织中，分析了从CT0-4类别进行的一次CT扫描的结果，分析时间为：2020年4月8日至2020年1月12日，以及11月（2020年11月1日至2020年1月12日）。根据标准协议在48台计算机断层扫描仪上执行CT，并通过ERIS处理。测试组包括由AI服务处理的CT，对照组为不包含AI的CT。分析包括5种AI服务：RADlogics COVID-19（美国RADLogics），COVID-IRA（俄罗斯的IRA实验室），Care Mentor AI，COVID（俄罗斯的CareMentor AI），第三意见。CT-COVID-19英寸（第三意见，俄罗斯），COVID-MULTIVOX（俄罗斯伽马迈德）。AI服务是随机编码的。

**结果：**分析了260594例患者的CT扫描结果（m / f% = 44/56，平均年龄-49.5）。测试组包括115,618次CT扫描，对照组-144976。根据特定的AI服务，对于CT-0类别的不同子组，其设置比对照组少2.3%至18.5%。与未使用AI相比，将CT3-4类别设置为比不使用AI少4.7%至27.6%，并且将CT-4类别与不使用AI设置成从40%至60%（p < 0.0001）。

对于11月（从01.11.2020到01.12.2020），分析了41386名患者的CT扫描结果（m / f% = 44/56，平均年龄-53.2岁）。测试组包括28881 CT扫描，对照组-12505。根据特定的AI服务，对于CT-0类别的不同子组，其设置比对照组小1%至2.6%。显示的CT3-4类别比没有使用AI的类别多出0.2%至15.7%；类别CT-4设置为比不使用AI时少25%（p = 0.001）。

**结论：**在门诊基础上将AI服务用于主要CT扫描会导致CT-0和CT3-4数量减少，从而影响管理COVID-19患者的策略。

**关键词：**COVID-19；社区获得性肺炎；CT扫描；人工智能。

## 引用本文：

Morozov SP, Chernina VYu, Andreychenko AE, Vladzimirsky AV, Mokienko OA, Gombolevskiy VA. 人工智能如何影响胸部CT扫描对COVID-19中肺损伤的评估? *Digital Diagnostics*. 2020;2(1):27-38. DOI: <https://doi.org/10.17816/DD60040>

收到: 04.02.2021

接受: 06.04.2021

发布时间: 09.04.2021



## Acronyms and abbreviations

**data set:** a set of data, a collection of logical records

**URIS:** Unified Radiological Information System

**AI service:** artificial intelligence software

**CT:** computed tomography

CT (computed tomography) 0–4 represents an empirical scale for visual assessment on the severity dependence of general condition of the nature and pronouncement of radiological changes in the lungs with Coronavirus disease 2019 (COVID-19) according to CT, where CT-0 implies the absence of signs of viral pneumonia; CT-1 indicates mild pneumonia with ground glass opacity areas,

with <25% severity of pathological changes; CT-2 is moderate pneumonia, with affection of 25%–50% of the lungs; CT-3 implies moderate pneumonia with 50%–75% of the lungs affected; and CT-4 is severe pneumonia, affecting >75% of the lungs.

**Digital Imaging and Communications in Medicine:** Structured Reporting is a standardized format of the medical industry standard for creating, storing, transferring, and visualizing digital medical images and documents of patients examined (structured reporting).

## BACKGROUND

In 2020, the Coronavirus disease 2019 (COVID-19) pandemic challenged healthcare systems worldwide, which prompted global governments to seek new solutions under resource-constrained conditions. On August 27, 2020, the government commission on digital development of the Russian Federation approved the certificate of the federal project “Artificial Intelligence” within the national program “Digital Economy”. Regardless of this, back in 2019, a Decree of the Moscow Government was drafted, followed by an Order of the Moscow Healthcare Department at the beginning of 2020 on conducting an experiment on the use of innovative technologies in the field of computer vision for the analysis of medical images and further application in the health care system of Moscow (Experiment) [1].

In the pandemic, computed tomography (CT) is used as a key tool for assessing changes in the lungs, associated with infection [2]. In the first months of the COVID-19 pandemic, semi-quantitative scales were mainly used to assess the severity of changes, with an insignificant frequency in routine clinical work [3–7]. Work with scales, which were based on severe acute respiratory syndrome viral pneumonia studies results, involves a separate calculation of the volume and type of lesions for lobes and segments of the lungs with subsequent summation of results [8]. A visual assessment was proposed based on the approximate volume determination of indurated tissue in both lungs without separate calculations for segments and lobes [9].

Radiologists in Moscow used the adapted CT 0–4 scale to assess visually the severity dependence of the general condition on the nature and pronouncement of radiological changes in the lungs with COVID-19 according to CT data. The percentage of damage was assessed separately for each lung, and the degree of change was assessed for the lung with the greatest lesion (regardless of postoperative changes). Every 25% of the volume of lung lesions increases the scale by one category [10, 11]. The proposed method of visual assessment CT 0–4 was validated by predicting lethal

outcomes in patients with COVID-19 [12]. The risk of lethal outcome increases by an average of 38% (95% confidence interval 17.1–62.6) with the transition from one CT 0–4 category to the next [12].

In case of a large stream of studies, the doctor may omit findings and make mistakes in assessing lung damage volume [13].

A task has been added to the experiment to process chest CT data for COVID-19 diagnostics using artificial intelligence software (AI services). The AI services added CT series with lung lesion segmentation, lesion volume information for each lung, and a CT 0–4 category.

This study aimed to compare the distribution of CT 0–4 categories in reports generated by radiographers with and without AI services.

## METHODS

### Study design

This is a retrospective study based on a study registered in Clinical Trials (NCT04489992). Data analyzed in the course of the work was provided by experts of the Moscow Information Technology Department.

### Compliance criteria

Inclusion and exclusion criteria were used to form the CT study group.

#### *Inclusion criteria:*

- CT scans of the chest organs of male and female patient who sought medical help with suspected COVID-19;
- age of patients over 18 years old;
- CT examinations of the chest organs were performed and interpreted by radiologists in the period from April 8, 2020 to December 1, 2020 in outpatient healthcare organizations;



- availability of information on the assessment category by CT 0–4 in protocols of medical reports of radiologists;
- CT description protocols were formed in the Unified Radiological Information System (URIS).

#### Exclusion criteria:

- CT studies with conclusion of other changes not associated with viral pneumonia.

### Implementation conditions

CT examinations were conducted in all medical organizations subordinate to the Moscow Healthcare Department, providing outpatient care for the adult population. During the pandemic, outpatient medical organizations were transformed into outpatient CT centers that provided a special round-the-clock operation. Taking into account the epidemiological situation, it can be assumed that the gender and age distribution of patients who underwent CT scan corresponds to the same distribution in Moscow.

### Study duration

The study was conducted in the period from April 8, 2020 to December 1, 2020. Additionally, an assessment was performed in November 2020 (from November 1, 2020 to December 1, 2020) (Fig. 1).

### Description of the medical intervention

Over the entire period under consideration and separately for November 2020, the test and control comparison groups were formed (Fig. 2). The test group included CTs processed by AI services, and the control group included CTs without AI processing.

Each algorithm was tested on a specially prepared calibration data set before including the AI service in the experiment. The calibration data set included CT scans of patients with laboratory-verified COVID-19 and an assessment by expert doctors. The criterion for inclusion of an AI service in the URIS was the algorithm accuracy not less than the area under the ROC curve (ROC AUC) of 0.81, according to the guidelines for clinical trials of software based on intelligent technologies [14].

Each AI service added a new series of AI-processed CT scans and information in Digital Imaging and Communications in Medicine: Structured Reporting (DICOM SR) format of the study. The additional CT series is based on the original CT series of the current study, with original image supplemented with the segmentation of lung lesions that are caused by COVID-19 according to the AI assumption. The AI developers participating in the experiment were advised to supplement the CT series sent by the AI service with summary information on lung damage and a CT 0–4 score. The DICOM SR data, available to each radiologist in the test group during the formation of the conclusion, contained information about a specific AI service, instructions for using the processing results, and automatically generated report including the severity assessment according to the CT 0–4 scale (Fig. 2).

CT examinations were performed on 48 computed tomographs (Toshiba Aquilion 64, Canon Medical Systems, Japan; HiSpeed GE, USA; Optima CT 660, GE, USA; Somatom Emotion 16, Siemens, Germany; Somatom Sensation 40, Siemens, Germany) according to standard chest scanning protocols recommended by manufacturers.

The comparison was conducted between categories on the CT 0–4 scale from the conclusions of radiologists who had access to AI service results and those who did not have such access.

### Main study outcome

AI services were included in the experiment after passing qualitative and quantitative tests on databases prepared by experts of the Scientific and Practical Clinical Center for Diagnostics and Telemedicine Technologies of the Moscow Healthcare Department. Research has been distributed randomly based on the computational capabilities of developers since the inclusion of five AI services. One study could be processed by several AI services. AI results were used only for research purposes, and the radiologist made the final decision on the category on the CT 0–4 scale.

### Subgroup analysis

The test group included subgroups since the experiment involved various AI services to diagnose changes in the lungs with COVID-19 according to CT data.

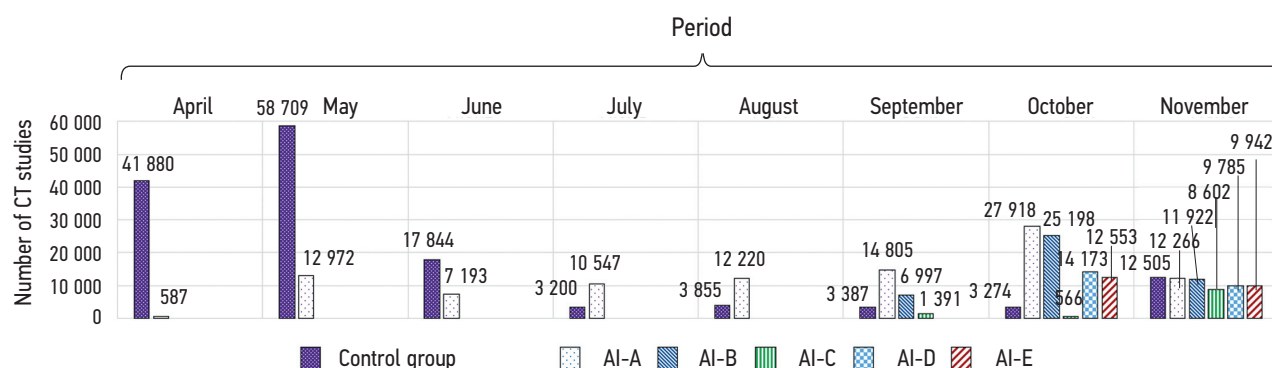
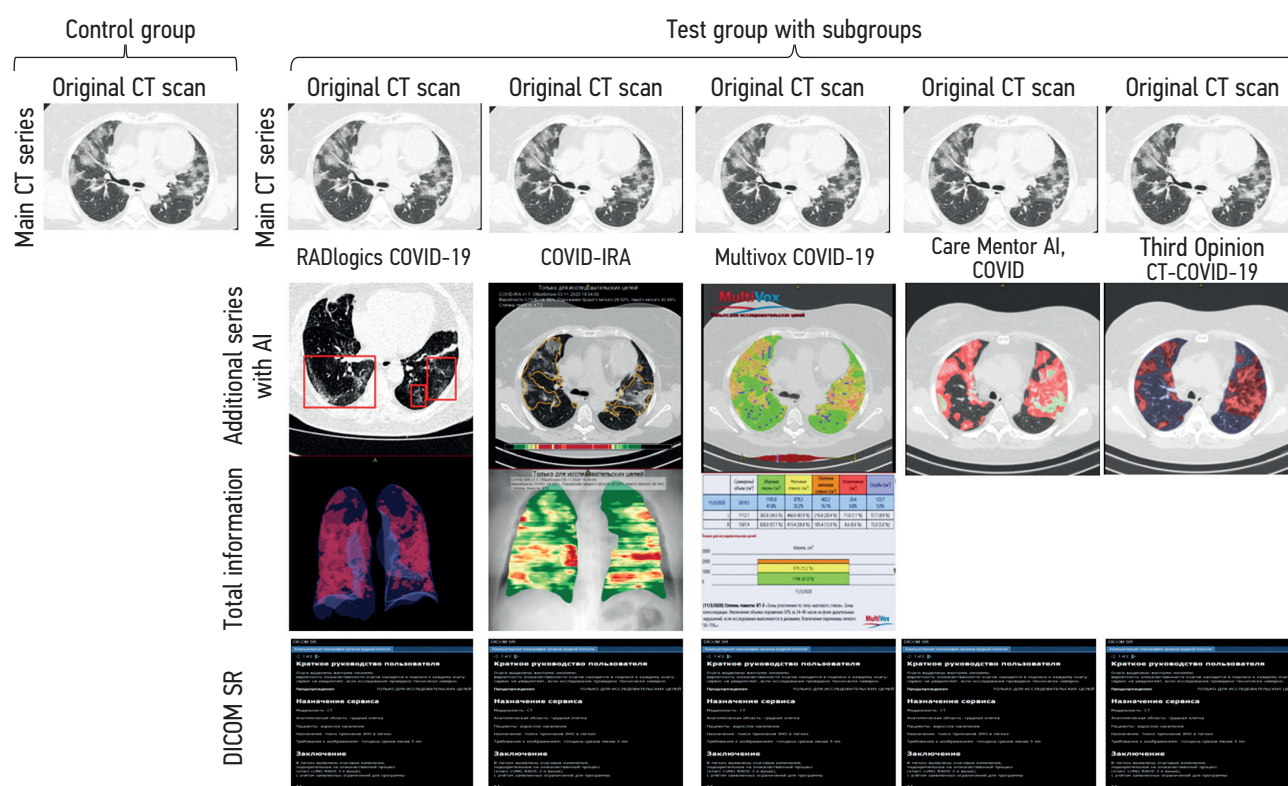


Fig. 1. Chronology of the use of AI services for COVID-19 diagnosis according to computed tomography of the thoracic organs (CT TO).



**Fig. 2.** Examples of original (control group) and additional CT series from various AI services (test group with subgroups) with demonstration of automatic image processing for segmentation of lung lesions in COVID-19, as well as summary information on lung damage and DICOM SR information.

The experiment involved 7 different AI services for diagnosing COVID-19, namely RADlogics COVID-19 (RADLogics, USA), COVID-IRA (IRA labs, Russia), Care Mentor AI, COVID (CareMertor AI, Russia), Third Opinion CT-COVID-19 (Third Opinion, Russia), Multivox COVID19 (Gammamed, Russia), IRYM (Russia), and CVL (CVisionLab, Russia); however, the last two were not included in the test subgroups due to the small number of processed studies over the entire study period. The remaining 5 AI services were randomly coded: AI-A, AI-B, AI-C, AI-D, and AI-E (Fig. 2).

## Ethical considerations

Approval of the Independent Ethics Committee of the Moscow Regional Branch of the Russian Society of Roentgenologists and Radiologists was obtained (Protocol No. 2 [1-II-2020] dated February 20, 2020).

## Statistical analysis

*Principles for calculating the sample size:* all those having valid data were included in the statistical analysis. Methods for restoration of missing data were not applied.

*Methods for statistical data analysis:* descriptive statistics methods were used to present results, indicating the absolute number ( $n$ ) and proportion (%) of cases in each category. Intergroup comparison of the frequency distribution in different categories between the control group and the test subgroups within each of the 2 periods was performed using the Pearson's chi-squared test ( $\chi^2$ ). The level of statistical

significance was considered as a value of 0.05. Statistical analysis was performed using the Stata 14 software.

## RESULTS

### Participants of the study

During the entire period, results of primary CT studies of 260,594 patients were analyzed (male/female ratio was 44%/56%, aged from 18 to 100 years, [average age 49.5 years]), performed and interpreted in the period from April 8, 2020 to December 1, 2020 in outpatient medical organizations in Moscow, repurposed for the pandemic period into outpatient CT centers.

### Main results of the study

The test group included 115,618 CT studies (44.4% of the total sample), and the control group included 144,976 CT studies (55.6%). The ratio of studies in the control and test groups was similar. Distribution by subgroups in the test group was as follows: 98,953 studies (37.9% of the total sample) were for AI-A, 44,194 (17%) for AI-B, 24,067 (9.2%) for AI-C, 22,679 (8.7%) for AI-D, and 10,645 (4.1%) for AI-E.

For different subgroups with AI services, 2.3%–18.5% fewer CT-0 categories were found (no COVID-19 lesions were detected) compared to the control group, and 4.7%–27.6% fewer CT 3–4 categories was found in different subgroups with AI services than in the control group.

In addition, 40%–60% fewer CT-4 categories were found in different subgroups with AI services than without AI (Fig. 3;  $p < 0.0001$ ).

In November 2020, results of primary CT scans of 41,386 patients were analyzed (male/female ratio was 44%/56%, aged from 18 to 100 years, with the average age of 53.2 years), performed and interpreted in the period from November 1, 2020 to December 1, 2020 in outpatient medical organizations in Moscow, repurposed for the period of the pandemic into outpatient CT centers.

The test group included 28,881 CT scans (69.8% of the total sample in November), and the control group included 12,505 CT scans (30.2%). Distribution by subgroups in the test group was as follows: 12,266 studies (29.6% of the total sample in November) were for AI-A, 11,922 (28.8%) for AI-B, 9,785 (23.6%) for AI-C, 9,942 (24%) for AI-D, and 8,602 (20.8%) for AI-E.

In different subgroups with AI services, 1%–2.6% fewer CT-0 (no COVID-19 lesions were detected), 0.2%–15.7% more CT 3–4, and 25% fewer CT-4 categories were found compared to the control group (Fig. 4;  $p = 0.0010$ ).

For the period of November 2020, statistically significant differences were revealed only for CT-0, whereas no differences were found for the rest of the categories. However, a minimal statistically significant difference was found in CT-0 (18.6% vs. 17.0%). By the general monitoring period, on the contrary, all categories were statistically significantly different between data “without AI” and “total for all AIs”. The critical  $\chi^2$  value was 4. For the total period, all CT 0–4 categories made a significant contribution to the differences. The minimum  $\chi^2$  value was 26.2 for CT-3 ( $p < 0.0001$ ).

## DISCUSSION

### Summary of the main result of the study

Study results revealed a change between the CT 0–4 scale categories generated by radiologists in the presence of results from processing by AI services and categories formed without the use of AI services.

### Discussion of the main result of the study

In general, prior to the COVID-19 pandemic, AI services were used to reveal radiological symptoms to detect diseases, classify and improve images, reduce radiation exposure, and improve the workflow [15].

Medical research makes AI applications more understandable, safer, more efficient, and more integrated into medical workflows [16]. It should be understood that validation of the AI algorithm should include not only a retrospective analysis of accuracy compared to the golden standard, but also a randomized clinical trial to assess the influence of AI on the decision making by healthcare professionals [17]. For example, in a randomized clinical study HYPE, the effect of the machine learning-based early diagnostics system of intraoperative hypotension was demonstrated, so in the intervention group, the median time of hypotension was 8.0 min versus 32.7 min in the control group ( $p < 0.001$ ), and the number of lethal outcomes in the intervention group was 0 versus 2 in the control group [18]. In another major study using AI to analyze chest X-rays in COVID-19, 20% of surveyed doctors reported that the algorithm influenced clinical decision making [19].

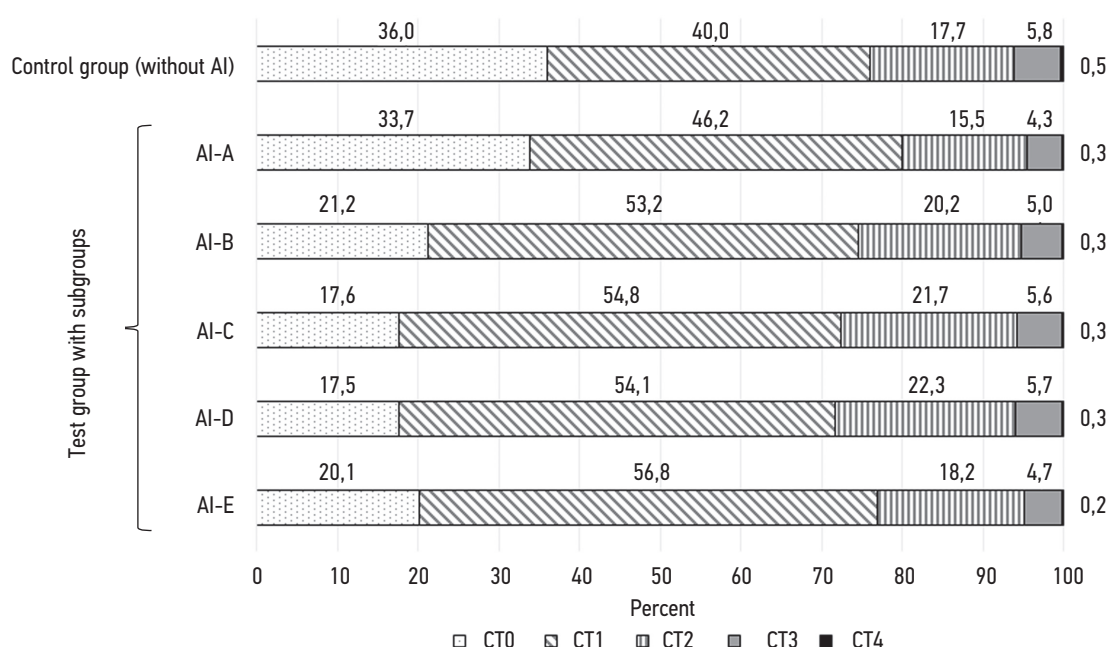


**Fig. 3.** Results of comparison of primary chest CT scans performed in outpatient CT centers in terms of the severity of CT 0–4 categories between the control group and test subgroups for the entire period (April 8, 2020–December 1, 2020).  $n=260\,594$ ;  $p < 0.0001$ .



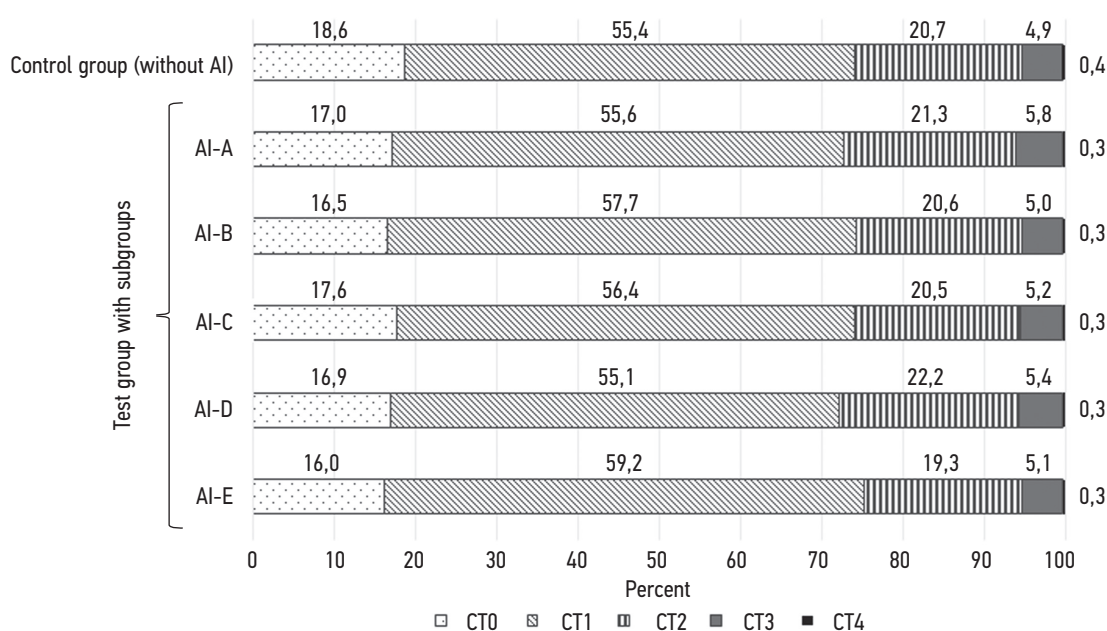


**Fig. 4.** Results of comparison of primary chest CT scans performed in outpatient CT centers, according to the severity of the CT 0–4 categories between the control group and test subgroups for November 2020.

$n=41\ 386$ ;  $p=0,0010$ .

Available literature provides no similar studies assessing the effect of AI results on the final decision making by radiologists when diagnosing lung changes with suspected COVID-19 based on chest CT data.

AI for COVID-19 has two tasks, namely detection and classification. The detection task is determined by the difference between CT-0 and all other categories. The classification task consists of identifying differences between different CT categories (CT1–CT4), i.e., different volumes of damage to the pulmonary parenchyma.

The finding 1 was the difference in the proportion of the CT-0 category between all subgroups. In the case of AI service A, the radiologist was shown only a part of the slices with changes characteristic of COVID-19, while all other AI services had equal number of slices as in the original CT series. Opinions of doctors without AI-A were close to those of the control group.

The finding 2 was the difference in the proportion of CT 3–4 categories between all subgroups. Probably, with a large amount of lung lesions, the empirical visual estimation of the radiologist may exaggerate the extent of the lesion. This overdiagnosis is compensated for when the radiologist monitors the segmentation of lung injuries, performed with the use of AI. This increases the degree of confidence in the automatic calculation of volume and category according to the CT 0–4 scale. Since a lung injury threshold of >50% (CT 3–4 categories) was used as justification for hospitalization, this, combined with clinical and laboratory findings, may reduce the number of hospitalizations.

Based on publications by S.P. Morozov et al. on prediction of lethal outcomes in COVID-19 according to chest CT, when transfer from one CT category to the next, the risk increased by an average of 38% (95% confidence interval

17.1–62.6), and in an additional study among patients with laboratory-verified COVID-19, the risk of lethal outcome with the CT-4 category was 3 times higher than with CT-0 [12, 20]. Our study has demonstrated a fewer CT-4 categories in the test subgroup than in the control one. Previous studies have revealed that CT-4 assessment of the degree of lung damage is associated with lethal outcomes in COVID-19 more than all other categories (CT 0–3) [12, 20]. Thus, the change in the number of patients with CT-4 categories is essential for the formation of calculators of mortality risks for patients with COVID-19.

Due to the pandemic, the simultaneous launch of all AI services was recognized to be limiting the potential benefits of using AI, since all developers would have to be expected to participate in the experiment. Therefore, throughout 2020, unevenness of different AI services in joining the experiment was reported. An analysis was performed for November obtained additional results when the number of CT studies in the control group and each test subgroup was comparable to each other.

According to the authors, the difference revealed between results of periods 1 and 2 is associated with several factors as follows:

- 1) different number of AI services;
- 2) technical factor, as until 2020, the AI services participating in the experiment did not have the opportunity to train their algorithms for assessing and diagnosing lung damage to diagnose COVID-19, therefore, during the experiment, the possibility of changing the AI based software version in order to improve the quality of algorithms and potentially more benefits was recognized justified;
- 3) the human factor, as until 2020, doctors did not use the assessment of the chest CT according to the CT 0–4

scale, which presents a certain difficulty in terms of assessing the volume of multiple lesions in the lungs. It should be noted that doctors could independently improve their skills in assessing the volume of lung lesions in COVID-19, since they evaluated a significant number of CT studies during the pandemic. In addition, doctors could gain experience by checking the markup performed by the AI service, which could lead to an improvement in the skill in more correct assessment of the lesion amount.

In URIS, the radiologist has the opportunity to leave feedback on the work of the AI service in a special feedback field. The study prospect is the comparison of distribution of categories on the CT 0–4 scale among radiologists who have not encountered AI services during the pandemic and use the results of AI services based on their feedback.

## Research limitations

Our research has a number of limitations. It did not include patients with positive results of the polymerase chain reaction test for COVID-19 verification, since results of these studies were after the CT scan. The study was not randomized. The extent of agreement of radiologists with the results of AI services was not assessed. In the test group, some of the CT scans were analyzed by several AI services. AI services were not registered as medical devices. Over the course of the pandemic, AI services were changed as the quality of CT processing improved, and this fact was not further evaluated in this study. The adaptation of radiologists to the use of the CT 0–4 scale was not taken into account.

URIS, where doctors formed medical reports, provides a special field for feedback on the work of AI services. However, at the time of the publication formation, results of feedback from doctors were being processed; therefore, it cannot be presented in the current study.

## CONCLUSION

Results reveal that the use of AI services for primary chest CT scans in outpatient settings leads to a decrease in

the number of CT-0 and CT 3–4 categories, which can influence the management of patients with COVID-19.

Additional research is required to assess whether reducing the choice of the above categories is appropriate for patient management, and how change in routing further affects recovery and mortality rates.

## ADDITIONAL INFORMATION

**Funding source.** The study had no sponsorship.

**Competing interests.** The authors declare that they have no competing interests.

**Author contribution.** The authors confirm that they meet the ICMJE international criteria for authorship (have read and approved the final version before publication). The largest contributions are distributed as follows: S.P. Morozov — research concept; V.Yu. Chernina — search for publications on the topic of the article, writing the text of the manuscript; A.E. Andreychenko — data set formation, editing the manuscript text; A.V. Vladzimirsky — editing the manuscript text; O.A. Mokienko — expert information evaluation, editing the manuscript text; V.A. Gombolevskiy — research concept, expert information evaluation, writing the manuscript text, approval of the final manuscript version.

**Acknowledgements:** The authors would like to express their gratitude to the teams of radiology departments of medical organizations of the Department of Healthcare of Moscow. The authors would like to thank the teams of the Department of Information Technology of the City of Moscow and Laval LLC for their concerted efforts in implementing artificial intelligence in practical healthcare at the level of a large metropolitan city. In addition, the authors thank separately the developers of Binomics ray, RADLogics, IRA labs, CareMentor AI, Third Opinion and Gammamed. Each of the contributors made important research efforts during a difficult time of the epidemic. The authors thank separately O.V. Omelyanskaya, E.G. Bakhteeva, I.A. Vinogradova, S.O. Ermolaev, L.G. Rodionova, K.V. Khripunova, K.M. Arzamasov, P.A. Nikolaev, S.F. Chetverikov, I.A. Blokhin, for administrative, pedagogical, and test work in preparing and implementing the Experiment; special thanks to V.G. Klyashtorny for statistical analysis.

## REFERENCES

1. Experiment on the use of innovative computer vision technologies for medical image analysis and subsequent applicability in the healthcare system of Moscow [cited 2021 Feb 04]. (In Russ). Available from: <https://mosmed.ai>
2. Morozov SP, Ledikhova NV, Panina EV, et al. Re: Controversy in coronaViral Imaging and Diagnostics (COVID). *Clin Radiol*. 2020;75(11):871–872. doi: 10.1016/j.crad.2020.07.023
3. Chang YC, Yu CJ, Chang SC, et al. Pulmonary sequelae in convalescent patients after severe acute respiratory syndrome: evaluation with thin-section CT. *Radiology*. 2005;236(3):1067–1075. doi: 10.1148/radiol.2363040958
4. Haseli S, Khalili N, Bakhshayeshkaram M, et al. Lobar distribution of COVID-19 pneumonia based on chest computed tomography findings. A retrospective study. *Arch Acad Emerg Med*. 2020;8(1):e55.
5. Inui S, Fujikawa A, Jitsu M, et al. Chest CT findings in cases from the cruise ship “Diamond Princess” with Coronavirus Disease 2019 (COVID-19). *Radiol Cardiothorac Imaging*. 2020;2(2):e200110. doi: 10.1148/ryct.2020200110
6. Prokop M, van Everdingen W, van Rees Vellinga T, et al. CO-RADS: A Categorical CT assessment scheme for patients suspected of having COVID-19—definition and evaluation. *Radiology*. 2020;296(2):97–104. doi: 10.1148/radiol.2020201473
7. Shen C, Yu N, Cai S, et al. Quantitative computed tomography analysis for stratifying the severity of Coronavi-

- rus Disease 2019. *J Pharm Anal.* 2020;10(2):123–129. doi: 10.1016/j.jpha.2020.03.004
8. Pan F, Ye T, Sun P, et al. Time course of lung changes at chest CT during recovery from Coronavirus Disease 2019 (COVID-19). *Radiology.* 2020;295(3):715–721. doi: 10.1148/radiol.2020200370
9. Revel MP, Parkar AP, Prosch H, et al. COVID-19 patients and the radiology department – advice from the European Society of Radiology (ESR) and the European Society of Thoracic Imaging (ESTI). *Eur Radiol.* 2020;30(9):4903–4909. doi: 10.1007/s00330-020-06865-y
10. Morozov SP, Protsenko DN, Smetanina SV, et al. Radiation diagnosis of coronavirus disease (COVID-19): organization, methodology, interpretation of results: preprint II. Version 2 of 17.04.2020. The series “Best practices of radiation and instrumental diagnostics”. Issue 65. Moscow: Research and Practical Clinical Center for Diagnostics and Telemedicine Technologies of the Moscow Health Care Department; 2020. 78 p. (In Russ).
11. Sinitsyn VE, Tyurin IE, Mitkov VV. Consensus Guidelines of Russian Society of Radiology (RSR) and Russian Association of Specialists in Ultrasound Diagnostics in Medicine (RASUDM) “Role of Imaging (X-ray, CT and US) in Diagnosis of COVID-19 Pneumonia” (version 2). *Journal of Radiology and Nuclear Medicine.* 2020;101(2):72–89. (In Russ). doi: 10.20862/0042-4676-2020-101-2-72-89
12. Morozov SP, Gornbolevskiy VA, Chernina VY, et al. Prediction of lethal outcomes in COVID-19 cases based on the results chest computed tomography. *Tuberculosis and Lung Diseases.* 2020;98(6):7–14. (In Russ). doi: 10.21292/2075-1230-2020-98-6-7-14
13. Howard J. Cognitive errors and diagnostic mistakes. A case-based guide to critical thinking in medicine. New York: Springer; 2019.
14. Morozov SP, Vladzimirsky AV, Klyashtorny VG, et al. Clinical trials of software based on intelligent technologies (radiation diagnostics). The series “Best practices of radiation and instrumental diagnostics”. Issue 57. Moscow: Research and Practical Clinical Center for Diagnostics and Telemedicine Technologies of the Moscow Health Care Department; 2019. 51 p. (In Russ).
15. Sahiner B, Pezeshk A, Hadjiiski LM, et al. Deep learning in medical imaging and radiation therapy. *Med Phys.* 2019;46(1):1–36. doi: 10.1002/mp.13264
16. Allen BJ, Seltzer SE, Langlotz CP, et al. A road map for translational research on artificial intelligence in medical imaging: from the 2018 national institutes of health/RSNA/ACR/The academy workshop. *J Am Coll Radiol.* 2019;16(9):1179–1189. doi: 10.1016/j.jacr.2019.04.014
17. Angus DC. Randomized clinical trials of artificial intelligence. *Jama.* 2020;323(11):1043–1045. doi: 10.1001/jama.2020.1039
18. Wijnberge M, Geerts BF, Hol L, et al. Effect of a machine learning-derived early warning system for intraoperative hypotension vs standard care on depth and duration of intraoperative hypotension during elective noncardiac surgery: the HYPE randomized clinical trial. *Jama.* 2020;323(11):1052–1060. doi: 10.1001/jama.2020.0592
19. Carlile M, Hurt B, Hsiao A, et al. Deployment of artificial intelligence for radiographic diagnosis of COVID-19 pneumonia in the emergency department. *J Am Coll Emerg Physicians Open.* 2020;1(6):1459–1464. doi: 10.1002/emp2.12297
20. Morozov SP, Chernina VYu, Blokhin IA, et al. Chest computed tomography for outcome prediction in laboratory-confirmed COVID-19: A retrospective analysis of 38,051 cases. *Digital Diagnostics.* 2020;1(1):27–36. (In Russ). doi: 10.17816/DD46791

## СПИСОК ЛИТЕРАТУРЫ

1. Эксперимент по использованию инновационных технологий в области компьютерного зрения для анализа медицинских изображений и дальнейшего применения в системе здравоохранения города Москвы [дата обращения: 04.02.2021]. Режим доступа: <https://mosmed.ai>. Дата обращения: 15.01.2021.
2. Morozov S.P., Ledikhova N.V., Panina E.V., et al. Re: Controversy in coronaViral Imaging and Diagnostics (COVID) // *Clin Radiol.* 2020. Vol. 75, N 11. P. 871–872. doi: 10.1016/j.crad.2020.07.023
3. Chang Y.C., Yu C.J., Chang S.C., et al. Pulmonary sequelae in convalescent patients after severe acute respiratory syndrome: evaluation with thin-section CT // *Radiology.* 2005. Vol. 236, N 3. P. 1067–1075. doi: 10.1148/radiol.2363040958
4. Haseli S., Khalili N., Bakhshayeshkaram M., et al. Lobar distribution of COVID-19 pneumonia based on chest computed tomography findings. A retrospective study // *Arch Acad Emerg Med.* 2020. Vol. 8, N 1. P. 55.
5. Inui S., Fujikawa A., Jitsu M., et al. Chest CT findings in cases from the cruise ship «Diamond Princess» with Coronavirus Disease 2019 (COVID-19) // *Radiol Cardiothorac Imaging.* 2020. Vol. 2, N 2. P. 200110. doi: 10.1148/ryct.2020200110
6. Prokop M., van Everdingen W., van Rees Vellinga T., et al. CO-RADS: A Categorical CT assessment scheme for patients suspected of having COVID-19-definition and evaluation // *Radiology.* 2020. Vol. 296, N 2. P. 97–104. doi: 10.1148/radiol.2020201473
7. Shen C., Yu N., Cai S., et al. Quantitative computed tomography analysis for stratifying the severity of Coronavirus Disease 2019 // *J Pharm Anal.* 2020. Vol. 10, N 2. P. 123–129. doi: 10.1016/j.jpha.2020.03.004
8. Pan F., Ye T., Sun P., et al. Time course of lung changes at chest CT during Recovery from Coronavirus Disease 2019 (COVID-19) // *Radiology.* 2020. Vol. 295, N 3. P. 715–721. doi: 10.1148/radiol.2020200370
9. Revel M.P., Parkar A.P., Prosch H., et al. COVID-19 patients and the radiology department – advice from the European Society of Radiology (ESR) and the European Society of Thoracic Imaging (ESTI) // *Eur Radiol.* 2020. Vol. 30, N 9. P. 4903–4909. doi: 10.1007/s00330-020-06865-y
10. Морозов С.П., Проценко Д.Н., Сметанина С.В., и др. Лучевая диагностика коронавирусной болезни (COVID-19): организация, методология, интерпретация результатов: препринт № ЦДТ-2020-II. Версия 2 от 17.04.2020. Серия «Лучшие практики лучевой и инструментальной диагностики». Вып. 65. Москва: ГБУЗ «НПКЦ ДиТ ДЗМ», 2020. 78 с.
11. Синицын В.Е., Тюрин И.Е., Митьков В.В. Временные методические рекомендации Российского общества рентгенологов и радиологов (РОРР) и Российской ассоциации специалистов ультразвуковой диагностики в медицине (РАСУДМ) «Методы лучевой диагностики пневмонии при новой коронавирусной инфекции при COVID-19» (версия 2) // *Вестник рентгенологии и радиологии.* 2020. Т. 101, № 2. С. 72–89. doi: 10.20862/0042-4676-2020-101-2-72-89



12. Морозов С.П., Гомболевский В.А., Чернина В.Ю., и др. Прогнозирование летальных исходов при COVID-19 по данным компьютерной томографии органов грудной клетки // Туберкулез и болезни лёгких. 2020. Т. 98, № 6. С. 7–14. doi: 10.21292/2075-1230-2020-98-6-7-14
13. Howard J. Cognitive errors and diagnostic mistakes. A case-based guide to critical thinking in medicine. New York: Springer; 2019.
14. Морозов С.П., Владимирский А.В., Кляшторный В.Г., и др. Клинические испытания программного обеспечения на основе интеллектуальных технологий (лучевая диагностика). Серия «Лучшие практики лучевой и инструментальной диагностики». Вып. 57. Москва: ГБУЗ «НПКЦ ДиТ ДЗМ», 2019. 51 с.
15. Sahiner B., Pezeshk A., Hadjiiski L.M., et al. Deep learning in medical imaging and radiation therapy // Med Phys. 2019. Vol. 46, N 1. P. 1–36. doi: 10.1002/mp.13264
16. Allen B.J., Seltzer S.E., Langlotz C.P., et al. A road map for translational research on artificial intelligence in medical imaging: from the 2018 national institutes of health/RSNA/ACR/The academy workshop // J Am Coll Radiol. 2019. Vol. 16, N 9. P. 1179–1189. doi: 10.1016/j.jacr.2019.04.014

## AUTHORS' INFO

**\*Victor A. Gombolevskiy**, Cand. Sci. (Med.);  
address: 24/1 Petrovka, Moscow, 127051, Russia;  
ORCID: <https://orcid.org/0000-0003-1816-1315>;  
eLibrary SPIN: 6810-3279; e-mail: [v.gombolevskiy@npcmr.ru](mailto:v.gombolevskiy@npcmr.ru)

**Sergey P. Morozov**, Dr. Sci. (Med.), Professor;  
ORCID: <https://orcid.org/0000-0001-6545-6170>;  
eLibrary SPIN: 8542-1720; e-mail: [morozov@npcmr.ru](mailto:morozov@npcmr.ru)

**Anna E. Andreychenko**, Cand. Sci. (Phys.-Math.);  
ORCID: <https://orcid.org/0000-0001-6359-0763>;  
eLibrary SPIN: 6625-4186; e-mail: [a.andreychenko@npcmr.ru](mailto:a.andreychenko@npcmr.ru)

**Valeria Yu. Chernina**, MD;  
ORCID: <http://orcid.org/0000-0002-0302-293X>;  
eLibrary SPIN: 8896-8051; e-mail: [v.chernina@npcmr.ru](mailto:v.chernina@npcmr.ru)

**Anton V. Vladzimirsky**, Dr. Sci. (Med.);  
ORCID: <https://orcid.org/0000-0002-2990-7736>;  
eLibrary SPIN: 3602-7120; e-mail: [a.vladzimirsky@npcmr.ru](mailto:a.vladzimirsky@npcmr.ru)

**Olesya A. Mokienko**, Cand. Sci. (Med.);  
ORCID: <https://orcid.org/0000-0002-7826-5135>;  
eLibrary SPIN: 8088-9921; e-mail: [Lesya.md@yandex.ru](mailto:Lesya.md@yandex.ru)

17. Angus D.C. Randomized clinical trials of artificial intelligence // Jama. 2020. Vol. 323, N 11. P. 1043–1045. doi: 10.1001/jama.2020.1039

18. Wijnberge M., Geerts B.F., Hol L., et al. Effect of a machine learning-derived early warning system for intraoperative hypotension vs standard care on depth and duration of intraoperative hypotension during elective noncardiac surgery: the HYPE randomized clinical trial // Jama. 2020. Vol. 323, N 11. P. 1052–1060. doi: 10.1001/jama.2020.0592

19. Carlile M., Hurt B., Hsiao A., et al. Deployment of artificial intelligence for radiographic diagnosis of COVID-19 pneumonia in the emergency department // J Am Coll Emerg Physicians Open. 2020. Vol. 1, N 6. P. 1459–1464. doi: 10.1002/emp2.12297

20. Морозов С.П., Чернина В.Ю., Блохин И.А., Гомболевский В.А. Прогнозирование исходов при лабораторно верифицированном COVID-19 по данным компьютерной томографии органов грудной клетки: ретроспективный анализ 38051 пациента // Digital Diagnostics. 2020. Т. 1, № 1. С. 27–36. doi: 10.17816/DD46791

## ОБ АВТОРАХ

**Гомболевский Виктор Александрович**, к.м.н.;  
адрес: Россия, 127051, Москва, ул. Петровка, д. 24/1;  
ORCID: <https://orcid.org/0000-0003-1816-1315>;  
eLibrary SPIN: 6810-3279; e-mail: [v.gombolevskiy@npcmr.ru](mailto:v.gombolevskiy@npcmr.ru)

**Морозов Сергей Павлович**, д.м.н., профессор;  
ORCID: <https://orcid.org/0000-0001-6545-6170>;  
eLibrary SPIN: 8542-1720; e-mail: [morozov@npcmr.ru](mailto:morozov@npcmr.ru)

**Андрейченко Анна Евгеньевна**, к.ф.-м.н.;  
ORCID: <https://orcid.org/0000-0001-6359-0763>;  
eLibrary SPIN: 6625-4186; e-mail: [a.andreychenko@npcmr.ru](mailto:a.andreychenko@npcmr.ru)

**Чернина Валерия Юрьевна**;  
ORCID: <http://orcid.org/0000-0002-0302-293X>;  
eLibrary SPIN: 8896-8051; e-mail: [v.chernina@npcmr.ru](mailto:v.chernina@npcmr.ru)

**Владимирский Антон Вячеславович**, д.м.н.;  
ORCID: <https://orcid.org/0000-0002-2990-7736>;  
eLibrary SPIN: 3602-7120; e-mail: [a.vladzimirsky@npcmr.ru](mailto:a.vladzimirsky@npcmr.ru)

**Мокиенко Олеся Александровна**, к.м.н.;  
ORCID: <https://orcid.org/0000-0002-7826-5135>;  
eLibrary SPIN: 8088-9921; e-mail: [Lesya.md@yandex.ru](mailto:Lesya.md@yandex.ru)



DOI: <https://doi.org/10.17816/DD60300>

# Radiation diagnostics of cerebral cavernous malformations

© Elena N. Giryа<sup>1</sup>, Valentin E. Sinitsyn<sup>2</sup>, Alexey S. Tokarev<sup>1, 3</sup>

<sup>1</sup> Sklifosovsky Research Institute for Emergency Medicine, Moscow, Russian Federation

<sup>2</sup> Lomonosov Moscow State University, Moscow, Russian Federation

<sup>3</sup> Moscow Health Department, Moscow, Russian Federation

## ABSTRACT

Cerebral cavernous malformations are a fairly common vascular pathology at the moment, with the number of detected cases increasing dramatically in recent years. This is because modern neuroimaging methods such as computed tomography (CT) and magnetic resonance imaging (MRI) have been introduced into clinical practice and are widely available. Prior to the advent of CT and MRI technologies, it was extremely difficult to diagnose this pathology, and the diagnosis was usually made intraoperatively or based on autopsy data. Further, the literature review is devoted to the radiological diagnosis of cerebral cavernous malformations (CM). The role of neuroimaging methods in the diagnosis of cavernous malformations, as well as the use of MRI for CM visualization, was analyzed. The advantages of MRI over other neuroimaging methods for this pathology have been demonstrated. Pulse sequences of MRI and signaling characteristics of various foci were characterized, depending on the morphological substrate. The significance of the susceptibility-weighted imaging sequence was also evaluated for the detection of multifocal lesions in cases of familial CM. The study of the main pulse sequences of MRI for visualization of CM will improve the protocol algorithm for the timely diagnosis of this pathology and the selection of therapeutic approach.

**Keywords:** radiation diagnostics; cavernous malformations; cavernous angiomas; hemangiomas; hidden vascular malformations.

To cite this article

Giryа EN, Sinitsyn VE, Tokarev AS. Radiation diagnostics of cerebral cavernous malformations. *Digital Diagnostics*. 2021;2(1):39–48.

DOI: <https://doi.org/10.17816/DD60300>

Received: 12.02.2021

Accepted: 25.03.2021

Published: 30.03.2021

DOI: <https://doi.org/10.17816/DD60300>

# Лучевая диагностика кавернозных мальформаций головного мозга

© Е.Н. Гирия<sup>1</sup>, В.Е. Синицын<sup>2</sup>, А.С. Токарев<sup>1, 3</sup>

<sup>1</sup> Научно-исследовательский институт скорой помощи имени Н.В. Склифосовского, Москва, Российская Федерация

<sup>2</sup> Московский государственный университет имени М.В. Ломоносова, Москва, Российская Федерация

<sup>3</sup> Департамент здравоохранения города Москвы, Москва, Российская Федерация

## АННОТАЦИЯ

Кавернозные мальформации головного мозга в настоящее время являются достаточно распространённой сосудистой патологией: число выявляемых случаев в последние годы резко возросло. Это связано с внедрением в клиническую практику и повсеместным распространением современных методов нейровизуализации, таких как компьютерная (КТ) и магнитно-резонансная (МРТ) томография. До появления КТ и МРТ диагностировать данную патологию было весьма трудно, и диагноз чаще всего устанавливался интраоперационно или по данным аутопсии. Обзор литературы посвящён лучевой диагностике кавернозных мальформаций (КМ) головного мозга. Проанализировано значение методов нейровизуализации для диагностики кавернозных мальформаций, а также применение МРТ для визуализации КМ. Выявлены преимущества МРТ перед другими методами нейровизуализации данной патологии. Охарактеризованы импульсные последовательности МРТ и сигнальные характеристики очагов различных типов в зависимости от морфологического субстрата. Проанализировано значение последовательности SWI (susceptibility weighted imaging) для обнаружения многоочаговых поражений в случаях семейных форм КМ. Изучение основных импульсных последовательностей МРТ для визуализации кавернозных мальформаций позволит оптимизировать алгоритм протокола для своевременной диагностики данной патологии и выбора тактики лечения.

**Ключевые слова:** лучевая диагностика; кавернозные мальформации; кавернозные ангиомы; гемангиомы; скрытые сосудистые мальформации.

## Как цитировать

Гирия Е.Н., Синицын В.Е., Токарев А.С. Лучевая диагностика кавернозных мальформаций головного мозга // *Digital Diagnostics*. 2021. Т. 2, №1. С. 39–48.  
DOI: <https://doi.org/10.17816/DD60300>

DOI: <https://doi.org/10.17816/DD60300>

## 脑洞畸形的放射诊断

© Elena N. Girya<sup>1</sup>, Valentin E. Sinitsyn<sup>2</sup>, Alexey S. Tokarev<sup>1,3</sup>

<sup>1</sup> Sklifosovsky Research Institute for Emergency Medicine, Moscow, Russian Federation

<sup>2</sup> Lomonosov Moscow State University, Moscow, Russian Federation

<sup>3</sup> Moscow Health Department, Moscow, Russian Federation

### 简评:

目前,脑海绵状畸形是相当普遍的血管病理:近年来发现的病例数量急剧增加。这是由于将其引入临床实践并广泛传播了现代神经成像方法,例如计算机断层扫描(CT)和磁共振成像(MRI)断层扫描。CT和MRI出现之前,很难诊断出这种病理,诊断通常是在术中或根据尸检数据进行的。文献综述致力于脑海绵状畸形(CM)的放射学诊断。分析了神经影像学方法对海绵状畸形的诊断的重要性,以及使用MRI对骨髓进行可视化的重要性。相比于这种病理学的其他神经影像学检查方法,MRI具有优势。根据形态学底物,对MRI的脉冲序列和各种类型灶的信号特征进行了表征。分析 SWI (susceptibility weighted imaging)序列的值用于检测家族性CM病例中的多灶性病变。对MRI的主要脉冲序列进行可视化以研究海绵状畸形的研究将有助于优化协议算法,以便及时诊断这种病理状况并选择治疗策略。

**关键字:** 放射诊断; 海绵状畸形; 海绵状血管瘤 血管瘤 隐藏的血管畸形。

### 引用本文:

Girya EN, Sinitsyn VE, Tokarev AS. 脑洞畸形的放射诊断. *Digital Diagnostics*. 2021;2(1):39–48. DOI: <https://doi.org/10.17816/DD60300>

收到: 12.02.2021

接受: 25.03.2021

发布时间: 30.03.2021

## BACKGROUND

Cavernous malformations (CMs) are vascular lesions of the brain and spinal cord; they have a low blood flow and consist of caverns with an endothelial lining [1–4]. They are also known as cavernous angiomas, cavernous hemangiomas, hidden vascular malformations, or cavernomas. They are found commonly in the supra- and infratentorial regions of the brain but less often in the spinal cord [5–8]. Such formations are the second-most common vascular malformations in the central nervous system after the development of venous anomalies [9–11]. The exact frequency and prevalence of CMs are unknown because the symptoms of these lesions do not manifest clinically in most cases; their diagnosis also requires neuroimaging techniques, which are usually used when they are clinically indicated. Despite the benign course of this disease, CMs can cause epileptic seizures and serious neurological deficits.

## DEVELOPMENT

### OF NEUROVISUALIZATION METHODS FOR DIAGNOSING CAVERNOUS MALFORMATIONS

Conventional radiography of the skull was first used to diagnose CMs in 1969 [12]. In skull radiographs, granular or gross macroscopic calcifications can be detected in about 7%–40% of cases. However, this method is insensitive and nonspecific in relation to CM detection.

Modern neuroimaging methods play a decisive role in the diagnosis, monitoring, and evaluation of the results of CM treatment. Before the advent of computed tomography (CT) and magnetic resonance imaging (MRI) tomography, detecting CM was difficult, so pathology was diagnosed during surgery. X-ray analysis and radionuclide scanning of the skull are also insensitive and nonspecific methods of CM detection.

With the development of CT, the sensitivity of diagnosis has significantly increased, thereby contributing to the first successful assessment of the incidence of CM [13]. Early studies reported that CMs can be fully detected via CT, with 100% detection [14, 15]. However, the resolution levels of scanners were limited to detecting small and relatively large foci [16].

As the only method for detecting CM, CT can be applied to diagnose foci only in 30%–50% of cases. CT images usually show hyperdense lesions and less often mixed hyper- and isodense lesions (Fig. 1) [17]. CT can also detect signs of lesion calcification.

With the introduction of a contrast agent, the definition of CM contours has improved, and sensitivity in detecting

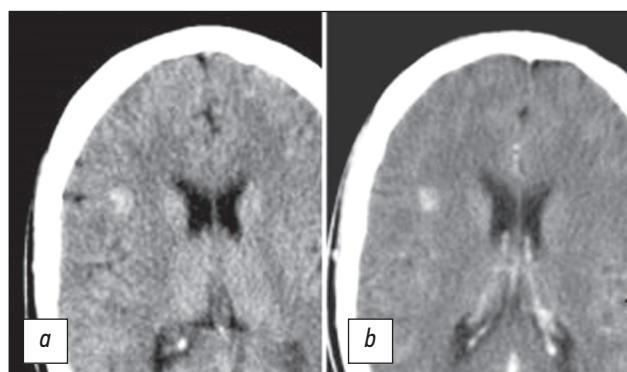


**Fig. 1.** CT sections of the brain in the axial view performed before (a) and after contrast agent administration (b). The images show a hyperdense focus in the right frontal lobe, without clear contours, and without contrast uptake.

isodense foci has increased. Some researchers [18] suggested the following signs of CM based on CT results: round shape, clearly defined edge, uneven density, absence of surrounding edema, and mass effect (in the absence of intracerebral hemorrhage). However, CT results in the diagnosis of CM are nonspecific. Thus, the differentiation of CM and partially calcified avascular gliomas is a significant problem.

Since the introduction of CT, the frequency of CM detection has increased significantly; as a result, a fundamental question on the appropriate therapeutic approach for the obtained lesion has been raised.

Cerebral angiography for detecting CMs remains difficult. Nevertheless, with this method, the presence of small feeding vessels, a decrease in the blood circulation rate, and the presence of thrombi in the vascular spaces of CMs can be detected. A. Jonutis et al. [19] presented the first case of CM detection as an angiographic anomaly.

Early reports on the use of this method described the signs of the presence of avascular mass lesions with the displacement of adjacent vessels but without pathological vasculature [20, 21]. The most common angiographic sign of CM is the presence of displaced avascular areas. Despite the progress of angiographic methods in recent decades, CMs cannot be detected in about 20%–85% of cases. Therefore, the effectiveness of this approach is limited.

With the introduction of MRI into clinical practice, the frequency of detection of this pathology has increased significantly. It requires an in-depth understanding of various aspects of the natural course of CM to develop ideas on the optimal tactics and timing of the treatment of such lesions.

As a sensitive method for detecting CM, MRI is less specific in the diagnosis of vascular malformations of the central nervous system. In such cases, angiography can be applied to exclude other lesions, particularly arteriovenous and venous malformations.



## USE OF MAGNETIC RESONANCE IMAGING FOR THE VISUALIZATION OF CAVERNOUS MALFORMATION

In 1987, D. Rigamonti et al. [16] demonstrated that MRI at a magnetic field level of 1.5 T is the most sensitive and specific method for detecting CM. Since then, this method has been used for the diagnosis of CM. T2-weighted (T2-WI) imaging is 100% sensitive to CM, whereas T1-weighted images (T1-WI) are significantly less sensitive.

Hemosiderin deposits in and around the CM are considered a typical sign of repeated subclinical hemorrhages or erythrocyte lysis; they provide magnetic susceptibility to this pathological lesion, especially at a high-magnetic-field strength. The heterogeneity of the magnetic field in the presence of hemosiderin also contributes to the differentiation of blood flow and the effects of hemosiderin in CMs (Fig. 2) [16, 17].

MRI findings are consistent with histologically confirmed CM findings with an acceptable reliability. MRI has been considered the preferred diagnostic method in terms of identifying and characterizing CMs.

The combination of a reduced signal rim with a reticular nucleus of mixed hyper- and hypointensity on T2-WI with a high probability is a diagnostic sign of CM. For smaller CM lesions, a point area of hypointensity is assessed on T2-WI. Vasogenic edema accompanies lesions in perifocal regions, which are indicated by an increased signal intensity on T2-WI, and the mass effect usually does not appear even with a sufficiently large lesion if no relatively recent bleeding has occurred (Fig. 3) [17, 22].

In CMs, a sign of a hyperintense signal around the lesion is described on T1 images. T. J. Yun et al. [23] considered that this signal variant is associated with the release of erythrocytes and plasma into the perivascular space during edema formation. A hyperintense signal around lesions on T1-WI is more common in CMs associated with recent clinically significant hemorrhage; in such cases, this sign is highly specific and prognostically significant for CM diagnosis.

Contrast-enhanced MRI in CM diagnosis may be useful in terms of identifying other lesions, such as neoplasms, arteriovenous malformations, or concomitant venous anomalies [21]. D. Rigamonti et al. [16] established a relationship between venous anomalies and in 1988. Subsequently, the association of these lesions is registered in almost 1/3 of cases of CMs [21]. However, this symptom is detected exclusively in sporadic but not familial forms of pathology [24].

J. Zabramski et al. [25] proposed a classification system that provides four different categories of CMs based on the correlation of MRI results by using the spin echo (SE) and gradient echo (GRE) sequences with histopathological examination data.

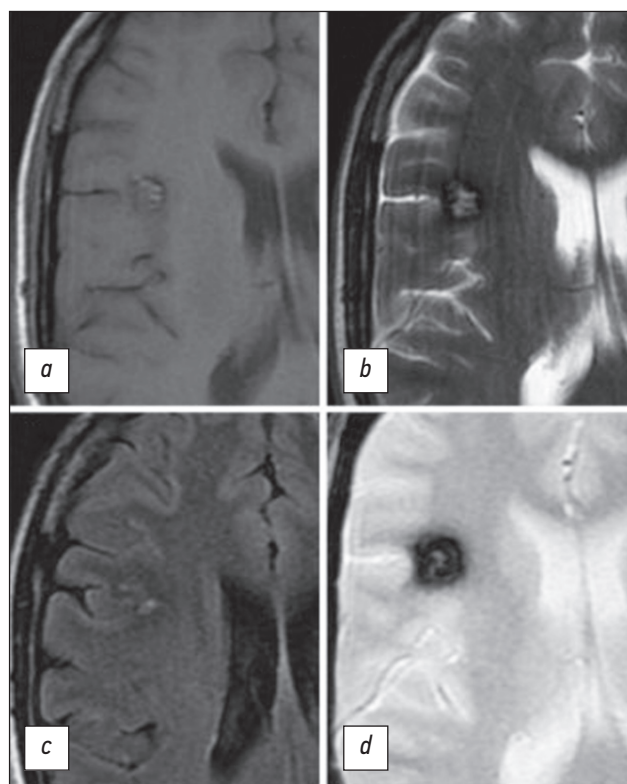


**Fig. 2.** MR images of the brain in the axial view in the T1-WI (a, c), T2-WI (b), and T2\*GRE (d) modes demonstrate a more detailed visualization of the CM structure (the same case as in Fig. 1). The images show a focal lesion of a characteristic cellular structure with a hypointense peripheral signal on T2-WI. The T2\*GRE sequence emphasizes the florid effect of hemosiderin.

According to this classification, the following types are described:

- Type I foci are characterized by a hyperintense nucleus on T1-weighted images and a hypo- or hyperintense nucleus on T2-weighted images depending on the intracellular or extracellular stage of methemoglobin. CMs are characterized and complicated by acute and subacute hemorrhages.
- Type II lesions are characterized by manifestations currently considered the pathognomonic MRI signs of CM and have a reticular nucleus with a mixed signal



**Fig. 3.** T2\*GRE image in the axial view shows a large cavernous angioma in the left occipital lobe. Despite the significant size of the lesion, no perifocal edema and mass effect on the surrounding structures are found.

intensity on T2–WI with the surrounding hypointensive ring, which is believed to be correlated with areas of ongoing thrombosis and the presence of hemorrhages of various ages.

- Type III foci are characterized by the pronounced hypointensity on T2-weighted images and an increase in the value of hypointensity when GRE sequences are used, with iso- or hypointensity observed in T1-weighted images. They reflect the signs of chronic hemorrhage with residual hemosiderin in and around the lesions.
- Type IV lesions are less characterized, and their origin is not entirely clear. They are poorly visualized using conventional SE sequences. These lesions appear as small punctate hypointensive lesions when GRE sequences are used. They are thought to reflect small hemosiderin deposits in either small CMs or possibly capillary telangiectasias.

The clinical relevance of MR classification of these lesions remains controversial, although J. Zabramski et al. [25] indicated that the clinical severity of CM manifestations may be associated with their reflection on MRI. In patients with signs of type I or II CM, this disease is almost always accompanied with an exacerbating condition. In the presence of type III or IV foci, symptoms appear only in 1/3 of patients. The exacerbation of CM symptoms is more often associated with type I foci.

In 1999, M. Essig et al. [26] proposed an MRI technique involving three-dimensional GRE known as susceptibility-weighted imaging (SWI). This type of sequence can be used to detect CMs based on the effects of the blood oxygen-dependent phase between venous blood and the surrounding cerebral parenchyma. With these characteristics, small venous vessels with a low blood flow velocity can be detected at submillimeter resolution. Thus, CM, capillary telangiectasias, and venous anomalies can be differentiated without the need for contrast enhancement.

B. Lee et al. [27] identified additional lesions in 2 out of 10 cases, which are not obvious on T2\*GRE images, by using SWI.

Subsequent studies have also demonstrated that the sensitivity of SWI in detecting multifocal familial CM is higher than that of T2\*GRE [28–30].

The superiority of SWI to T2\*GRE imaging in detecting sporadic CM is less obvious. N.M. de Champfleure et al. [31] reported no differences in sensitivity when they used these sequences for the diagnosis of CM. H.T. Bulut et al. [30] proposed to include type V foci in the classification of J. Zabramski et al. [25] to characterize lesions detectable on SWI images but not on T2\*GRE.

The advantage of SWI is generally found in the detection of CM and telangiectasias in the absence of signs of overt hemorrhage [32]. However, the size of foci is often overestimated because of a significant susceptibility artifact in the

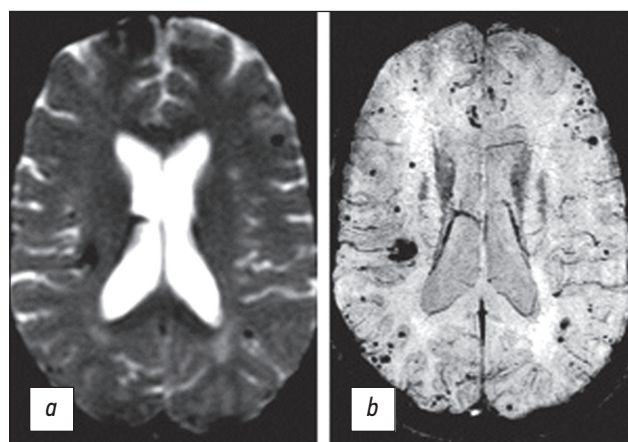


**Fig. 4.** MR images of the brain in the axial view in the T2\*GRE (A) and SWI (B) modes. SWI images can reveal additional CM lesions not visible in the T2\*GRE.

presence of paramagnetic hemosiderin in chronic stasis or previous bleeding in SWI image analysis [31].

Thus, correlation with conventional SE sequences can be used to delineate anatomical details in the resulting images more accurately. K. Pinker et al. [33] demonstrated the possibility of using high-resolution SWI at 3 T to identify the intrafocal tubular structures of CMs, which correspond to vascular canals in hyaline collagen revealed during post-mortem examination.

SWI sequences can be used to determine the dynamics of CMs and assess whether they are increasing in number and size or the detected new lesions are subsequently bleeding from previously unrecognized small CMs.

In general, T2\*GRE sequences can be utilized to reveal the “blooming” effect of hemosiderin and increase the sensitivity of CM detection. SWI sequences, especially with a magnetic field level of 3 T, can be used to identify multifocal lesions in the case of familial CMs that cannot be identified with T2\*GRE images (Fig. 4) [27]. With such approaches, the diagnostic capabilities of MRI significantly increase.

CM with hemorrhagic microangiopathy or cerebral microbleeds, especially in the presence of age-related changes in the brain, can be differentially diagnosed by increasing the sensitivity of methods. In some cases, such as metastases of malignant tumors, differential diagnosis is also feasible. MRI can be applied to perform functional imaging of the primary sensorimotor, speech, and visual areas of the cortex and assess the state of brain structures through diffusion tensor imaging technologies; in turn, these technologies improve the planning of surgical interventions [34].

New MRI options have been proposed for quantitative susceptibility mapping and dynamic contrast-enhanced quantitative perfusion, which have been developed to measure iron deposition and vascular permeability in CM. The latter indicators are considered potential biomarkers of a disease activity.

## CONCLUSION

CMs are cerebral vascular neoplasms whose development mechanism is based on vascular proliferation, dysmorphism, and hemorrhagic angiopathy. This disease is characterized by iron deposits in the structure of the cavernoma and perifocal substance of the brain. It often leads to manifestations of epileptogenesis in lesions. However, improving the methods of the diagnosis and treatment of this disease is a multidisciplinary problem.

The analysis of literature data shows that MRI is the preferred method for diagnosing CM because of its high sensitivity and specificity. The validity of MRI is insufficient to assess the results of modern CM treatment methods, such as stereotaxic radiosurgical treatment and proton therapy. However, studies have yet to provide the diagnostic characteristics of the MRI protocols used in the treatment of CMs. A generally accepted algorithm for the use of MRI protocols has yet to be developed to evaluate the results at various times after the stereotactic radiosurgical treatment of CM.

## REFERENCES

1. Mukha AM, Dashyan VG, Krylov VV. Cavernous malformations of the brain. *Nevrologicheskii zhurnal*. 2013;18(5):46–51. (In Russ).
2. Popov VE, Livshits MI, Bashlachev MG, Nalivkin AE. Cavernous malformations in children: a literature review. *Almanach klinicheskoy mediciny*. 2018;46(2):146–159. (In Russ).
3. Caton MT, Shenoy VS. Cerebral Cavernous Malformations. In: StatPearls [Internet]. Treasure Island (FL): StatPearls Publishing; 2020. Available from: <https://www.ncbi.nlm.nih.gov/books/NBK538144>
4. Flemming KD, Brown RD. Epidemiology and natural history of intracranial vascular malformations. In: H.R. Winn, ed. *Youmans and Winn neurological surgery*, 7th ed. Amsterdam: Elsevier; 2017. P. 3446–3463e7.
5. Gotko AV, Kivelev JV, Son AS. Cavernous malformations of the brain and spinal cord. *Ukrainskij neyroxirurgicheskij zhurnal*. 2013;(3):10–15. (In Russ).
6. Rodich A, Smeyanovich A, Sidorovich R, et al. Modern approaches to the surgical treatment of cavernous angiomas of the brain. *Nauka i innovacii*. 2018;10(188):70–73. (In Russ).
7. Gross BA, Du R. Natural history of cerebral arteriovenous malformations: a meta-analysis. *J. Neurosurg.* 2013;118(2):437–443. doi: 10.3171/2012.10.JNS121280
8. Kearns KN, Chen CJ, Tvrdik P, et al. Outcomes of Surgery for Brainstem Cavernous Malformations: A Systematic Review. *Stroke*. 2019;50(10):2964–2966. doi: 10.1161/STROKEAHA.119.026120
9. Sazonov IA, Belousova OB. Cavernous malformation, which caused the development of extensive acute subdural hematoma. Case study and literature review. *Voprosy neyrokhirurgii imeni N.N. Burdenko*. 2019;3(3):73–76. (In Russ).
10. Mouchtouris N, Chalouhi N, Chitale A, et al. Management of cerebral cavernous malformations: from diagnosis to treatment. *Scientific World Journal*. 2015;2015:808314. doi: 10.1155/2015/808314
11. Negoto T, Terachi S, Baba Y, et al. Symptomatic brainstem cavernoma of elderly patients: timing and strategy of surgical treatment. Two case reports and review of the literature. *World Neurosurg.* 2018;111:227–234. doi: 10.1016/j.wneu.2017.12.111
12. Runnels JB, Gifford DB, Forsberg PL, et al. Dense calcification in a large cavernous angioma. Case report. *J Neurosurg.* 1969;30(3):293–298. doi: 10.3171/jns.1969.30.3part1.0293
13. Batra S, Lin D, Recinos PF, et al. Cavernous malformations: natural history, diagnosis and treatment. *Nat Rev Neurol.* 2009;5(12):659–670. doi: 10.1038/nrneurol.2009.177
14. Vaquero J, Leunda G, Martinez R, et al. Cavernomas of the brain. *Neurosurgery*. 1983;12:208–210. doi: 10.1227/00006123-198302000-00013
15. Tagle P, Huete I, Mendez J, et al. Intracranial cavernous angioma: presentation and management. *J Neurosurg.* 1986;64:720–723. doi: 10.3171/jns.1986.64.5.0720
16. Rigamonti D, Drayer BP, Johnson PC, et al. The MRI appearance of cavernous malformations (angiomas). *J Neurosurg.* 1987;67(4):518–524. doi: 10.3171/jns.1987.67.4.0518
17. Cortés V, Concepción A, Ballenilla M, et al. Cerebral cavernous malformations: Spectrum of neuroradiological findings. *Radiologia*. 2012;54(5):401–409. doi: 10.1016/j.rx.2011.09.016
18. Pozzati E, Padovani R, Morrone B, et al. Cerebral cavernous angiomas in children. *J Neurosurg.* 1980;5(3):826–832. doi: 10.3171/jns.1980.53.6.0826
19. Jonutis AJ, Sondheim FK, Klein HZ, et al. Intracerebral cavernous hemangioma with angiographically demonstrated pathologic vasculature. *Neuroradiology*. 1971;3(3):57–63. doi: 10.1007/BF00339895
20. Kamrin RB, Buchsbaum HW. Large vascular malformations of the brain not visualized by serial angiography. *Arch Neurol.* 1965;13(4):413–420. doi: 10.1001/archneur.1965.00470040079013
21. Jain KK, Robertson E. Recurrence of an excised cavernous hemangioma in the opposite cerebral hemi-



- sphere. Case report. *J Neurosurg.* 1970;33(4):453–456. doi: 10.3171/jns.1970.33.4.0453
22. Batra S, Lin D, Recinos PF, et al. Cavernous malformations: natural history, diagnosis and treatment. *Nat Rev Neurol.* 2009;5(12):659–670. doi: 10.1038/nrneurol.2009.177.
23. Yun TJ, Na DG, Kwon BJ, et al. A T1 hyperintense perilesional signal aids in the differentiation of a cavernous angioma from other hemorrhagic masses. *AJNR Am J Neuroradiol.* 2008;29(3):494–500. doi: 10.3174/ajnr.A0847
24. Petersen TA, Morrison LA, Schrader RM, et al. Familial versus sporadic cavernous malformations: differences in developmental venous anomaly association and lesion phenotype. *AJNR Am J Neuroradiol.* 2019;31(2):377–382. doi: 10.3174/ajnr.A1822
25. Zabramski JM, Wascher TM, Spetzler RF, et al. The natural history of familial cavernous malformations: results of an ongoing study. *J Neurosurg.* 1994;80(3):422–432. doi: 10.3171/jns.1994.80.3.0422
26. Essig M, Reichenbach JR, Schad LR, et al. High-resolution MR venography of cerebral arteriovenous malformations. *Magn Reson Imaging.* 1999;17(3):1417–1425. doi: 10.1007/s001170050989
27. Lee BC, Vo KD, Kido DK, et al. MR high-resolution blood oxygenation level-dependent venography of occult (low-flow) vascular lesions. *AJNR Am. J. Neuroradiol.* 1999;20(7):1239–1242.
28. Cooper AD, Campeau NG, Meissner I. Susceptibility-weighted imaging in familial cerebral cavernous malformations. *Neurology.* 2008;71(5):382. doi: 10.1212/01.wnl.0000319659.86629.c8
29. De Souza JM, Domingues RC, Cruz J, et al. Susceptibility-weighted imaging for the evaluation of patients with familial cerebral cavernous malformations: a comparison with t2-weighted fast spin-echo and gradient-echo sequences. *AJNR Am J Neuroradiol.* 2008;29(1):154–158. doi: 10.3174/ajnr.A0748
30. Bulut HT, Sarica MA, Baykan AH. The value of susceptibility weighted magnetic resonance imaging in evaluation of patients with familial cerebral cavernous angioma. *Int J Clin Exp Med.* 2014;7(12):5296–5302.
31. De Champfleury NM, Langlois C, Ankenbrandt WJ, et al. Magnetic resonance imaging evaluation of cerebral cavernous malformations with susceptibility-weighted imaging. *Neurosurgery.* 2011;68(3):641–648. doi: 10.1227/NEU.0b013e31820773cf
32. Campbell PG, Jabbour P, Yadla S, Awad IA. Emerging clinical imaging techniques for cerebral cavernous malformations: a systematic review. *Neurosurg Focus.* 2010;29(3):E6. doi: 10.3171/2010.5.FOCUS10120
33. Pinker K, Stavrou I, Szomolanyi P, et al. Improved preoperative evaluation of cerebral cavernomas by high-field, high-resolution susceptibility-weighted magnetic resonance imaging at 3 Tesla: comparison with standard (1.5 T) magnetic resonance imaging and correlation with histopathological findings – preliminary results. *Invest Radiol.* 2007;42(6):346–351. doi: 10.1097/01.rli.0000262744.85397.fc
34. Flores BC, Whittemore AR, Samson DS, Barnett SL. The utility of preoperative diffusion tensor imaging in the surgical management of brainstem cavernous malformations. *J Neurosurg.* 2015;122(3):653–662. doi: 10.3171/2014.11.JNS13680

## СПИСОК ЛИТЕРАТУРЫ

1. Муха А.М., Дашьян В.Г., Крылов В.В. Кавернозные мальформации головного мозга // Неврологический журнал. 2013. Т. 18, № 5. С. 46–51.
2. Попов В.Е., Лившиц М.И., Башлачев М.Г., Наливкин А.Е. Кавернозные мальформации у детей: обзор литературы // Альманах клинической медицины. 2018. Т. 46, № 2. С. 146–159. doi: 10.18786/2072-0505-2018-46-2-146-159
3. Caton M.T., Shenoy V.S. Cerebral cavernous malformations. In: StatPearls [Internet]. Treasure Island (FL): StatPearls Publishing; 2020. Available from: <https://www.ncbi.nlm.nih.gov/books/NBK538144>
4. Flemming K.D., Brown R.D. Epidemiology and natural history of intracranial vascular malformations. In: H.R. Winn, ed. Youmans and Winn neurologic surgery, 7th ed. Amsterdam: Elsevier; 2017. P. 3446–3463e7.
5. Готко А.В., Кивелев J.V., Сон А.С. Кавернозные мальформации головного и спинного мозга // Український нейрохірургічний журнал. 2013. № 3. С. 10–15.
6. Родич А., Смянович А., Сидорович Р. и др. Современные подходы к хирургическому лечению кавернозных ангиом головного мозга // Наука и инновации. 2018. Т. 10, № 188. С. 70–73.
7. Gross B.A., Du R. Natural history of cerebral arteriovenous malformations: a meta-analysis // J Neurosurg. 2013. Vol. 118, № 2. P. 437–443. doi: 10.3171/2012.10.JNS121280
8. Kearns K.N., Chen C.J., Tvrdik P., et al. Outcomes of surgery for brainstem cavernous malformations: a systematic review // Stroke. 2019. Vol. 50, № 10. P. 2964–2966. doi: 10.1161/STROKEAHA.119.026120
9. Сазонов И.А., Белоусова О.Б. Кавернозная мальформация, вызвавшая развитие обширной острой субдуральной гематомы. Случай из практики и обзор литературы // Вопросы нейрохирургии имени Н.Н. Бурденко. 2019. Т. 83, № 3. С. 73–76. doi: 10.17116/neiro20198303173
10. Mouchtouris N., Chalouhi N., Chitale A., et al. Management of cerebral cavernous malformations: from diagnosis to treatment // Scientific World Journal. 2015. Vol. 2015. P. 808314. doi: 10.1155/2015/808314
11. Negoto T., Terachi S., Baba Y., et al. Symptomatic brainstem cavernoma of elderly patients: timing and strategy of surgical treatment. Two case reports and review of the literature // World Neurosurg. 2018. Vol. 111. P. 227–234. doi: 10.1016/j.wneu.2017.12.111
12. Runnels J.B., Gifford D.B., Forsberg P.L., et al. Dense calcification in a large cavernous angioma. Case report // J Neurosurg. 1969. Vol. 30, № 3. P. 293–298. doi: 10.3171/jns.1969.30.3part1.0293
13. Batra S., Lin D., Recinos P.F., et al. Cavernous malformations: natural history, diagnosis and treatment // Nat Rev Neurol. 2009. Vol. 5, № 12. P. 659–670. doi: 10.1038/nrneurol.2009.177
14. Vaquero J., Leunda G., Martinez R., et al. Cavernomas of the brain // Neurosurgery. 1983. Vol. 12. P. 208–210. doi: 10.1227/00006123-198302000-00013
15. Tagle P., Huete I., Mendez J., et al. Intracranial cavernous angioma: presentation and management // J Neurosurg. 1986. Vol. 64. P. 720–723. doi: 10.3171/jns.1986.64.5.0720
16. Rigamonti D., Drayer B.P., Johnson P.C., et al. The MRI appearance of cavernous malformations (angio-

- mas) // J Neurosurg. 1987. Vol. 67, № 4. P. 518–524. doi: 10.3171/jns.1987.67.4.0518
17. Cortés V., Concepción A., Ballenilla M., et al. Cerebral cavernous malformations: spectrum of neuroradiological findings // Radiologia. 2012. Vol. 54, № 5. P. 401–409. doi: 10.1016/j.rx.2011.09.016
18. Pozzati E., Padovani R., Morrone B., et al. Cerebral cavernous angiomas in children // J Neurosurg. 1980. Vol. 5, № 3. P. 826–832. doi: org/10.3171/jns.1980.53.6.0826
19. Jonutis A.J., Sondheimer F.K., Klein H.Z., et al. Intracerebral cavernous hemangioma with angiographically demonstrated pathologic vasculature // Neuroradiology. 1971. Vol. 3, № 3. P. 57–63. doi: 10.1007/BF00339895
20. Kamrin R.B., Buchsbaum H.W. Large vascular malformations of the brain not visualized by serial angiography // Arch Neurol. 1965. Vol. 13, № 4. P. 413–420. doi: 10.1001/archneur.1965.00470040079013
21. Jain K.K., Robertson E. Recurrence of an excised cavernous hemangioma in the opposite cerebral hemisphere. Case report // J Neurosurg. 1970. Vol. 33, № 4. P. 453–456. doi: 10.3171/jns.1970.33.4.0453
22. Batra S., Lin D., Recinos P.F., et al. Cavernous malformations: natural history, diagnosis and treatment // Nat Rev Neurol. 2009. Vol. 5, № 12. P. 659–670. doi: 10.1038/nrneurol.2009.177
23. Yun T.J., Na D.G., Kwon B.J., et al. A T1 hyperintense perilesional signal aids in the differentiation of a cavernous angioma from other hemorrhagic masses // AJNR Am J Neuroradiol. 2008. Vol. 29, № 3. P. 494–500. doi: 10.3174/ajnr.A0847
24. Petersen T.A., Morrison L.A., Schrader R.M., et al. Familial versus sporadic cavernous malformations: differences in developmental venous anomaly association and lesion phenotype // AJNR Am J Neuroradiol. 2019. Vol. 31, № 2. P. 377–382. doi: 10.3174/ajnr.A1822
25. Zabramski J.M., Wascher T.M., Spetzler R.F., et al. The natural history of familial cavernous malformations: results of an ongoing study // J Neurosurg. 1994. Vol. 80, № 3. P. 422–432. doi: 10.3171/jns.1994.80.3.0422
26. Essig M., Reichenbach J.R., Schad L.R., et al. High-resolution MR venography of cerebral arteriovenous malformations // Magn Reson Imaging. 1999. Vol. 17, № 3. P. 1417–1425. doi: 10.1007/s001170050989
27. Lee B.C., Vo K.D., Kido D.K., et al. MR high-resolution blood oxygenation level-dependent venography of occult (low-flow) vascular lesions // AJNR Am J Neuroradiol. 1999. Vol. 20, № 7. P. 1239–1242.
28. Cooper A.D., Campeau N.G., Meissner I. Susceptibility-weighted imaging in familial cerebral cavernous malformations // Neurology. 2008. Vol. 71, № 5. P. 382. doi: 10.1212/01.wnl.0000319659.86629.c8
29. De Souza J.M., Domingues R.C., Cruz J., et al. Susceptibility-weighted imaging for the evaluation of patients with familial cerebral cavernous malformations: a comparison with t2-weighted fast spin-echo and gradient-echo sequences // AJNR Am J Neuroradiol. 2008. Vol. 29, № 1. P. 154–158. doi: 10.3174/ajnr.A0748
30. Bulut H.T., Sarica M.A., Baykan A.H. The value of susceptibility weighted magnetic resonance imaging in evaluation of patients with familial cerebral cavernous angioma // Int J Clin Exp Med. 2014. Vol. 7, № 12. P. 5296–5302.
31. De Champfleury N.M., Langlois C., Ankenbrandt W.J. et al. Magnetic resonance imaging evaluation of cerebral cavernous malformations with susceptibility-weighted imaging // Neurosurgery. 2011. Vol. 68, № 3. P. 641–648. doi: 10.1227/NEU.0b013e31820773cf
32. Campbell P.G., Jabbour P., Yadla S., Awad I.A. Emerging clinical imaging techniques for cerebral cavernous malformations: a systematic review // Neurosurg Focus. 2010. Vol. 29, № 3. P. E6. doi: 10.3171/2010.5.FOCUS10120
33. Pinker K., Stavrou I., Szomolanyi P., et al. Improved preoperative evaluation of cerebral cavernomas by high-field, high-resolution susceptibility-weighted magnetic resonance imaging at 3 Tesla: comparison with standard (1.5 T) magnetic resonance imaging and correlation with histopathological findings – preliminary results // Invest Radiol. 2007. Vol. 42, № 6. P. 346–351. doi: 10.1097/01.rli.0000262744.85397.fc
34. Flores B.C., Whittemore A.R., Samson D.S., Barnett S.L. The utility of preoperative diffusion tensor imaging in the surgical management of brainstem cavernous malformations // J Neurosurg. 2015. Vol. 122, № 3. P. 653–662. doi: 10.3171/2014.11.JNS13680

## AUTHORS' INFO

\* **Elena N. Girya**, MD; address: 3 Bol'shaya Sukharevskaya ploshcad, 129010, Moscow, Russia; tel.: +7 (495) 608-34-50; ORCID: <https://orcid.org/0000-0001-5875-1489>; eLibrary SPIN: 4793-7748; e-mail: mishka\_77@list.ru

**Valentin E. Sinitsyn**, MD, Dr. Sci. (Med.), Professor; ORCID: <https://orcid.org/0000-0002-5649-2193>; eLibrary SPIN: 8449-6590; e-mail: vsini@mail.ru

**Alexey S. Tokarev**, MD, Cand. Sci. (Med.); ORCID: <https://orcid.com/0000-0002-8415-5602>; eLibrary SPIN: 1608-0630; e-mail: alex\_am\_00@mail.ru

## ОБ АВТОРАХ

\* **Гиря Елена Николаевна**; адрес: Россия, 129010, Москва, Большая Сухаревская пл., д. 3; тел.: +7 (495) 608-34-50; ORCID: <https://orcid.org/0000-0001-5875-1489>; eLibrary SPIN: 4793-7748; e-mail: mishka\_77@list.ru

**Синицын Валентин Евгеньевич**, д.м.н., профессор; ORCID: <https://orcid.org/0000-0002-5649-2193>; eLibrary SPIN: 8449-6590; e-mail: vsini@mail.ru

**Токарев Алексей Сергеевич**, к.м.н.; ORCID: <https://orcid.com/0000-0002-8415-5602>; eLibrary SPIN: 1608-0630; e-mail: alex\_am\_00@mail.ru





DOI: <https://doi.org/10.17816/DD60635>

# Reference medical datasets (MosMedData) for independent external evaluation of algorithms based on artificial intelligence in diagnostics

© Nikolay A. Pavlov, Anna E. Andreychenko, Anton V. Vladzemyrskyy, Anush A. Revazyan, Yuri S. Kirpichev, Sergey P. Morozov

Moscow Center for Diagnostics and Telemedicine, Moscow, Russian Federation

## ABSTRACT

The article describes a novel approach to creating annotated medical datasets for testing artificial intelligence-based diagnostic solutions. Moreover, there are four stages of dataset formation described: planning, selection of initial data, marking and verification, and documentation. There are also examples of datasets created using the described methods. The technique is scalable and versatile, and it can be applied to other areas of medicine and healthcare that are being automated and developed using artificial intelligence and big data technologies.

**Keywords:** artificial intelligence; medical data; dataset; marking; computer-assisted learning; big data; verification.

## To cite this article

Pavlov NA, Andreychenko AE, Vladzemyrskyy AV, Revazyan AA, Kirpichev YS, Morozov SP. Reference medical datasets (MosMedData) for independent external evaluation of algorithms based on artificial intelligence in diagnostics. *Digital Diagnostics*. 2021;2(1):49–65. DOI: <https://doi.org/10.17816/DD60635>

Received: 11.02.2021

Accepted: 23.03.2021

Published: 30.03.2021

DOI: <https://doi.org/10.17816/DD60635>

## Эталонные медицинские датасеты (MosMedData) для независимой внешней оценки алгоритмов на основе искусственного интеллекта в диагностике

© Н.А. Павлов, А.Е. Андрейченко, А.В. Владзимирский, А.А. Ревазян, Ю.С. Кирпичев, С.П. Морозов

Научно-практический клинический центр диагностики и телемедицинских технологий Департамента здравоохранения г. Москвы, Москва, Российская Федерация

### АННОТАЦИЯ

В статье описывается оригинальный подход к формированию аннотированных медицинских датасетов для проверки диагностических решений, основанных на технологиях искусственного интеллекта. Описаны 4 этапа формирования датасета — планирование, отбор исходных данных, разметка и верификация, документирование. Приведены примеры созданных по описанной методике датасетов. Методика является масштабируемой и универсальной, а значит, может быть использована в других областях медицины и здравоохранения, которые подлежат автоматизации и развитию с помощью технологий искусственного интеллекта и технологий больших данных.

**Ключевые слова:** искусственный интеллект; медицинские данные; датасет; разметка; машинное обучение; большие данные; верификация.

### Как цитировать

Павлов Н.А., Андрейченко А.Е., Владзимирский А.В., Ревазян А.А., Кирпичев Ю.С., Морозов С.П. Эталонные медицинские датасеты (MosMedData) для независимой внешней оценки алгоритмов на основе искусственного интеллекта в диагностике // *Digital Diagnostics*. 2021. Т. 2, №1. С. 49–65. DOI: <https://doi.org/10.17816/DD60635>

DOI: <https://doi.org/10.17816/DD60635>

# 标准医疗日期(MosMedData)独立外部评价的算法在诊断的人工智能基础上

© Nikolay A. Pavlov, Anna E. Andreychenko, Anton V. Vladzemyrskyy,  
Anush A. Revazyan, Yuri S. Kirpichev, Sergey P. Morozov

Moscow Center for Diagnostics and Telemedicine, Moscow, Russian Federation

## 简评:

这篇文章介绍了一个独特的方法来创建附加说明的医疗日期，以测试基于人工智能技术的诊断解决方案。描述了数据集形成的四个阶段-计划，初始数据选择，标记和验证，文档。所举的例子是根据上述日期方法建立的。该方法是广泛而普遍的，因此可以应用于医学和卫生的其他领域，它是由人工智能技术和高数据技术的自动化和发展。

**关键字:** 关键词: 人工智能 医疗数据; 数据集 标记; 机器学习; 大数据; 确认。

## 引用本文:

Pavlov NA, Andreychenko AE, Vladzemyrskyy AV, Revazyan AA, Kirpichev YS, Morozov SP. 标准医疗日期 (MosMedData) 独立外部评价的算法在诊断的人工智能基础上. *Digital Diagnostics*. 2021;2(1)49–65. DOI: <https://doi.org/10.17816/DD60635>

收到: 11.02.2021

接受: 23.03.2021

发布时间: 30.03.2021

## List of abbreviations

**GB, MB, TB** — digital storage capacity: gigabyte, megabyte, terabyte

**Dataset; Data set** — a structured set of information united according to certain logical principles, suitable for machine processing by computed methods of data analysis. A dataset is a complex concept characterized by four main stages: the presence of content (observations, values, records, files, etc.); the presence of a goal (for example, a knowledge base, use for a specific task); the presence of groupings (aggregation and organization of content into sets, collections, etc.); and the presence of cohesion (relation to the subject, integration, logical collection of content, etc.)

**UMIAS** — Unified Medical Information Analysis System of Moscow

**URIS** — Unified Radiological Information Service of Moscow

**AI (artificial intelligence)** — the science and technology of creating intelligent computer programs capable of performing tasks for which, as a rule, human intelligence is required

**CT** — computed tomography

**CT 0–4** — classification of COVID-19 CT signs developed by the Scientific and Practical Clinical Center for Diagnostics and Telemedicine Technologies of the Moscow Department of Health in 2020. CT0 is the norm and the absence of CT signs of viral pneumonia. CT1 — areas of induration with the appearance of frosted glass; involvement of the lung parenchyma is  $\leq 25\%$ . CT2 — areas of induration by the type of frosted glass; involvement of the lung parenchyma is 25%–50%. CT3 — areas of induration by the type of frosted glass and consolidation; involvement of the lung parenchyma is 50%–75%.

**CT4** — diffuse induration of the lung tissue with the appearance of ground glass and consolidation in combination with reticular changes; involvement of the lung parenchyma is  $>75\%$

**MIS** — Medical Information System

**MMG** — mammography

**LDCT** — low-dose computed tomography

**Chest** — thoracic organs

**X-ray** — X-ray study

**FLG** — fluorography

**COVID-19** — an infectious disease caused by the SARS-CoV-2 virus the spread of which in 2020 was characterized by the World Health Organization as a pandemic. According to the International Classification of Diseases of the 10th revision, it is coded as U07.1 or U07.2, depending on the presence/absence of laboratory identification of the virus, respectively

**DICOM (Digital Imaging and Communications in Medicine)** — medical industry standard for the creation, storage, transmission, and visualization of digital medical images and documents of examined patients

**MeSH (Medical Subject Headings)** — a thesaurus containing key medical terms used to index, catalog, and search articles in an English textual database of medical and biological publications created by the US National Center for Biotechnology Information (PubMed)

**README** — in *English*, «Read me» is a well-established name for a document accompanying an executable code, database, or other software product, usually containing basic information about files in the same directory.

**SARS-CoV-2** — enveloped single-stranded (+)RNA virus of *Betacoronavirus*

## BACKGROUND

Progress in artificial intelligence (AI) technologies and their practical uses in various fields, medicine in particular, demonstrates the potential utility of such technologies in applications such as automated diagnostic systems; systems for recognizing unstructured medical records and understanding natural language, analyzing and predicting events, and automatic classification and verification of information; and automatic chat bots to support patients [1]. In connection with the rapid development of deep machine learning and the associated computer recognition of images and patterns within them, considerable attention among all areas of application of automated diagnostic systems is currently being paid to the analysis of medical images, in particular, radiation studies [2].

In practical healthcare, the task of automating diagnostic processes is one of the top priorities for the aging population, increase the availability and, accordingly, the number of diagnostic procedures which are not compensated for by an increase in the number of qualified personnel necessary to ensure proper interpretation of results and, as a result, provide timely medical care. This problem is particularly acute in radiation diagnostics [3], which is based on the visual analysis of images by a doctor. For most modern methods in radiation diagnostics, the number of two-dimensional images per patient requiring interpretation can reach 1000 or more. In this regard, radiation diagnostics is currently an area of active development of deep learning technologies, which is part of the AI concept, for creating computer vision systems that automate the interpretation of medical images. A distinctive feature of deep learning from other



machine learning methods is that the accuracy, reliability, and practical value of the created models depends directly on the quantity and quality of the data used in the learning, validation (fine-tuning), and testing processes [4].

That is why one of the main barriers to the development of AI-based solutions in medical diagnostics is the absence of verified (free from incomplete and erroneous) and high-quality (unified, prepared for automatic machine processing) data sets [5]. Annotated datasets [6] are necessary not only for “training” AI, particularly for machine learning of computer neural networks, but also for testing networks trained on other data.

The requirements for datasets do not allow the use of simple unloading from a medical information system but require that a number of manipulations be carried out with data before they become an annotated dataset suitable for effective use by AI models. The difference between medical data and data in other areas in which machine learning is actively used (for example, banking and other services) lies in the historically established culture of medical records, the absence of structure or minimal structuring, and the limited comparison of different studies of the same patient with each other. At the moment, the literature on the preparation of medical datasets is represented by few publications [7–9]. With this publication, the authors aim to expand the understanding of the problem and the features of preparing datasets based on medical data among medical specialists related to or involved in the development or testing of AI as well as programmers and data scientists to improve the process of independent evaluation of algorithms for AI-based applications.

This article presents a unified approach (methodology) to the development of datasets for objective (as far as possible in each specific case) testing of solutions using AI technologies in the field of radiation diagnostics. In the course of describing the stages of our proposed methodology, we give practical examples of datasets developed by us in the period from September 2019 to December 2020 using data

from the departments of radiological diagnostics of medical outpatient and inpatient institutions in Moscow deposited in the Unified Radiological Information Service (URIS UMIAS) [10]. The basic principles described in the article can be used to form medical datasets in other areas of medicine.

## METHODS AND RESULTS

A dataset differs from a simple collection of medical data in that it is endowed with special properties: data unification and structuring; a lack of gross inaccuracies or erroneous research; the presence of additional information (categories and values of attributes or characteristics of data items); and the presence of accompanying documentation. In the Russian Federation, a dataset is equated to a database and is subject to voluntary state registration as a result of intellectual activity. In foreign practice, datasets are often published not only as datasets available for download but also as scientific publications in journals. Each dataset is unique not only in the composition of the studies but also in the way they are classified and the approaches to markup, and the process of creating a dataset is exploratory in nature. Even in the presence of a structured method of dataset formation, at certain stages, departures, exceptions, and changes to the original dataset are possible, depending on its purpose.

The whole process can be divided into four major stages: planning, selection of initial data, markup and verification, and documentation (Fig. 1).

### 1. Planning stage

The preparation of a dataset, as in scientific research, begins with the planning stage, which consists of the following steps:

- formulation of a clinical and/or practical problem in the field of medicine, which is (potentially) subject to automation by intelligent systems;
- compilation of a list of features and/or characteristics of the initial data, information about which will be

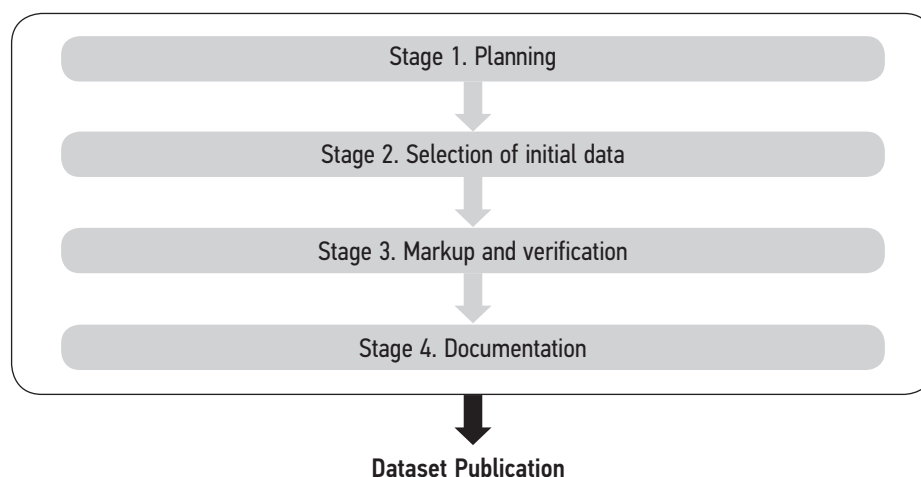


Fig. 1. Stages of forming a medical dataset.

received from the intelligent system in the process of solving the problem and by which it is possible to assess the correctness of the solution adopted by the system;

- determination of the verification methodology for the values of the selected features and/or characteristics of the elements of the generated data set;
- definition of data sources;
- description of the steps planned for data anonymization;
- determination of criteria for inclusion and exclusion of a study from the dataset;
- determination of significant data characteristics necessary to assess not only the accuracy but also the limits of the reliability and scalability of an intelligent system.

*Setting a clinical task* is one of the most important tasks facing the creator of a dataset. Insufficient attention to it leads to sudden pop-up questions both in the process of preparing a dataset and when introducing a diagnostic algorithm based on AI into clinical practice. (Fig. 2).

In order for the task to correspond to the class of tasks in which AI has established itself as a promising technology and, at the same time, has an important socioeconomic component from the point of view of clinical specialists, a working group of professionals of various profiles, namely clinicians, specialists on medical data processing, research engineers (machine learning or validating AI solutions), and administrators who access and upload raw data, should participate in task definition.

The clinical task should allow the creators of the dataset to answer the following questions:

- 1) What modalities, procedures, clinical, demographic, and similar information should be taken as input to the algorithm to solve it, and what should be taken as one data

unit?

- 2) What features should be determined using AI technologies?
- 3) What nosology or groups of nosology are the desired signs?
- 4) How does the solution to the problem help the clinical specialist?
- 5) How many data units are necessary and sufficient for the purpose of using the created dataset (AI validation, machine learning, etc.)?

An important criterion for the selection of the number of data units and characteristics of the study is the purpose of applying the dataset in relation to AI. The following classification of datasets can be given by their purpose:

- 1) general sets:
  - a self-test to check the AI for technical compliance;
  - a clinical test to assess the metrics of the accuracy and productivity of AI;
  - «additional training» for tweaking the already trained AI model;
  - machine learning for learning new models underlying AI and solving new clinical problems;
- 2) specialized kits:
  - dynamic sets for assessing changes over time (linking several data items to one subject);
  - technological defects to assess the stability and reliability of diagnostic solutions based on AI when attempting to analyze a defective study.

The number of research units required for a self-test is usually calculated individually for each type or model of the diagnostic device; the number of research units in dynamic sets and datasets for a clinical test is usually between 10 and 100; datasets for training and «additional training» can contain from several hundred to several tens of thousands of studies. The indicated quantities are rough estimates and

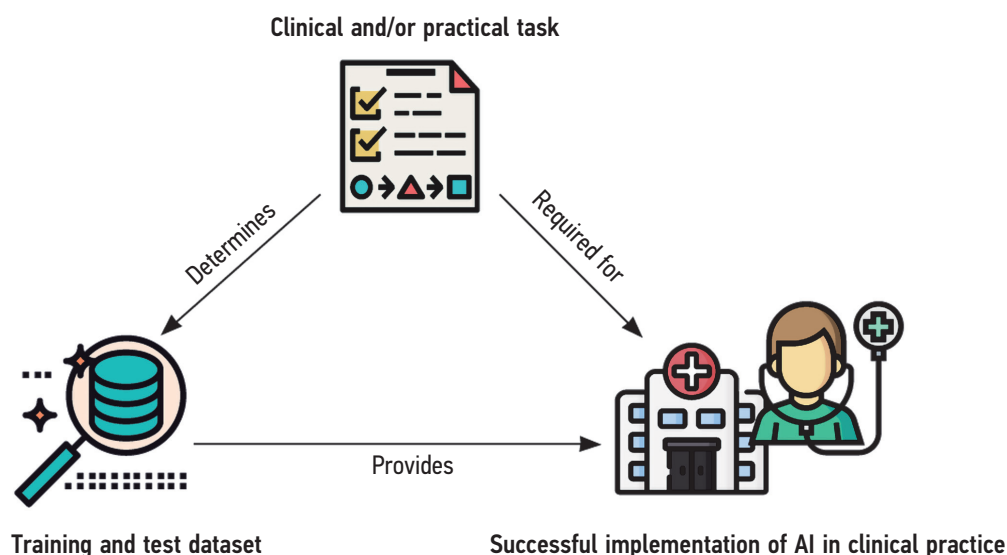


**Fig. 2.** Relationships among the clinical task, dataset, and success in the implementation of a solution based on artificial intelligence (AI) in routine clinical practice.

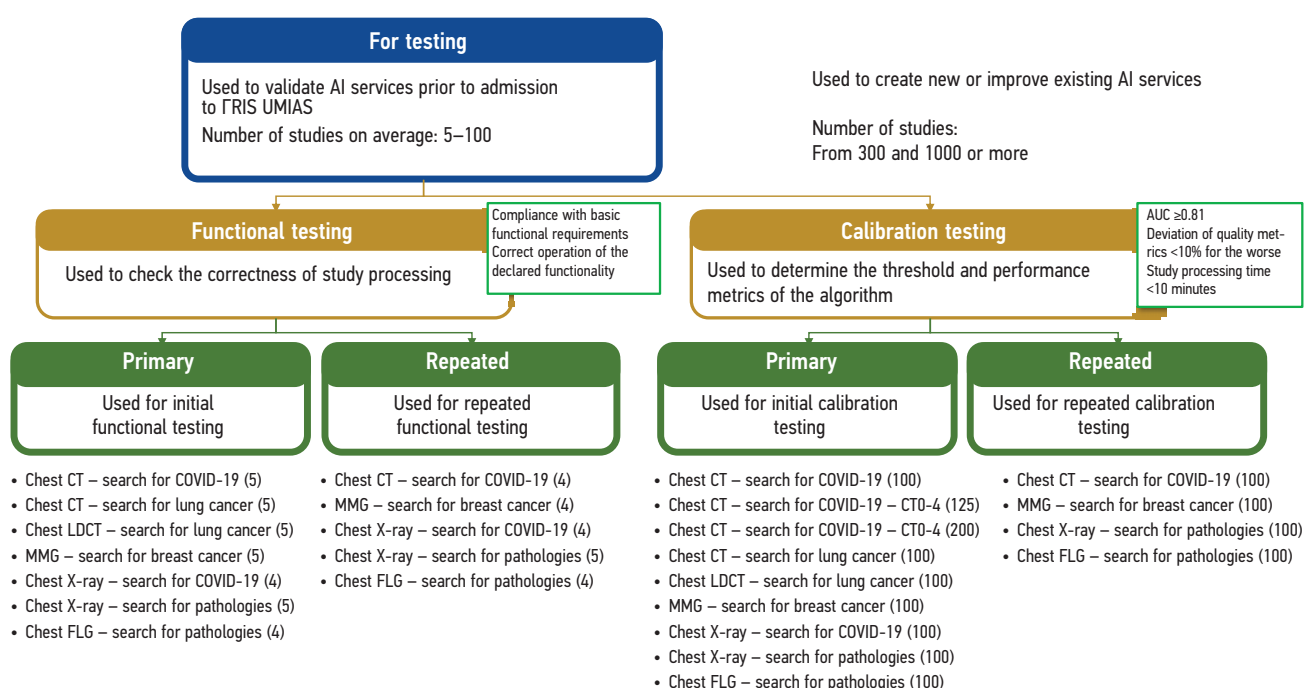


**Fig. 3.** Datasets of the Moscow experiment on the use of innovative technologies in the field of computer vision for the analysis of medical images and further use in the healthcare system of Moscow, prepared according to this method.

can vary widely depending on the availability of studies in the data source, the complexity of the clinical task, the detail and laboriousness of annotating the data, and other factors.

After the clinical task is defined, the criteria by which the intelligent system decides whether to assign a particular study or the area found in the image to a group of interest logically follows from it (basic diagnostic requirements for the work of AI). Diagnostic requirements include a formal description of the desired features of the study and also make up a list of features and/or characteristics, on the basis of which the data will be marked up in the dataset in the future. This information allows developers to more accurately customize solutions to determine the required features and for dataset preparation specialists to draw up instructions for marking and verifying data.

The balance of classes, namely in what proportion the studies in the dataset are distributed related to various features and/or characteristics, is of key importance for the value and significance of the obtained analysis of systems based on AI technologies using a dataset. In the simplest case, to assess the performance of intelligent diagnostic systems that provide dichotomous responses, an equal division is used between the two categories (for example, 50% of studies with signs of pathology according to the basic diagnostic requirements for the work of AI and 50% of studies without signs of pathology). In more complex cases, the division between several classes may be uneven and depend on the comparison method that will be used at a subsequent time.

Studies divided into classes according to a significant trait may have other differences, both in clinical (for example, the prevalence of female patients in the category with

signs of pathology, due to the age and sex pattern of morbidity) and in technical (for example, artificial sampling bias due to the preference for directing patients with an already-identified pathology to a study performed on a device with a higher resolution) aspects. In order to avoid systematic errors, it is necessary to identify signs, even though to do so will not contribute significantly to the solution to a clinical problem but will affect the operation of the diagnostic intelligent system, and when selecting studies in a dataset, we should strive to present different examples in each of the classes. The question of systematizing such signs and characteristics for a wide range of clinical tasks (that is, the issue of class balance in datasets) remains open and is being actively investigated at the present time [9].

At the end of the planning stage, *the sources of the initial data are determined, as well as the criteria for inclusion, non-inclusion, and exclusion* of studies from the dataset.

To create the most representative dataset, data sources should, if possible, be either the same or relevant to those information systems in which the implementation of AI-based solutions is planned in the future. For Moscow healthcare, an example of such a source is URIS UMIAS, which unites storage systems for the departments of radiological diagnostics of dozens of outpatient and inpatient medical institutions in Moscow.

Inclusion and exclusion criteria are often determined by a clinical and/or practical task, while exclusion criteria are usually supplemented in the course of working with primary data, since certain criteria are found that negatively affect the structure and unification of the data set. These criteria can be both medical (for example, age from 18 to 99 years;

presence of intact structure of the target organ, etc.), and technical (CT filter — soft tissue, convolution core — FC51, etc.). Data unification is necessary for the reliable operation of tools for evaluating the work of an AI-based solution (see Section 3 “Markup and verification”).

Take as an example the dataset “MosMedData: results of ultra-low-dose computed tomography with lesions in the lungs.”<sup>1</sup> The purpose of creating a database is to ensure the possibility of verifying the readiness of automated systems (including those using AI) to work in ERIS UMIAS. The clinical task is the search for and identification of pulmonary foci during lung cancer screening. For the dataset, anonymized computed tomography (CT) studies in DICOM format were selected, carried out in a special ultra-low-dose tomography mode (effective dose of radiation exposure less than 1 mSv at an increased voltage of 135 kV). One unit is one chest CT (CT) scan that meets the criteria below.

#### A. Inclusion criteria:

1. The patient's age is over 55 years and under 75 years.
2. Experience of smoking more than 30 packs per year (at least 1 pack per day for 30 years or 2 packs per day for 15 years, etc.).
3. Current smoking or smoking cessation no more than 15 years ago.
4. The study was carried out in the mode of ultra-low-dose CT in the first round of screening for lung cancer.

#### B. Criteria for non-inclusion:

1. Lung cancer detected within 2 years after the first round of lung cancer screening using ultra-low-dose CT.
2. History of lung cancer and/or lung surgery (not including percutaneous lung biopsy).
3. History of cancer diagnosed less than 5 years ago, with the exception of skin cancer and cervical cancer in situ.
4. The presence of pronounced pathology of the cardiovascular, immune, respiratory, or endocrine systems, as well as a life expectancy of less than 5 years.
5. Acute disease of the respiratory system.
6. Antibiotic treatment in the past 12 weeks.
7. Presence of hemoptysis or weight loss of more than 10 kg in the last year.

#### C. Criteria for exclusion:

1. Absence of pulmonary foci in the first round of Moscow lung cancer screening.

The target value of the number of studies in the final dataset (300) is sufficient for testing AI-based automated diagnostic systems (the total number is 312 units).

## 2. Stage of selection of initial data

After access is gained to the source of the initial data, the stage of selecting the initial (“raw”) data begins. The

approach to obtaining (unloading) the data depends on the source and method of data storage.

Medical data can be accumulated during the routine diagnostic process in a medical institution (MeSH: Routinely Collected Health Data), by direct data collection from the patient and/or his relatives and social workers (MeSH: Patient Generated Health Data), or as a result of targeted data collection, for example, during a clinical trial. Data collected on a routine basis usually has wide variability in parameters and allows the user to create the most representative dataset. When analyzing the data collected in the course of a clinical trial, attention is drawn to (1) the criteria for inclusion, non-inclusion, and exclusion of subjects from the study, set by its design and limiting the possibilities for preparing the dataset, as well as (2) the amount of data, which is limited by the power of the study.

Digitizing documents that are not primarily electronic makes little sense; documents stored on external media are often poorly structured, and digitizing and/or transferring data from other media can be costly (for example, transferring a radiation imaging database stored on CD-ROMs). The presence of a medical information system (MIS; MeSH: Health Information Systems) simplifies unloading, since it allows the user to apply filters and select the necessary studies by such criteria as, for example, the presence of a particular study or diagnosis. However, the necessary information is not contained in electronic medical records for all clinical tasks: lists of patients suitable for the criteria of a clinical task can be generated separately from the MIS, and the selection of studies for patients from these lists takes a significant amount of time.

The general principles for selecting “raw” data are the following:

- 1) Choose the largest possible range of studies of the modality and procedure of interest.
- 2) Preserve the amount of accompanying information necessary for solving the clinical problem (including text documents describing the results of the study, the clinical diagnosis of the patient who ended the medical case, etc.).
- 3) If possible, depersonalize the research “on the spot,” without leaving the information circuit of the institution in which the data is selected.

At the selection stage, the criteria for including and exclusion of the study in the future dataset are also applied. This operation can be carried out both directly, during the selection of studies in the MIS, and immediately after unloading (already outside the information circuit of a medical organization). It should be borne in mind that this step can lead to a 10-fold or greater decrease in the size of the dataset.

During study selection, the class balance identified in Step 1 should be borne in mind.

For example, for the dataset “MosMedData: Results of ultralow-dose computed tomography with lesions in the

<sup>1</sup> Morozov S.P., Gonchar A.P., Nikolaev A.E. et al. MosMedData: results of studies of ultra-low-dose computed tomography with lesions in the lungs (database). Certificate of state registration of the database No. 2020622727 dated 21.12.2020.

lungs" mentioned in the description of stage 1, stage 2 can consist of the following steps:

- 1) selection of patients in the MIS who underwent a study of low-dose chest CT in order to screen for malignant lung tumors;
- 2) analysis of electronic medical records of selected patients (life history, history of previous diseases, data from previous studies) to select patients in accordance with the inclusion and exclusion criteria formed at stage 1;
- 3) decision-making to include studies in the dataset in accordance with the desired balance of classes.

### 3. Markup and verification stage

Markup is the process of determining the value of attributes or characteristics for a data item in a dataset. Based on the markup, it becomes possible to classify elements and assign them to a particular group. For markup, both the information already available at the time of selection of the initial data (retrospective markup) and markup made by a specialist with medical education and/or work experience after the selection stage (prospective markup) can be used [9].

For retrospective markup, data from accompanying documents (such as, for example, the texts of conclusions for the results of instrumental studies), MIS, electronic medical records, etc. can be used. An example is the metadata generated automatically by the device during the study and stored in the initial data. The obvious advantage of retrospective markup is that it takes significantly less time on the part of healthcare professionals, since most of the preparatory work is performed by the data scientist.

Prospective markup involves the active involvement of medical professionals in the process of "saturation" of the dataset with additional information, for example, allowing the user to effectively divide the elements of the dataset into classes and categories. In radiation diagnostics, markup is most often understood as the classification of studies by classes (the presence or absence of radiological signs of the selected disease) as well as the graphic designation of the area of interest corresponding to the desired signs (for example, foci of demyelination in multiple sclerosis on MR images of the brain). The degree of involvement can be divided into more or less costly: in the first case, experts are asked to outline the contour of the area of interest and in the second, to designate its coordinates with a simple geometric figure.

In cases where expert opinion is the most significant factor in determining the values of features or characteristics of the data, it is reasonable to conduct a simultaneous reading of the study by two independent experts. In case of inconsistency between two experts, the disputed research is sent to a third, more qualified expert (based on practical experience, degree or other criteria). Studies that remain controversial after reading by three experts may be considered controversial and excluded from the dataset. From our practice of preparing a dataset consisting

of 100 chest CT with signs of various pathologies of the respiratory system, up to one quarter of the studies may be controversial after two independent readings; up to 4% of studies may remain controversial after being read by a third, more qualified expert (who has more than 5 years of medical experience).

Before proceeding with prospective markup, it is necessary to determine the scope of research of each specialist; the criteria for markup signs; and software that allows textual, graphic, or other designation of the desired features and prepare a markup of physician's instructions. In the process of preparing such instructions, if possible, the same working group that defined the clinical task at the planning stage should be involved.

Markup verification provides a degree of "trust" in markup on the part of developers or evaluators of intelligent systems. Markup verification can be divided into:

- low (the fact of the presence of a find) – based on the documentation;
- average (classification of finds) – based on expert opinion;
- high (confirmed diagnosis) – based on the results of a more sensitive research method or dynamic observation (repeated performance of the same method after a certain time interval).

The classification of markup types is shown in Fig. 4. Part of the dataset can have one class, while the other has a different class; a combination of retro- and prospective markup is allowed in the same dataset. An important part of the markup process is its correct documentation in the accompanying documentation (see clause 4 "Documentation stage").

For both retro- and prospective markup, various data automation tools can be used (for example, viewing medical imaging results and creating binary masks, analyzing databases) using various technologies and programming languages (C / C ++, Python, Kotlin, Java, etc.) [11].

### 4. Documentation stage

After the dataset has passed all the previous stages and is ready for transfer to third parties, it is considered "ready for publication." The publication of the dataset is accompanied by the release of the first major version (1.0.0), as well as the preparation and publication of accompanying documentation (README file).

In the process of preparing a dataset, certain criteria are inevitably overlooked that pop up when end users work directly with the dataset (specialists in validation of AI-based solutions or researchers using machine learning). Making adjustments to the dataset should be transparent to all process participants and users. Dataset versioning keeps track of such changes.

We have proposed the following original approach to solving the described problem as a variation of semantic versioning [12]:



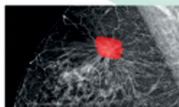
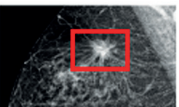
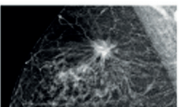
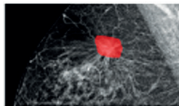
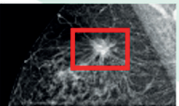
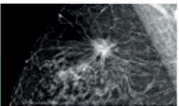
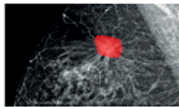
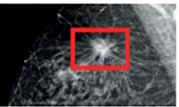
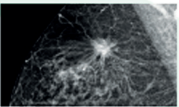
Markup classes		A		B		C	
		PROSPECTIVE				RETROSPECTIVE	
VALUE		Pixelized mask		Area coordinates		Metadata	
1	Confirmed diagnosis		Breast cancer (histological data)		Breast cancer (histological data)		Breast cancer (histological data)
2	Classification of findings		BI-RADS 2		BI-RADS 2		BI-RADS 2
3	Presence of findings		Foci are absent / Foci are present		Foci are absent / Foci are present		Foci are absent / Foci are present

Fig. 4. Classification of markup by labor costs and degree of verification

1. Major version (Major): increases when significant parameters of the dataset change, related to the clinical task, purpose, and principles of data marking and verification.
2. Minor version (Minor): increases when replacing, adding, or deleting data units in the dataset without changing other significant parameters of the dataset; in this case, the learning or validation algorithms can use the new minor version without changing the code. When a new major version is released, the minor version is set to 0.
3. Patch version (Patch): increases when making adjustments to the accompanying documentation, correcting typos and other errors in markup files, while the quantity and quality of data units in the dataset does not change. When a new major and/or minor version is released, the patch version is set to 0.

For ease of use of the dataset, a file named README.md in Markdown format and the generated README.pdf in Adobe PDF format are placed in the root directory. A unified approach to the structure of the README file will allow future organization of convenient searching and filtering of all published datasets. The basic structure of the README file is shown in Fig. 5; however, other sections can be added to the file if necessary.

For convenience of reporting, a single register of prepared data sets is of practical value, an example of which is given in Table 1 [13].

The minimum set of recommended registry fields is the following:

1. The sequential number of the registry entry.
2. An internal code unique to the dataset in the current registry and/or institution.


Dataset name

Organization logo

Abstract (1–2 sentences)

Disclaimer

- dataset name
- license conditions (main)
- special conditions prohibiting the use of the dataset

 License designation

License designation

Dataset name

- Name
- Internal code
- Markup classes
- Key words
- Language
- Financing
- Version
- Constant reference
- Publication date

Affiliation and authors

- Authors
- Affiliation

Structure of dataset

- Directory and file structure diagram
- Description of files in the root directory
- Description of the principle of naming directories
- Description of the principle of naming files

Data review

Parameter	Value

- Features of research preparation
- Principles of data markup
- Principles of data markup verification

Terms of use and distribution

- License
- Copyright
- Recommended citation form
- Distribution rules

Fig. 5. Basic structure of the README file.

3. The purpose and scope of the dataset.
4. Modality/procedure (characteristics of studies, suitable for their search and selection in the IIA).
5. Searched signs and/or target pathology (if possible, indicating the code of the International Classification of Diseases).
6. The definition of a data unit.
7. The number of data units (if possible, indicating the output volume of data in MB, GB, or TB).
8. Markup classes indicating the number of records in each class.

## DISCUSSION

This paper presents an experimental approach to the formation of sets of medical data (datasets) for use in the development and evaluation of intelligent medical diagnostic systems using AI technologies.

The use of a large-scale MIS (URIS UMIAS) as a data source for a dataset is a certain guarantee of its representativeness. The performance parameters of the AI algorithm after implementation in the diagnostic process will most likely correspond to the parameters obtained during validation on such a dataset. At the same time, it is necessary to account for the variability of the fleet of diagnostic devices, as well as variations in the physical parameters of the studies being carried out, while attempting to present the widest range of studies in the dataset. The value of the variability of devices from different manufacturers presented in datasets can be of practical importance for fine-tuning the threshold of AI systems in order to ensure their reliable operation [14].

Another advantage of working with URIS UMIAS is practically unlimited access to hundreds of thousands of beam studies of various modalities, which permits the creation of datasets with extremely diverse sets of technical, demographic, and clinical characteristics. Such variations ensure the value of the generated datasets for assessing not only the accuracy but also the scalability and reliability of the AI systems being developed and tested.

The proposed approach was developed and tested during the creation of 25 datasets in seven directions in radiation diagnostics with a total of more than 1400 data units (studies), including during the implementation of the Moscow experiment on the use of innovative technologies in the field of computer vision for the analysis of medical images and further application in the healthcare system in Moscow [15] (see Fig. 3). A complete list of datasets is given in the table 1. The provisions described in this article are consistent with the criteria for reference datasets included in the guidelines for clinical trials of software based on intelligent technologies in radiation diagnostics [16].

Over the course of the Moscow experiment, an independent external assessment of AI algorithms is provided in two stages (functional and calibration testing, respectively): at the first stage, relatively small datasets (up to five data

units) are used to check the technical feasibility of reading and processing studies; at the second stage, medium-sized datasets are used (on average, from 100 to 200 data units) to compare the results of processing AI studies with a verified markup. In cases where, as a result of initial testing, the developer of an AI-based solution receives recommendations for finalizing their solution, it is possible to retest said solution on a different dataset.

An important part of the life cycle of a dataset in the post-publication phase is the scientific presentation of the work in relevant publications and manuscripts. One of the portals that support free placement of information on public datasets is medRxiv<sup>2</sup> — service of preprints on biomedical topics. The advantage of the service is the absence of external peer review of publications, which allows the community to be informed about the results of their work as soon as possible. An example of a publication about a dataset on the medRxiv portal is presented in [17].

It should be noted that datasets generated by this method are successfully used by domestic and foreign research teams, as evidenced by recent publications [18, 19]. The use of the work product in practice confirms the timeliness and adequacy of the formulated approaches and methodology.

When the necessary changes are made, the technique can be fully or partially used not only for other areas in radiation diagnostics but also outside of it, in other areas of practical medicine, in which primary electronic information is accumulated in the course of medical activity (electroencephalograms, electrocardiograms, and other records of physiological signals, records from bedside resuscitation monitors, log records of modern laboratory equipment, such as chemical analyzers, etc.). In particular, the principles of formulating a clinical and/or practical problem, working with MIS for unloading initial data, general principles of marking and documenting in an experimental mode were successfully tested in the formation of a data set of electrocardiograms with signs of cardiovascular diseases. In the future, this technique can be included in the state standard, thereby ensuring the continuity and unification of medical datasets for teaching and testing AI technologies at the national level.

A hotly debated issue is the problem of depersonalization of medical data, especially the results of radiation studies. There is currently no generally accepted standard for anonymizing medical images. Professionals working with this kind of data must follow a sound logic to prevent the disclosure of the patient's confidential medical information and personal data. It should be remembered that the results of a radiation study in and of themselves can serve as a source of personal data: for example, it is possible to reconstruct a three-dimensional image of the soft tissues of the facial skull from head cuts, which in turn makes it possible to sufficiently identify a person. Despite the absence of explicit legislative norms or standards for depersonalization in such

<sup>2</sup> Access mode: <https://medrxiv.org>. Access date: 15.01.2021.

**Table 1.** List of medical DATASets developed using the described experimental approach

No.	Internal code	Purpose	Modality/Procedure	Desired signs and/ or target nosology	Data unit	Number of data units	Markup classes (number of data units)
1	DS_FT-I_CT_OGK_CANCER	FT-I	CHEST CT	Lung cancer	CT	5	Without signs of pathology (2), with signs of pathology (2), with technical defect (1)
2	DS_FT-I_CT_OGK_COVID	FT-I	CHEST CT	Viral pneumonia (COVID-19)	CT	5	
3	DS_FT-II_CT_OGK_COVID	FT-II	CHEST CT	Viral pneumonia (COVID-19)	CT	4	Without signs of pathology (2), with signs of pathology (2)
4	DS_FT-I_LDCT_OGK_CANCER	FT-I	CHEST LDCT	Lung cancer	CT	5	Without signs of pathology (2), with signs of pathology (2), with technical defect (1)
5	DS_FT-I_MMG_CANCER	FT-I	MMG	Breast cancer	MMG	5	
6	DS_FT-II_MMG_CANCER	FT-II	MMG	Breast cancer	MMG	4	Without signs of pathology (2), with signs of pathology (2)
7	DS_FT-I_DX_OGK_PAT	FT-I	CHEST X-RAY	Respiratory pathology	X-ray study	5	Without signs of pathology (2), with signs of pathology (2), with technical defect (1)
8	DS_FT-II_DX_OGK_PAT	FT-II	CHEST X-RAY	Respiratory pathology	X-ray study	5	
9	DS_FT-I_DX_OGK_COVID	FT-I	CHEST X-RAY	Viral pneumonia (COVID-19)	X-ray study	4	
10	DS_FT-II_DX_OGK_COVID	FT-II	CHEST X-RAY	Viral pneumonia (COVID-19)	X-ray study	4	Without signs of pathology (2), with signs of pathology (2)
11	DS_FT-I_FLG_OGK_PAT	FT-I	CHEST FLG	Respiratory pathology	FLG	4	
12	DS_FT-II_FLG2_OGK_PAT	FT-II	CHEST FLG	Respiratory pathology	FLG	4	
13	DS_CT-I_CT_OGK_CANCER	CIT-I	CHEST CT	Lung cancer	CT	100	Without signs of pathology (50), with signs of pathology (50)
14	DS_CT-I_CT_OGK_COVID	CIT-I	CHEST CT	Viral pneumonia (COVID-19)	CT	100	

Table. Continuation.

No.	Internal code	Purpose	Modality/Procedure	Desired signs and/or target nosology	Data unit	Number of data units	Markup classes (number of data units)
	DS_CT-II_CT_OGK_COVID	CIT-II	CHEST CT	Viral pneumonia (COVID-19)	CT	100	Without signs of pathology (50), with signs of pathology (50)
	DS_CT-II_CT_OGK_COVID_2	CIT-I	CHEST CT	Viral pneumonia (COVID-19)	CT	125	CT0 (25), CT1 (25), CT2 (25), CT3 (25), CT4 (25)
	DS_CT-II_CT_OGK_COVID_3	CIT-I	CHEST CT	Viral pneumonia (COVID-19)	CT	200	CT0 (100), CT1 (25), CT2 (25), CT3 (25), CT4 (25)
	DS_CT-I_LDCT_OGK_CANCER	CIT-I	CHEST LDCT	Lung cancer	CT	100	
	DS_CT-I_MMG_CANCER	CIT-I	MMG	Breast cancer	MMG	100	
	DS_CT-II_MMG_CANCER	CIT-II	MMG	Breast cancer	MMG	100	
	DS_CT-I_DX_OGK_CANCER	CIT-I	CHEST X-RAY	Respiratory pathology	X-ray study	100	Without signs of pathology (50), with signs of pathology (50)
	DS_CT-II_DX_OGK_CANCER	CIT-II	CHEST X-RAY	Respiratory pathology	X-ray study	100	
	DS_CT-I_DX_OGK_COVID	CIT-I	CHEST X-RAY	Viral pneumonia (COVID-19)	X-ray study	100	
	DS_CT-I_FLG_OGK_CANCER	CIT-I	CHEST FLG	Respiratory pathology	FLG	100	
	DS_CT-II_FLG_OGK_CANCER	CIT-II	CHEST FLG	Respiratory pathology	FLG	100	

Note. FT-I — primary functional testing; FT-II — repeated functional testing; CIT-I — primary calibration testing; CIT-II — repeated calibration testing; CT — computed tomography; MMG — mammography; X-ray — X-ray study; FLG — fluorography; Chest — thoracic organs; CT1 — areas of induration by the type of frosted glass; involvement of the lung parenchyma is  $\leq 25\%$ . CT2 — areas of induration by the type of frosted glass; involvement of the lung parenchyma is 25–50%. CT3 — areas of induration by the type of frosted glass and consolidation; involvement of the lung parenchyma is 50–75%. CT4 — diffuse induration of the lung tissue like ground glass and consolidation in combination with reticular changes; involvement of the lung parenchyma is  $> 75\%$  [13].

situations, the author of the dataset should make the decision to remove the record of soft tissues of the head from the studies, starting from the clinical and/or practical task and continuing with the purpose of the dataset.

To maintain the growth rates of the market for AI technologies in medicine, one should, if possible, consider providing free access to datasets, subject to all the anonymization conditions described above. Portals such as arXiv (<https://arxiv.org>), medRxiv (<https://medrxiv.org>), and Zenodo (<https://zenodo.org>) are used to publish articles describing datasets. There are a large number of public repositories of open datasets, as well as integral search on them, for example, Google's Dataset Search<sup>3</sup>. One of the ways to not only ensure legal access to datasets but also to attract attention from the AI developer community is to conduct online competitions among AI developers on platforms such as Kaggle<sup>4</sup>.

A promising direction of development is the use of "digital twins of the disease," extensive sets of information about patients of various profiles (social, demographic, behavioral, etc.) for the formation of statistical signs characteristic of patients suffering from a specific disease. The use of such information can make it possible to create more representative medical datasets, including the widest range of signs and factors of the disease that are significant for the clinical and/or practical task. The basis for the creation of a "digital twin of a disease" is, first of all, the analysis and processing of impersonal information obtained from "digital twins of patients" containing the widest possible set of diverse information about a patient.

The approach presented in this article makes it possible to systematize and standardize the preparation of datasets and their life cycle for subsequent use in the testing of intelligent systems (including those based on AI) and registering tested systems for their further use in the healthcare sector. Such a step-by-step and detailed methodology for dataset

formation will allow developers to objectively evaluate their products and regulators to ensure the objectivity and transparency of the assessment process using datasets created on the basis of the proposed methodology.

## CONCLUSION

The task of forming sets of medical data for training and validating diagnostic systems based on AI technologies is gaining critical importance in connection with active development of this field. The original approaches described in the article can serve as a starting point for the creation of a full-fledged methodology for the preparation and standardization of medical datasets of various modalities and types of data. Moreover, they can be used to determine the conditions and factors necessary for the successful practical application of this methodology.

## ADDITIONAL INFORMATION

**Funding source.** This study was not supported by any external sources of funding.

**Competing interests.** The authors declare that they have no competing interests.

**Author contribution.** N.A. Pavlov — manuscript design and writing, development of an approach for dataset formation, formation of dataset examples; S.P. Morozov — concept of research; A.E. Andreychenko — study design, manuscript curation and editing; A.V. Vladzymyrskyy — scientific rationale for dataset formation; A.A. Revazyan — literature review, formation of dataset examples; Yu.S. Kirpichev — formation of dataset examples. All authors made a substantial contribution to the conception of the work, acquisition, analysis, interpretation of data for the work, drafting and revising the work, final approval of the version to be published and agree to be accountable for all aspects of the work.

## REFERENCES

1. Gusev AV. Prospects for neural networks and deep machine learning in creating health solutions (Complex medical information system, Russian). *Vrach i Informatsionnye Tekhnologii*. 2017;(3):92–105. (In Russ).
2. Ranschaert ER, Morozov S, Algra PR, eds. Artificial intelligence in medical imaging. Cham: Springer International Publishing; 2019. doi: 10.1007/978-3-319-94878-2
3. Griffith B, Kadom N, Straus CM. Radiology Education in the 21st Century: Threats and Opportunities. *J Am Coll Radiol*. 2019;16(10):1482–1487. doi: 10.1016/j.jacr.2019.04.003
4. Savadjiev P, Chong J, Dohan A, et al. Demystification of AI-driven medical image interpretation: past, present and future. *Eur Radiol*. 2019;29(3):1616–1624. doi: 10.1007/s00330-018-5674-x
5. Ng A. What artificial intelligence can and can't do right now. Harvard Business Review; 2016. Available from: <https://hbr.org/2016/11/what-artificial-intelligence-can-and-cant-do-right-now>
6. Renear H, Sacchi S, Wickett KM. Definitions of dataset in the scientific and technical literature. *Proceedings of the American Society for Information Science and Technology*. 2010;47(1):1–4. doi: 10.1002/meet.14504701240
7. Tan SL, Gao G, Koch S. Big data and analytics in healthcare. *Methods Inf Med*. 2015;54(6):546–547. doi: 10.3414/ME15-06-1001
8. Kohli MD, Summers RM, Geis JR. Medical image data and datasets in the era of machine learning—whitepaper from the 2016 C-MIMI meeting dataset session. *J Digit Imaging*. 2017;30(4):392–399. doi: 10.1007/s10278-017-9976-3
9. Willemink MJ, Koszek WA, Hardell C, et al. Preparing medical imaging data for machine learning. *Radiology*. 2020;295(1):4–15. doi: 10.1148/radiol.2020192224

<sup>3</sup> <https://datasetsearch.research.google.com>. Accessed: 15.01.2021.

<sup>4</sup> <https://kaggle.com>. Accessed: 15.01.2021.



10. Morozov SP, Shelekhov PV, Vladzimirsky AV. Modern approaches to the radiology service improvement. *Health Care Standardization Problems*. 2019;(5-6):30–34. (In Russ). doi: 10.26347/1607-2502201905-06030-034
11. Kulberg NS, Gusev MA, Reshetnikov RV, et al. Methodology and tools for creating training samples for artificial intelligence systems for recognizing lung cancer on CT images. *Health Care Russian Federation*. 2021;64(6):343–350. doi: 10.46563/0044-197x-2020-64-6-343-350
12. Preston-Werner T. Semantic Versioning 2.0.0 [Internet]. Available from: <https://semver.org>
13. Morozov SP, Protsenko DN, Smetanina SV, et al. Radiation diagnostics of coronavirus disease (COVID-19): organization, methodology, interpretation of results: Preprint No.CDT — 2020 — II. Version 2 from 17.04.2020. The series “Best practices of radiation and instrumental diagnostics”. Issue 65. Moscow : Scientific and Practical Clinical Center for Diagnostics and Telemedicine Technologies of the Moscow Department of Health; 2020. 80 p. (In Russ). Available from: <https://tele-med.ai/biblioteka-dokumentov/luchevaya-diagnostika-koronavirusnoj-bolezni-covid-19-organizaciya-metodologiya-interpretaciya-rezultatov>
14. Pavlov N. ECR 2021: Value of technical stratification of medical datasets for AI services. Moscow, 2021. [Internet]. Available from: <https://connect.myesr.org/course/ai-in-breast-imaging/>
15. Morozov SP, Vladzimirsky A, Andreychenko A, et al. Moscow experiment on computer vision in radiology: involvement and participation of radiologists. *Vrach i informacionnye tehnologii*. 2020;(4):14–23. doi: 10.37690/1811-0193-2020-4-14-23
16. Morozov SP, Vladzimirsky AV, Klyashtorny VG, et al. Clinical acceptance of software based on artificial intelligence technologies (radiology). Series “Best practices in medical imaging”. Issue 57. Moscow; 2019. 45 p.
17. Morozov SP, Andreychenko AE, Pavlov NA, et al. MosMedData: Chest CT scans with COVID-19 related findings dataset. *medRxiv*. 2020. doi: 10.1101/2020.05.20.20100362
18. Sushentsev N, Bura V, Kotniket M, et al. A head-to-head comparison of the intra- and interobserver agreement of COVID-RADS and CO-RADS grading systems in a population with high estimated prevalence of COVID-19. *BJR Open*. 2020;2(1):20200053. doi: 10.1259/bjro.20200053
19. Jin C, Chen W, Caoet Y, et al. Development and evaluation of an artificial intelligence system for COVID-19 diagnosis. *Nat Commun*. 2020;11(1):5088. doi: 10.1038/s41467-020-18685-1

## СПИСОК ЛИТЕРАТУРЫ

1. Гусев А.В. Перспективы нейронных сетей и глубокого машинного обучения в создании решений для здравоохранения // Врачи и информационные технологии. 2017. № 3. С. 92–105.
2. Ranschaert E.R., Morozov S., Algra P.R., eds. Artificial intelligence in medical imaging. Cham: Springer International Publishing; 2019. doi: 10.1007/978-3-319-94878-2
3. Griffith B., Kadom N., Straus C.M. Radiology Education in the 21st Century: Threats and Opportunities // J Am Coll Radiol. 2019. Vol. 16, N 10. P. 1482–1487. doi: 10.1016/j.jacr.2019.04.003
4. Savadjiev P., Chong J., Dohan A., et al. Demystification of AI-driven medical image interpretation: past, present and future // European Radiology. 2019. Vol. 29, N 3, P. 1616–1624. doi: 10.1007/s00330-018-5674-x
5. Ng A. What artificial intelligence can and can't do right now. Harvard Business Review; 2016. Available from: <https://hbr.org/2016/11/what-artificial-intelligence-can-and-cant-do-right-now>
6. Renear H., Sacchi S., Wickett K.M. Definitions of dataset in the scientific and technical literature // Proceedings of the American Society for Information Science and Technology. 2010. Vol. 47, N 1. P. 1–4. doi: 10.1002/meet.14504701240
7. Tan S.L., Gao G., Koch S. Big data and analytics in health-care // Methods Inf Med. 2015. Vol. 54, N 6. P. 546–547. doi: 10.3414/ME15-06-1001
8. Kohli M.D., Summers R.M., Geis J.R. Medical image data and datasets in the era of machine learning—whitepaper from the 2016 C-MIMI meeting dataset session // J Digit Imaging. 2017. Vol. 30, N 4. P. 392–399. doi: 10.1007/s10278-017-9976-3
9. Willeminck M.J., Koszek W.A., Hardell C., et al. Preparing medical imaging data for machine learning // Radiology. 2020. Vol. 295, N 1. P. 4–15. doi: 10.1148/radiol.2020192224
10. Морозов С.П., Шелехов П.В., Владимирский А.В. Современные стандартизованные подходы к совершенствованию службы лучевой диагностики // Проблемы стандартизации в здравоохранении. 2019. № 5-6. С. 30–34. doi: 10.26347/1607-2502201905-06030-034
11. Kulberg N.S., Gusev M.A., Reshetnikov R.V., et al. Methodology and tools for creating training samples for artificial intelligence systems for recognizing lung cancer on CT images // Health Care Russian Federation. 2021. Vol. 64, N 6. P. 343–350. doi: 10.46563/0044-197x-2020-64-6-343-350
12. Preston-Werner T. Semantic Versioning 2.0.0 [Internet]. Available from: <https://semver.org>
13. Морозов С.П., Проценко Д.Н., Сметанина С.В. и др. Лучевая диагностика коронавирусной болезни (COVID-19): организация, методология, интерпретация результатов : препринт № ЦДТ — 2020 — II. Версия 2 от 17.04.2020. Серия «Лучшие практики лучевой и инструментальной диагностики». Вып. 65. Москва : ГБУЗ НПКЦ ДиТ ДЗМ, 2020. 80 с. Режим доступа: <https://tele-med.ai/biblioteka-dokumentov/luchevaya-diagnostika-koronavirusnoj-bolezni-covid-19-organizaciya-metodologiya-interpretaciya-rezultatov>. Дата обращения: 15.01.2021.
14. Pavlov N. ECR 2021: Value of technical stratification of medical datasets for AI services. Moscow, 2021. [Internet]. Available from: <https://connect.myesr.org/course/ai-in-breast-imaging/>
15. Морозов С.П., Владимирский А.В., Ледихова Н.В. и др. Московский эксперимент по применению компьютерного зрения в лучевой диагностике: вовлеченность врачей-рентгенологов // Врачи и информационные технологии. 2020. № 4. С. 14–23. doi: 10.37690/1811-0193-2020-4-14-23
16. Morozov S.P., Vladzimirsky A.V., Klyashtorny V.G., et al. Clinical acceptance of software based on artificial intelligence tech-

nologies (radiology). Series «Best practices in medical imaging». Issue 57. Moscow; 2019. 45 p.

**17. Morozov S.P., Andreychenko A.E., Pavlov N.A., et al.** MosMed-Data: Chest CT scans with COVID-19 related findings dataset // medRxiv. 2020. doi: 10.1101/2020.05.20.20100362

**18. Sushentsev N., Bura V., Kotniket M., et al.** A head-to-head comparison of the intra- and interobserver agreement of COVID-RADS

and CO-RADS grading systems in a population with high estimated prevalence of COVID-19 // BJR Open. 2020. Vol. 2, N 1. P. 20200053. doi: 10.1259/bjro.20200053

**19. Jin C., Chen W., Caoet Y., et al.** Development and evaluation of an artificial intelligence system for COVID-19 diagnosis // Nat Commun. 2020. Vol. 11, N 1. P. 5088. doi: 10.1038/s41467-020-18685-1

## AUTHORS' INFO

**\*Nikolay A. Pavlov, MD;**

address: 28-1, Srednyaya Kalitnikovskaya street, 109029, Moscow, Russia; tel.: +7 (495) 276-04-36;

ORCID: <https://orcid.org/0000-0002-4309-1868>;

eLibrary SPIN: 9960-4160; e-mail: n.pavlov@npcmr.ru

**Anna E. Andreychenko, PhD;**

ORCID: <https://orcid.org/0000-0001-6359-0763>;

eLibrary SPIN: 6625-4186; e-mail: a.andreychenko@npcmr.ru

**Anton V. Vladzymyrskyy, MD, Dr. Sci. (Med.);**

ORCID: <https://orcid.org/0000-0002-2990-7736>;

eLibrary SPIN: 3602-7120; e-mail: a.vladimirsky@npcmr.ru

**Anush A. Revazyan;**

ORCID: <http://orcid.org/0000-0003-1589-2382>;

e-mail: anushrevazyan@gmail.com

**Yury S. Kirpichev;**

ORCID: <http://orcid.org/0000-0002-9583-5187>;

eLibrary SPIN: 3362-3428; e-mail: y.kirpichev@npcmr.ru

**Sergey P. Morozov, MD, Dr. Sci. (Med.), Professor;**

ORCID: <http://orcid.org/0000-0001-6545-6170>;

eLibrary SPIN: 8542-1720; e-mail: morozov@npcmr.ru

## ОБ АВТОРАХ

**\*Павлов Николай Александрович;**

адрес: Россия, 109029, Москва, ул. Средняя Калитниковская, д. 28, стр. 1; тел.: +7 (495) 276-04-36;

ORCID: <https://orcid.org/0000-0002-4309-1868>;

eLibrary SPIN: 9960-4160; e-mail: n.pavlov@npcmr.ru

**Андрейченко Анна Евгеньевна, к.ф.-м.н.;**

ORCID: <https://orcid.org/0000-0001-6359-0763>;

eLibrary SPIN: 6625-4186; e-mail: a.andreychenko@npcmr.ru

**Владимирский Антон Вячеславович, д.м.н.;**

ORCID: <https://orcid.org/0000-0002-2990-7736>;

eLibrary SPIN: 3602-7120; e-mail: a.vladimirsky@npcmr.ru

**Ревазян Ануш Артуровна;**

ORCID: <http://orcid.org/0000-0003-1589-2382>;

e-mail: anushrevazyan@gmail.com

**Кирпичев Юрий Сергеевич;**

ORCID: <http://orcid.org/0000-0002-9583-5187>;

eLibrary SPIN: 3362-3428; e-mail: y.kirpichev@npcmr.ru

**Морозов Сергей Павлович, д.м.н., профессор;**

ORCID: <http://orcid.org/0000-0001-6545-6170>;

eLibrary SPIN: 8542-1720; e-mail: morozov@npcmr.ru





DOI: <https://doi.org/10.17816/DD60493>

# MRI evaluation of the neoadjuvant chemoradiation therapy result in a patient with rectal cancer, supplemented with T2-WI texture analysis of the tumor: a clinical case

© Yana A. Dayneko, Tatiana P. Berezovskaya, Sofia A. Myalina, Ivan A. Orekhov, Alexey A. Nevolskikh

A. Tsyb Medical Radiological Research Centre – branch of the National Medical Research Radiological Centre, Obninsk, Russian Federation

## ABSTRACT

The article presents a clinical case of using the active follow-up strategy (the so-called watch & wait) in a 73-year-old patient with cancer of the lower rectum with a good response to neoadjuvant chemoradiation therapy (NCRT). After 3 years of regular follow-up, including digital rectal examination, rectoscopy and MRI, indicating the absence of tumor progression, PET/CT with 18F-FDG was obtained, which revealed a region of hypermetabolic activity in the lower rectum (SUVmax 27.1), in connection with which it was decided to carry out surgical treatment. When discussing the issue of the volume of the operation, MRI data were taken into account, supplemented by the results of T2-weighted texture analysis, which confirmed the absence of progression. The patient underwent organ-preserving treatment in the amount of trans-anal tumor resection. Pathomorphological examination after surgery established the inflammatory changes in the intestinal wall and absence of tumor. This case demonstrates the effectiveness of the standard examination volume when using the watch & wait strategy and the possibility of using T2-WI texture analysis to increase the reliability of MRI assessment of tumor response to chemotherapy.

**Keywords:** rectal cancer; magnetic resonance imaging; texture analysis; neoadjuvant chemoradiotherapy; response assessment on treatment.

## To cite this article

Dayneko YaA, Berezovskaya TP, Myalina SA, Orekhov IA, Nevolskikh AA. MRI evaluation of the neoadjuvant chemoradiation therapy result in a patient with rectal cancer, supplemented with T2-WI texture analysis of the tumor: a clinical case. *Digital Diagnostics*. 2021;2(1):67–74. DOI: <https://doi.org/10.17816/DD60493>

Received: 10.02.2021

Accepted: 03.03.2021

Published: 12.03.2021



DOI: <https://doi.org/10.17816/DD60493>

# **МРТ-оценка результата неоадьювантной химиолучевой терапии у больной раком прямой кишки, дополненная текстурным анализом Т2-ВИ опухоли (клинический случай)**

© Я.А. Дайнеко, Т.П. Березовская, С.А. Мялина, И.А. Орехов, А.А. Невольских

Медицинский радиологический научный центр имени А.Ф. Цыба – филиал ФГБУ «Национальный медицинский исследовательский центр радиологии», Обнинск, Российская Федерация

## **АННОТАЦИЯ**

В работе представлен клинический случай использования стратегии активного динамического наблюдения (watch & wait) у 73-летней больной раком нижнеампулярного отдела прямой кишки с хорошим ответом на неоадьювантную химиолучевую терапию. После трёх лет регулярного наблюдения, включающего пальцевое ректальное исследование, ректоскопию и магнитно-резонансную томографию (МРТ), указывавших на отсутствие прогрессирования опухоли, были получены результаты позитронно-эмиссионной томографии с <sup>18</sup>F-фтордезоксиглюкозой, совмещённой с компьютерной томографией, выявившей в нижнеампулярном отделе прямой кишки участок гиперметаболической активности (SUV<sub>max</sub> 27,1), в связи с чем было принято решение о проведении хирургического лечения. При обсуждении вопроса об объёме операции были учтены данные МРТ, дополненные результатами текстурного анализа Т2-ВИ, подтвердившие отсутствие прогрессирования. Пациентке было проведено органосохраняющее лечение в объёме трансанальной резекции опухоли. Патоморфологическое исследование операционного препарата установило воспалительные изменения в стенке кишки и отсутствие опухоли. Данный случай демонстрирует эффективность стандартного объёма обследования при использовании стратегии watch & wait и возможность использования текстурного анализа Т2-ВИ для повышения надёжности МРТ-оценки ответа опухоли на химиолучевую терапию.

**Ключевые слова:** рак прямой кишки; магнитно-резонансная томография; неоадьювантная химиолучевая терапия; текстурный анализ; ответ опухоли на лечение.

## **Как цитировать**

Дайнеко Я.А., Березовская Т.П., Мялина С.А., Орехов И.А., Невольских А.А. МРТ-оценка результата неоадьювантной химиолучевой терапии у больной раком прямой кишки, дополненная текстурным анализом Т2-ВИ опухоли (клинический случай) // *Digital Diagnostics*. 2021. Т. 2, №1. С. 67–74. DOI: <https://doi.org/10.17816/DD60493>

DOI: <https://doi.org/10.17816/DD60493>

# MRI评价1例直肠癌新辅助放化疗结果，辅以肿瘤T2WI结构分析（临床病例）

© Yana A. Dayneko, Tatiana P. Berezovskaya, Sofia A. Myalina, Ivan A. Orekhov, Alexey A. Nevolskikh

A. Tsyb Medical Radiological Research Centre – branch of the National Medical Research Radiological Centre, Obninsk, Russian Federation

## 简评：

本文报告一名对新辅助化疗有良好反应的73岁下段壶腹直肠癌患者，采用积极动态随访策略（Watch & Wait策略）的临床病例。经过三年的定期随访，包括指状直肠检查、直肠镜检查 and 磁共振成像（MRI），表明肿瘤没有进展，得到了18F氟脱氧葡萄糖正电子发射断层摄影与计算机断层摄影的结果。结果显示直肠下段壶腹部有一个高代谢活动的部位（SUV<sub>max</sub> 27.1），因此决定进行手术治疗。讨论手术范围时，考虑MRI资料，辅以T2WI分析结果，证实无疾病进展。患者接受了保留器官的经肛门肿瘤切除体积的治疗。手术准备的病理形态学检查确定了肠壁炎症改变和肿瘤的消失。本案例证明了标准调查体积在使用Watch & Wait策略时的有效性，以及使用T2WI分析来提高MRI评估肿瘤对放化疗反应的可靠性的可能性。

**关键词：**直肠癌；磁共振成像；新辅助化疗；结构分析；肿瘤对治疗的反应。

## 引用本文：

Dayneko YaA, Berezovskaya TP, Myalina SA, Orekhov IA, Nevolskikh AA. MRI评价1例直肠癌新辅助放化疗结果，辅以肿瘤 T2WI结构分析（临床病例）. *Digital Diagnostics*. 2021;2(1):67–74. DOI: <https://doi.org/10.17816/DD60493>

收到: 10.02.2021

接受: 03.03.2021

发布时间: 12.03.2021

## BACKGROUND

The current standard of treatment for rectal lower ampullary cancer is the combination of neoadjuvant chemoradiation therapy (NHRT) and surgery [1]. Some patients with a complete or almost complete response to NHRT no longer need an aggressive surgical treatment; instead, they undergo moderate techniques, such as transanal endoscopic microsurgery. Others may even completely refuse surgery in favor of an active monitoring (i.e., watch and wait) strategy, which includes regular digital rectal examination, rectoscopy, and magnetic resonance imaging (MRI). However, in the case of obtaining conflicting clinical and diagnostic data during follow-up, additional criteria are required, thereby increasing the reliability of diagnostics. Such criteria can be established via the radiomic analysis of diagnostic images; consequently, the structural heterogeneity of a tumor tissue and its changes as a result of treatment can be described using quantitative indicators obtained through the computer processing of medical images [2].

## CLINICAL CASE

In the clinic of the A.F. Tsyba National Medical Research Radiological Center (Obninsk), a 73-year-old patient was followed up, diagnosed with C20 rectal cancer in accordance with ICD-10, cT3N0M0, and received NHRT (total focal dose of 50 Gy + capecitabine) and four cycles of consolidating polychemotherapy in accordance with the FOLFOX<sup>1</sup> scheme. The pre-MRI treatment is presented in Fig. 1. At the end of neoadjuvant treatment, the set of control examination data (i.e., the MRI of the small pelvis, the endoscopic presentation of the tumor, and the results of digital rectal examination) indicated that the patient had a complete clinical response.

A case follow-up was prescribed to and agreed upon by the patient.

MRI was performed eight times throughout the 3-year follow-up, and the baseline MR image was obtained 1 month after the end of NHRT. This image was characterized by the replacement of the tumor located along the posterior semi-circle of the rectum at a distance of 4 cm from the anal edge with a 1.5 cm-long thin fibrous scar that had no signs of diffusion limitation but had an increase in the initial coefficient (apparent diffusion coefficient, ADC) of up to  $1.66 \times 10^{-3} \text{ mm}^2/\text{s}$ . No suspicious lymph nodes were found in the mesorectum and near the pelvic walls. Therefore, the MR image corresponded to the tumor of the lower ampullar rectum (ymrT1-0N0), TRG2 (Fig. 2). The described MR image was retained without significant changes during the follow-up period.

Colonoscopy revealed no pathology of the colon 1 year after the treatment. In the lower ampullar rectum, a 4.5 cm whitish stellate scar was found, whereas a tumor tissue was not detected. Therefore, this finding showed the endoscopic presentation of the complete intraluminal regression of the rectal tumor during treatment.

After 3 years of follow-up, the patient underwent positron emission tomography with 18F-fluorodeoxyglucose combined with computed tomography because of an increase in the level of tumor markers (Fig. 3). The results revealed a tumor with a length of 43 mm ( $\text{SUV}_{\text{max}}^2 27.1$ ) at the level of the lower ampullar rectum. On the basis of these results, the patient was admitted to the clinic of the A.F. Tsyba National Medical Research Radiological Center for surgical treatment in the scope of laparoscopic abdominal perineal resection.

The patient was examined during surgical treatment preparation. An elastic movable scar was observed after digital rectal examination. During colonoscopy, a 4.5 cm-long

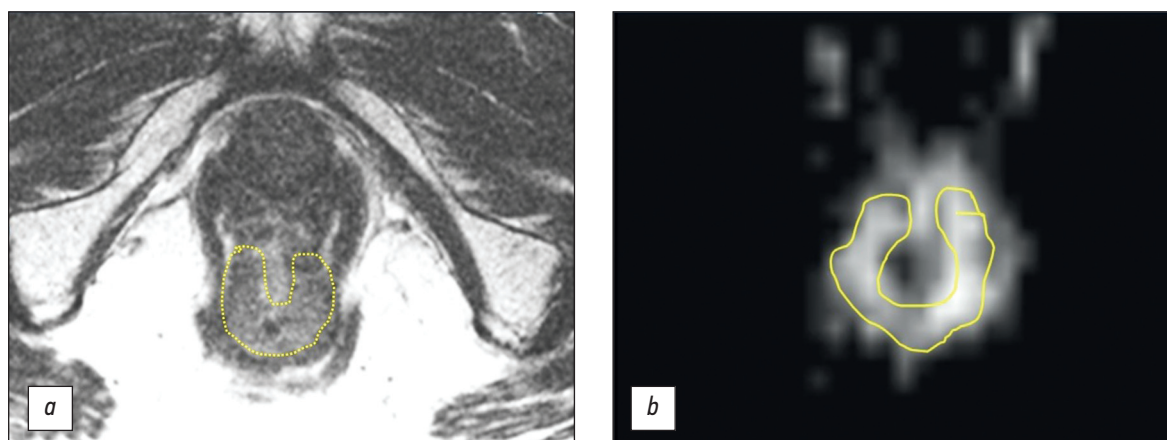


**Fig. 1.** Magnetic resonance imaging of the tumor of the lower rectal ampulla before treatment, mrT3a: *a* — T2-WI; *b* — diffusion-weighted image. The tumor is encircled.

<sup>1</sup> FOLFOX — chemotherapy regimen used to treat colorectal cancer: (FOL) inacid, calcium salt — folinic acid as calcium folinate (leucovorin), (F) fluorouracil, (OX)aliplatin.

<sup>2</sup> SUV (standardized uptake value) — стандартизированный уровень накопления радиофармпрепарата.

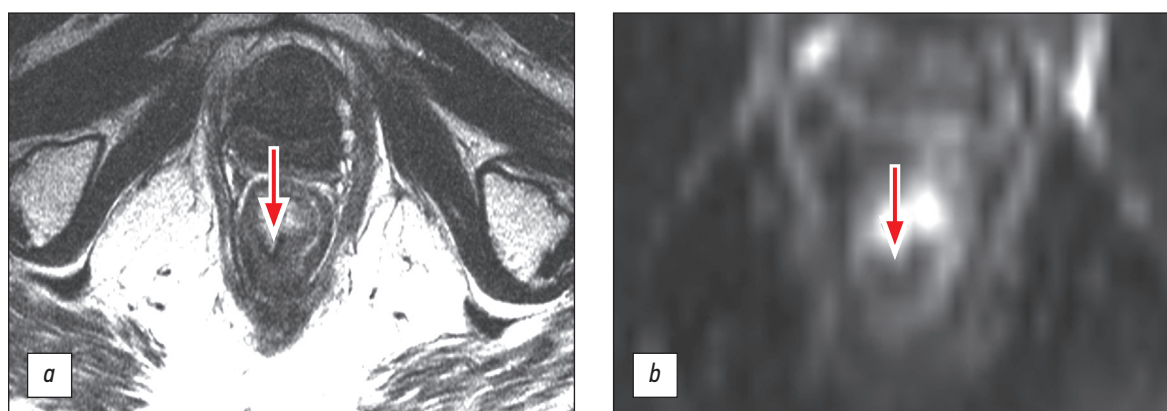


**Fig. 2.** Magnetic resonance imaging of the tumor of the lower ampullar rectum 1 month after neoadjuvant chemoradiation therapy, ymrT1-0, TRG2: *a* — T2-WI; *b* — diffusion-weighted images. The tumor was replaced with a thin fibrous scar that had no signs of diffusion restriction (arrows).



**Fig. 3.** Positron emission tomography with 18F-fluorodeoxyglucose combined with computed tomography: *a* — mono-mode positron emission tomography at the tumor level (arrow); *b* — computed tomography at the tumor level (arrow); *c* — three-dimensional reconstruction with a focus of 18F-fluorodeoxyglucose hyperfixation in the lower ampullar rectum (arrow).

whitish stellate scar without signs of tumor tissues remained in the lower ampullar rectum.

Another MRI examination of the pelvic organs did not reveal any deterioration (Fig. 4). However, given the difficulties of standard MRI in differentiating fibrosis and tumor tissue, T2-WI texture analysis was performed using the MaZda ver. 4.6<sup>3</sup> computer program based on a gray-level co-occurrence matrix [3]. Our scoring system was used to interpret the obtained parameters of texture analysis [4]. In particular, if the sum of the points of the five parameters of texture analysis is  $\geq 3$ , then the patient responded to NHRT; otherwise, the patient did not respond to NHRT. The results of the texture analysis of this patient and the assessment criteria are presented in Table 1. Texture analysis indicated no signs of tumor progression.

Organ sparing surgery in the volume of transanal tumor resection was performed on the basis of the obtained data. Under endotracheal anesthesia, a rectal speculum was installed in the anal canal, and the retraction of the mucous membrane for 1 cm was visually determined along the

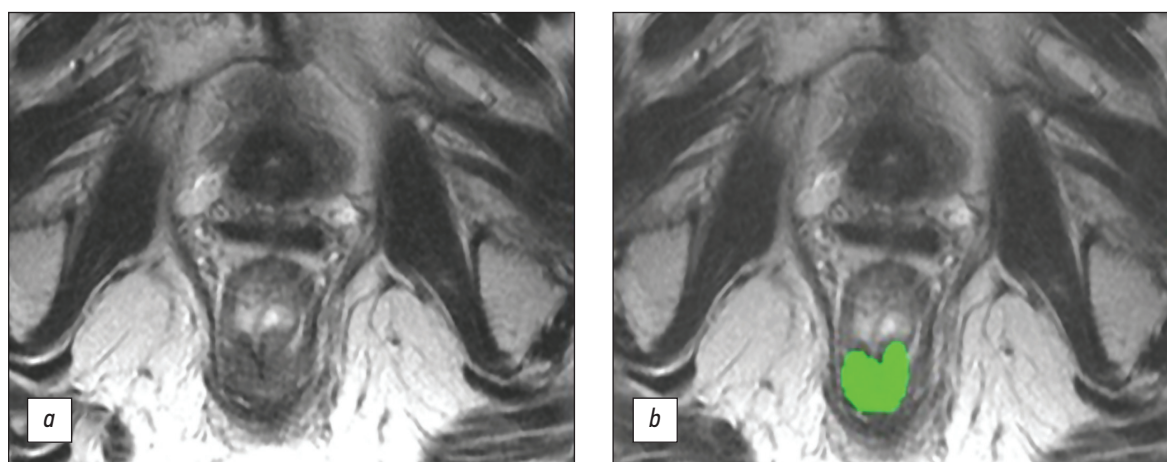


**Fig. 4.** Magnetic resonance imaging of the tumor of the lower ampullar rectum 3 years after neoadjuvant chemoradiation therapy: *a* — T2-WI; *b* — segmentation of the zone of interest for texture analysis (highlighted in green).

<sup>3</sup> Computer software for the calculation of texture parameters in digitized images. Available from: <http://www.eletel.p.lodz.pl/programy/mazda/>



**Table 1.** Results and evaluation of the parameters of T2-WI texture analysis based on the patient's magnetic resonance imaging before surgery.

Parameter	Value	Scoring system		Score
		1 point	0 points	
AngScMom	0.0041	$\geq 0.0022$	$< 0.0022$	1
InvDfMom	0.15	$\geq 0.12$	$< 0.12$	1
Entropy	2.5	$\leq 2.75$	$> 2.75$	1
DifEntrp	1.32	$\leq 1.32$	$> 1.32$	1
SumEntrp	1.74	$\leq 1.8$	$> 1.8$	1
Total	-	-	-	5

posterior wall in the area of the internal sphincter. The lesion was excised through sharp dissection. A wipe tampon was inserted in the rectum. A fragment of the bright red mucous membrane with a size of 2.0 cm  $\times$  0.4 cm  $\times$  0.2 cm and a dense bright red sample of the wall with the largest dimension of 0.4 cm were pathomorphologically examined.

The two fragments of the mucous membrane covered with a multilayer scaly nonsquamous epithelium were morphologically examined. The results revealed that the stroma in the submucous layer with diffused and weak lymphocytic-leukocytic and plasmocytic infiltration and hemorrhage was fibrotic. No tumors were found.

## DISCUSSION

NHRT efficacy evaluation is essential for the individualized treatment of patients with lower ampullary cancer of the rectum. The ability to preserve the sphincter with a good response to neoadjuvant treatment significantly improves the quality of life of patients by eliminating their permanent colostomy. It also reduces the risk of postoperative complications. Through endoscopic diagnostics, the response of the intraluminal component of tumors can be assessed. By comparison, MRI is performed to examine the entire intestinal wall, mesorectal tissue, and fascia and the status of regional lymph nodes. For the MRI assessment of tumor responses, the TRG system is generally used, but its accuracy is reduced because of difficulties in differentiating residual tumor tissues and fibrosis. Nevertheless, this problem can be solved with diffusion-weighted images (DWIs), which have recently supplemented T2-WI. Through DWI, small areas of residual tumors in the presence of fibrosis can be distinguished. Consequently, the diagnostic specificity increases up to 90%, but its sensitivity is still 64%. This relatively low sensitivity is mainly due to the erroneous interpretation of a high MR signal in the normal postradiation intestinal wall as a residual tumor [5]. In addition, the susceptibility of the method to artifacts, including brightness and geometric distortions, as well as false images, often complicates the interpretation of DWI.

Currently, a radiomic approach is being developed to assess the efficiency of chemoradiation therapy. It is based on the high-technology extraction of information from medical images; thus, tissue heterogeneity can be characterized quantitatively [6].

Various approaches are used to interpret texture analysis results and assess the efficiency of NHRT. N. Horvat et al. [7] retrospectively studied 118 patients with rectal cancer. They used a machine learning algorithm to create a high-resolution radiomic classifier of the parameters of T2-WI texture analysis and identify patients who suffer from rectal cancer and have a complete response to NHRT. In our study, the radiomic score was significantly superior to the visual assessment of T2-WI or the combination of T2-WI and DWI in terms of overall accuracy ( $p = 0.02$ ), specificity, and positive predictive value ( $p = 0.0001$ ). The sensitivity and negative predictive value did not differ significantly. The parameters of texture analysis were characterized using the score based on the points of separation and the direction of our previously established correlation [4]. The presented clinical case with the prospective application of the proposed system for evaluating texture analysis demonstrated its efficiency. The analyzed image and the images during the development of the scoring system were obtained using similar parameters of fast spin echo sequences but on different MR tomographs (Ingenia 1.5T, Philips and Symphony 1.5T, Siemens, respectively). This finding suggested that the reproducibility of the texture analysis parameters was good. It also confirmed the suitability of further large-scale studies in this field.

## CONCLUSION

The presented radiomic approach with high-resolution T2-WI texture analysis shows potential for application in the assessment of the efficiency of NHRT in patients with regional rectal cancer. However, this approach should be further developed, its implementation and systems for texture parameter evaluation should be improved, and the reproducibility of results should be studied.



## ADDITIONAL INFORMATION

**Funding source.** This study was not supported by any external funding sources.

**Competing interests.** The authors declare that they have no competing interests.

**Authors' contributions.** Ya.A. Dayneko — collection and processing of the material, analysis of the received data, and writing of the text; T.P. Berezovskaya — concept and design of the study, analysis of the received data, writing of the text, and editing;

S.A. Myalina — collection and processing of the material and writing of the text; I.A. Orekhov — collection and processing of the material and analysis of the received data; and A.A. Nevolskikh — editing. All authors made a substantial contribution to the conception of the work, acquisition, analysis, data interpretation, drafting and revision, and final approval of the version to be published. They agreed to be accountable for all aspects of the work.

**Patient's permission.** Written consent was obtained from the patient for the publication of relevant medical information and all the accompanying images within the manuscript.

## REFERENCES

1. Fedyanin MYu, Artamonova EV, Barsukov YuA, et al. Practical recommendations for the drug treatment of rectal cancer. Malignant tumors: Practical recommendations of RUSSCO. Russian Society of Clinical Oncology; 2020. (In Russ). doi: 10.18027/2224-5057-2020-10-3s2-23
2. Gillies RJ, Kinahan PE, Hricak H. Radiomics: images are more than pictures, they are data. *Radiology*. 2016;278(2):563–577. doi: 10.1148/radiol.2015151169
3. Haralick RM, Shanmugam K, Dinstein I. Textural features for image classification. *IEEE Transactions on Systems, Man, and Cybernetics*. 1973;SMC-3(6):610–621. doi: 10.1109/TSMC.1973.4309314
4. Berezovskaya TP, Dayneko YaA, Nevolskikh AA, et al. A system for evaluating the effectiveness of neoadjuvant chemo radiotherapy in patients with colorectal cancer based on a texture analysis of post-therapeutic T2-WI magnetic resonance imaging. *REJR*. 2020;10(3):92–101. doi: 10.21569/2222-7415-2020-10-3-92-101
5. Lambregts DM, Rao SX, Sassen S, et al. MRI and Diffusion-weighted MRI volumetry for identification of complete tumor responders after preoperative chemoradiotherapy in patients with rectal cancer: a bi-institutional validation study. *Ann Surg*. 2015;262(6):1034–1039. doi: 10.1097/SLA.0000000000000909
6. Lambin P, Rios-Velazquez R, Leijenaar S, et al. Radiomics: Extracting more information from medical images using advanced feature analysis. *Eur J Cancer*. 2012;48(4):441–446. doi: 10.1016/j.ejca.2011.11.036
7. Horvat N, Veeraraghavan H, Pelossof RA, et al. Radiogenomics of rectal adenocarcinoma in the era of precision medicine: A pilot study of associations between qualitative and quantitative MRI imaging features and genetic mutations. *Eur J Radiol*. 2019;113:174–181. doi: 10.1016/j.ejrad.2019.02.022

## СПИСОК ЛИТЕРАТУРЫ

1. Федянин М.Ю., Артамонова Е.В., Барсуков Ю.А. и др. Практические рекомендации по лекарственному лечению рака прямой кишки. Злокачественные опухоли: Практические рекомендации RUSSCO. Российское общество клинической онкологии, 2020. doi: 10.18027/2224-5057-2020-10-3s2-23
2. Gillies R.J., Kinahan P.E., Hricak H. Radiomics: images are more than pictures, they are data // *Radiology*. 2016. Vol. 278, N 2. P. 563–577. doi: 10.1148/radiol.2015151169
3. Haralick R.M., Shanmugam K., Dinstein I. Textural features for image classification // *IEEE Transactions on Systems, Man, and Cybernetics*. 1973. Vol. SMC-3, N 6. P. 610–621. doi: 10.1109/TSMC.1973.4309314
4. Бerezovskaya T.P., Dayneko Ya.A., Nevolskikh A.A. и др. Система оценки эффективности неoadъювантной химиолучевой терапии у больных раком прямой кишки на основе текстурного анализа посттерапевтического T2-взвешенного магнитно-резонансного изображения опухоли // *REJR*. 2020. Т. 10, № 3. С. 92–101. doi: 10.21569/2222-7415-2020-10-3-92-101
5. Lambregts D.M., Rao S.X., Sassen S., et al. MRI and Diffusion-weighted MRI volumetry for identification of complete tumor responders after preoperative chemoradiotherapy in patients with rectal cancer: a bi-institutional validation study // *Ann Surg*. 2015. Vol. 262, N 6. P. 1034–1039. doi: 10.1097/SLA.0000000000000909
6. Lambin P., Rios-Velazquez R., Leijenaar S., et al. Radiomics: Extracting more information from medical images using advanced feature analysis // *Eur J Cancer*. 2012. Vol. 48, N 4. P. 441–446. doi: 10.1016/j.ejca.2011.11.036
7. Horvat N., Veeraraghavan H., Pelossof R.A., et al. Radiogenomics of rectal adenocarcinoma in the era of precision medicine: A pilot study of associations between qualitative and quantitative MRI imaging features and genetic mutations // *Eur J Radiol*. 2019. Vol. 113. P. 174–181. doi: 10.1016/j.ejrad.2019.02.022

## AUTHORS' INFO

\* **Tatiana P. Berezovskaya**, MD, Dr. Sci. (Med.) Professor, Chief Researcher; address: 4 Korolev st., Obninsk, 249036, Russia; ORCID: <http://orcid.org/0000-0002-3549-4499>; eLibrary SPIN: 5837-3465; e-mail: [berez@mrrc.obninsk.ru](mailto:berez@mrrc.obninsk.ru)

## ОБ АВТОРАХ

\* **Березовская Татьяна Павловна**, д.м.н., профессор, гл. науч. сотр.; адрес: Россия, 249036, Обнинск, ул. Королева, д. 4; ORCID: <http://orcid.org/0000-0002-3549-4499>; eLibrary SPIN: 5837-3465; e-mail: [berez@mrrc.obninsk.ru](mailto:berez@mrrc.obninsk.ru)

**Yana A. Dayneko**, MD, Research Associate;  
ORCID: <https://orcid.org/0000-0002-4524-0839>;  
eLibrary SPIN: 1841-7759; e-mail: vorobeyana@gmail.com

**Sofia A. Myalina**, MD, Junior Research Associate;  
ORCID: <https://orcid.org/0000-0001-6686-5419>;  
e-mail: samyalina@mail.ru

**Ivan A. Orekhov**, MD, Junior Research Associate;  
ORCID: <https://orcid.org/0000-0001-6543-6356>;  
eLibrary SPIN: 6040-8930; e-mail: ivan.orekhov.vgma@gmail.com

**Alexey A. Nevolskikh**, MD, Dr. Sci. (Med.);  
ORCID: <http://orcid.org/0000-0001-5961-2958>;  
eLibrary SPIN: 3787-6139; e-mail: nevol@mrrc.obninsk.ru

**Дайнеко Яна Александровна**, науч. сотр.;  
ORCID: <https://orcid.org/0000-0002-4524-0839>;  
eLibrary SPIN: 1841-7759; e-mail: vorobeyana@gmail.com

**Мялина Софья Анатольевна**, мл. науч. сотр.;  
ORCID: <https://orcid.org/0000-0001-6686-5419>;  
e-mail: samyalina@mail.ru

**Орехов Иван Анатольевич**, мл. науч. сотр.;  
ORCID: <https://orcid.org/0000-0001-6543-6356>;  
eLibrary SPIN: 6040-8930; e-mail: ivan.orekhov.vgma@gmail.com

**Невольских Алексей Алексеевич**, д.м.н.;  
ORCID: <http://orcid.org/0000-0001-5961-2958>;  
eLibrary SPIN: 3787-6139; e-mail: nevol@mrrc.obninsk.ru

DOI: <https://doi.org/10.17816/DD59690>

# Diagnosis of solitary eosinophilic granuloma by CT, MRI, and 18F-FDG PET/CT: two clinical cases

© Pavel B. Gelezhe<sup>1, 2</sup>, Dmitriy V. Bulanov<sup>2, 3</sup>

<sup>1</sup> Moscow Center for Diagnostics and Telemedicine, Moscow, Russian Federation

<sup>2</sup> Joint-Stock Company "European Medical Center", Moscow, Russian Federation

<sup>3</sup> The Russian National Research Medical University named after N.I. Pirogov, Moscow, Russian Federation

## ABSTRACT

This paper presents two clinical cases of eosinophilic granuloma of bone diagnosed by CT, MRI, and 18F-FDG PET/CT. In both cases the patients were admitted to the clinic with suspected primary malignant bone tumor and the diagnosis of a solitary eosinophilic granuloma was made based on the results of comprehensive radiological diagnostic examination and histological verification. Solitary eosinophilic granuloma of bone is an infrequent condition, occurring in less than 1% of cases of skeletal tumor masses. The most common eosinophilic granuloma is found in the parietal and frontal bones of the skull and is an osteolytic volumetric mass that gradually increases in size. Although most bone tumors can be detected by radiography, computed tomography is preferred, primarily because of its superior ability to detect cortical bone destruction. The diagnostic accuracy of computed tomography and magnetic resonance imaging may be different. The combined use of radiological and radionuclide methods allows us to narrow the spectrum of differential diagnosis. Unfortunately, relatively low specificity of existing radiological diagnostic studies in most cases does not allow to establish a precise diagnosis, and biopsy with subsequent pathological examination remains the method of choice. These clinical observations demonstrate the need to include eosinophilic granuloma in the differential diagnosis when a solitary osteolytic focus is detected.

**Keywords:** eosinophilic granuloma; osteolytic focus; computed tomography; magnetic resonance imaging; positron emission tomography; case report.

## To cite this article

Gelezhe PB, Bulanov DV. Diagnosis of solitary eosinophilic granuloma by CT, MRI, and 18F-FDG PET/CT: two clinical cases. *Digital Diagnostics*. 2021;2(1):75–82. DOI: <https://doi.org/10.17816/DD59690>

Received: 29.01.2021

Accepted: 02.03.2021

Published: 12.03.2021

DOI: <https://doi.org/10.17816/DD59690>

## Два случая верифицированной солитарной эозинофильной гранулёмы: визуализация методами КТ, МРТ и 18F-ФДГ ПЭТ/КТ

© П.Б. Гележе<sup>1, 2</sup>, Д.В. Буланов<sup>2, 3</sup>

<sup>1</sup> Научно-практический клинический центр диагностики и телемедицинских технологий Департамента здравоохранения города Москвы, Москва, Российская Федерация

<sup>2</sup> Акционерное общество «Европейский Медицинский Центр», Москва, Российская Федерация

<sup>3</sup> Российский национальный исследовательский медицинский университет имени Н.И. Пирогова, Москва, Российская Федерация

### АННОТАЦИЯ

В работе представлены два клинических наблюдения эозинофильной гранулёмы кости, диагностированной методами компьютерной, магнитно-резонансной и позитронно-эмиссионной томографии с 18F-фтордезоксиглюкозой, совмещённой с компьютерной томографией. В обоих случаях пациенты поступили в клинику с подозрением на первичную злокачественную опухоль кости, по результатам комплексного лучевого диагностического исследования и гистологической верификации установлен диагноз солитарной эозинофильной гранулёмы. Солитарная эозинофильная гранулёма кости — достаточно редкое (менее 1% случаев всех опухолевых объёмных образований скелета) заболевание. Наиболее часто эозинофильная гранулёма обнаруживается в теменной и лобных костях черепа и представляет собой остеолитическое объёмное образование, постепенно увеличивающееся в размерах. Несмотря на то, что большую часть опухолей костной ткани можно выявить при помощи рентгенографии, предпочтительно применение компьютерной томографии, в первую очередь из-за её превосходной способности визуализировать структуры кортикального слоя кости. Диагностическая точность компьютерной и магнитно-резонансной томографии может быть различна. Комплексное применение методов лучевой и радионуклидной диагностики позволяет сузить спектр дифференциального диагноза. К сожалению, относительно низкая специфичность существующих лучевых диагностических исследований в большинстве случаев не позволяет установить точный диагноз, и методом выбора остаётся биопсия с последующим патоморфологическим исследованием. Данные клинические наблюдения показывают необходимость включения эозинофильной гранулёмы в дифференциальный диагноз при обнаружении солитарного остеолитического очага.

**Ключевые слова:** эозинофильная гранулёма; остеолитический очаг; компьютерная томография; магнитно-резонансная томография; позитронно-эмиссионная томография; клинический случай.

### Как цитировать

Гележе П.Б., Буланов Д.В. Два случая верифицированной солитарной эозинофильной гранулёмы: визуализация методами КТ, МРТ и 18F-ФДГ ПЭТ/КТ // *Digital Diagnostics*. 2021. Т. 2, №1. С. 75–82. DOI: <https://doi.org/10.17816/DD59690>

DOI: <https://doi.org/10.17816/DD59690>

## 2例证实的孤立性嗜酸性肉芽肿 CT、MRI和18F-FDG PET/CT成像

© Pavel B. Gelezhe<sup>1,2</sup>, Dmitriy V. Bulanov<sup>2,3</sup>

<sup>1</sup> Moscow Center for Diagnostics and Telemedicine, Moscow, Russian Federation

<sup>2</sup> Joint-Stock Company "European Medical Center", Moscow, Russian Federation

<sup>3</sup> The Russian National Research Medical University named after N.I. Pirogov, Moscow, Russian Federation

### 简评:

本文介绍计算机诊断嗜酸性骨肉芽肿、磁共振和18F氟脱氧葡萄糖正电子发射断层扫描以及计算机断层扫描的两个临床观察。根据综合的放射学诊断研究和组织学证实,确诊为孤立性嗜酸性肉芽肿,两例患者都因怀疑原发性恶性骨肿瘤而入院。孤立性嗜酸性肉芽肿是一种相当罕见的疾病(不到1%的骨骼肿瘤体积形成病例)。最常见的是,嗜酸性肉芽肿见于头骨的顶骨和额骨,是一种溶骨体积的形成,逐渐增大。虽然大多数骨肿瘤可以通过X线摄影发现,计算机体层摄影术是首选,主要是因为它能很好地显示骨皮质层的破坏情况。计算机断层扫描和磁共振成像的诊断准确性可能不同。辐射和放射性核素诊断方法的复杂应用使能够缩小鉴别诊断的范围。在大多数病例中,现有的放射学诊断研究的特异性较低,不能做出准确的诊断,选择的方法仍然是活检后进行病理形态学检查。这些临床观察表明,当发现孤立的溶骨性病灶时,鉴别诊断需要包括嗜酸性肉芽肿。

**关键词:** 嗜酸性肉芽肿; 溶骨性病灶; 计算机断层扫描; 磁共振成像; 正电子发射断层扫描; 临床病例.

### 引用本文:

Gelezhe PB, Bulanov DV. 2例证实的孤立性嗜酸性肉芽肿 CT、MRI和18F-FDG PET/CT成像. *Digital Diagnostics*. 2021;2(1):75–82.  
DOI: <https://doi.org/10.17816/DD59690>

收到: 29.01.2021

接受: 02.03.2021

发布时间: 12.03.2021



## BACKGROUND

The newly diagnosed osteolytic focus in young patients leads inevitably to an extensive differential diagnosis, which involves a variety of pathological processes. Under conditions of oncological alertness of radiologists and general practitioners, the osteolytic focus is often unambiguously interpreted as a manifestation of a malignant tumor. It should be remembered that benign and inflammatory processes can also cause the emergence of an osteolytic focus.

The paper presents two clinical cases of solitary eosinophilic granuloma of the bone, which is a rare pathological process that must be included in the differential range when a solitary osteolytic focus is detected.

## DESCRIPTION OF THE CASES

### Clinical case 1

A 30-year-old female patient considers herself sick since August 2016, when pain began in the lumbar region on the left, progressing over the course of a year. She visited the clinic in August 2017 after experiencing severe pain.

The studies of the pelvis were performed using magnetic resonance imaging (MRI) and computed tomography (CT). MRI revealed a cystic formation measuring  $2.2 \times 1.4 \times 2.0$  cm on the gluteal surface of the upper sections of the left iliac crest, along with edema of the musculus gluteus medius with a vertical length of up to 7 cm. A trabecular edema of the iliac crest on the left with a length of 5.0 cm was determined. The CT scan showed an osteolytic focus of the upper sections of the wing of the left iliac bone of up to  $1.8 \times 1.2 \times 1.2$  cm with clear uneven contours, destructed cortical layer of the bone, and signs of generalization beyond its limits (Fig. 1).

Mono-mode positron emission tomography (PET) with  $^{18}\text{F}$ -fluorodeoxyglucose ( $^{18}\text{F}$ -FDG) was performed, which revealed a single focus of the radiopharmaceutical agent hyperfixation in the area of the wing of the left iliac bone ( $\text{SUV}_{\text{max}}^1 13.1$ ) (Fig. 2); therefore, the widespread metastatic process was ruled out.

CT-guided  $^{18}\text{G}$  needle biopsy was performed from the wing formation of the left iliac bone (Fig. 3). The histological study (No. 2017-10802-01) concluded on the morphoimmunohistochemical presentation, which is most consistent with Langerhans cell histiocytosis (eosinophilic granuloma, histiocytosis X) (Fig. 4).

### Clinical case 2

A 12-year-old boy, during his football practice, he hit the ball with his head. According to his parents and the child himself, after which, they noticed swelling in the



Fig. 1. Computed tomography reveals an osteolytic focus in the wing of the left iliac bone.

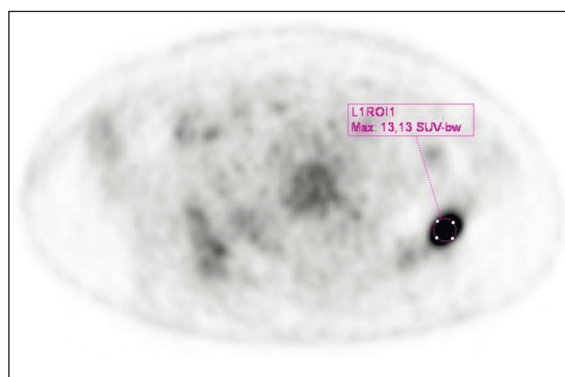


Fig. 2. A hypermetabolic focus in the projection of the wing of the left iliac bone on mono-mode positron emission tomography with  $^{18}\text{F}$ -fluorodeoxyglucose.

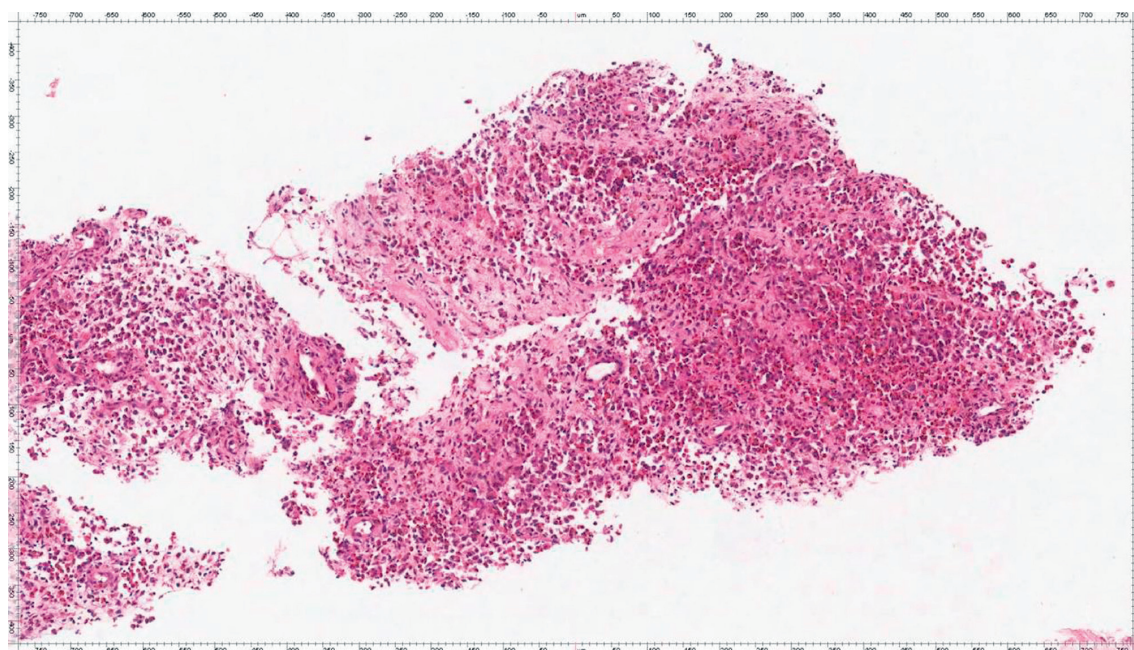


Fig. 3. The process of needle biopsy by computed tomography.

forehead area, which gradually increased in the subsequent days. A CT scan was performed, as recommended by the doctor of the primary health care facility, which revealed an osteolytic rounded defect of the frontal bone with a diameter of about 3.5 cm, punch-type destruction of the external and internal cortical laminas, and soft tissue parosseous formation. MRI was recommended as further examination.

According to the brain MRI data, a subcutaneously located space-occupying lesion was detected in the frontal region parasagittally, with a mild right-sided priority, with a non-uniformly increased MR signal in the T2-WI and T2-dark fluid modes, with signs of diffusion restriction, of

<sup>1</sup> SUV (standardized uptake value) — стандартизированный уровень накопления радиофармпрепарата.



**Fig. 4.** Histological specimen: fibrovascular tissue fragments with polymorphic-cellular infiltration consisting numerous granulocytes, including an abundance of eosinophils, plasma cells, and individual cells with bean-shaped nuclei are noted. Hematoxylin-eosin staining  $\times 200$ .

an ovoid shape with indistinct uneven boundaries, sized  $47 \times 17 \times 35$  mm. It was widely adjacent to the squama of the frontal bone, with destruction of the external and internal cortical plates with a minimal intracranial soft tissue component, limited by the brain dura mater (Fig. 5).

Lymphocytosis of up to 49.5%, neutropenia of 39.3%, and thrombocytosis 491 were noticeable in the general blood

test, as well as an increase in the erythrocyte sedimentation rate of up to 29 mm/h and an increase in C-reactive protein up to 10.65 mg/L.

According to the results of the studies, a neoplastic lesion of the frontal bone was suggested. Differential diagnostics was made between lymphoma, plasmacytoma, and sarcoma. In order to search for a primary tumor focus,  $^{18}\text{F}$ -FDG PET/CT was performed. In the frontal region, along the midline, an ovoid lesion of  $30 \times 15$  mm in size was revealed, with a significant accumulation of the radiopharmaceutical agent (SUVmax up to 11.2), destruction of the external and internal cortical lamina of the frontal bone (Fig. 6). For the rest of the  $^{18}\text{F}$ -FDG foci, no positive neoplastic process was detected; therefore, a widespread metastatic process was ruled out.

An incisional biopsy of the subcutaneous lesion of the frontal region was performed for histological verification. Percutaneous puncture biopsy of the frontal region lesion was performed in the supine position with a thick needle. When aspirated with a syringe, no tissue was obtained. A 1-cm transverse linear incision was made along the hair-line of the frontal region soft tissues. A biopsy sample of the pathological tissue, which was represented by gray soft tissue masses, was taken using a Volkmann curet and Royce forceps. According to the histological conclusion No. 2015-11688-01, the changes are more consistent with Langerhans cell histiocytosis (eosinophilic cell granuloma).

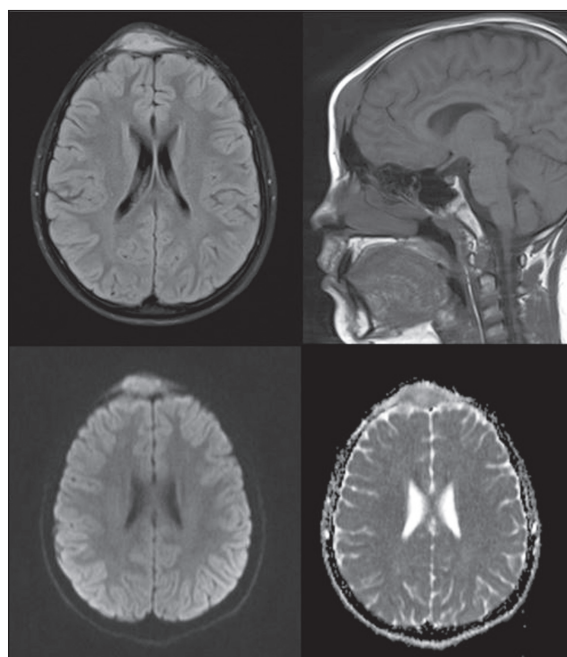


**Fig. 5.** Magnetic resonance imaging of the head. Top row from left to right: T2-TIRM, T1-WI; bottom row from left to right: diffusion-weighted image (B-factor 800 mm<sup>2</sup>/s), measured diffusion coefficient. Subcutaneous space-occupying lesion of increased signal in T2-TIRM, isointense in T1-WI, with signs of diffusion restriction.

## DISCUSSION

Solitary eosinophilic granuloma of bone is a relatively uncommon occurrence, accounting for less than 1% of tumor-like bone lesions. A histological sign of histiocytosis X,



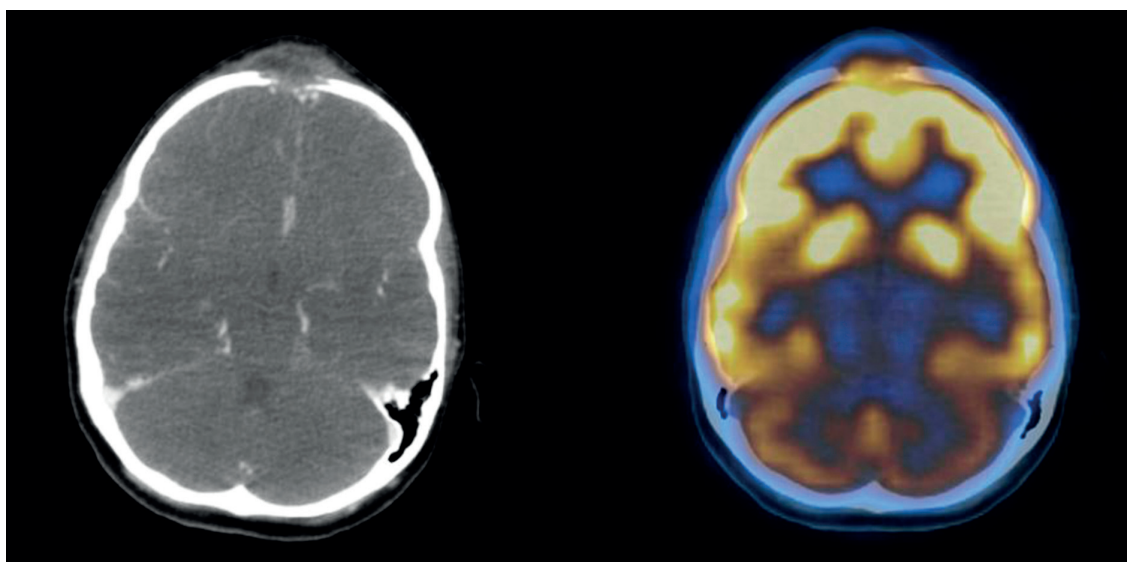


**Fig. 6.** Positron emission tomography with 18F-fluorodeoxyglucose, combined with computed tomography. Left: computed tomography with intravenous contrast enhancement; right: combined image of positron emission and computed tomography. A hypermetabolic focus with destruction of the external and internal cortical lamina of the frontal bone is visible.

including eosinophilic granuloma, is the presence of proliferating histiocytes (Langerhans histiocytes) [1]. The histiocyte contains puffed oval nuclei and eosinophilic cytoplasm. Birbeck granules are cytoplasmic organelles found in Langerhans cells, but their function is still unclear. The granuloma also comprises a large number of eosinophils and giant multinucleated cells.

In their work, K. M. Herzog et al. [2] reported that the skull is the most common site of eosinophilic granuloma (43%), whereas the femur is the second most common site. C. Arseni et al. [3] reported the lesion of the skull was solitary in 80% of the patients with eosinophilic granuloma, as in our clinical case 1.

Eosinophilic granuloma of the skull is manifested as an osteolytic space-occupying lesion, gradually increasing in size, often with localization in the parietal and frontal bones. On the basis of 25 patients with a total of 41 eosinophilic granulomas, L. Ardekian et al. [4] found that pain, often accompanied by local edema, was the most common symptom (92% of cases).

Although X-ray can accurately identify and distinguish most bone foci, CT is the preferred method, mainly due to its excellent ability to detect bone cortical layer destruction.

The radiographic characteristics vary significantly depending on the lesion location. The lesion in the skull is usually 1 to 4 cm in diameter, demonstrating punch-type clear boundaries, with frequent destruction of the external and internal cortical lamina. At the same time, there can be sequestrum inside the focus. Flat bone lesions are characterized by a periosteal reaction, thinning of the cortical layer, and local swelling of the bone. A hole within a hole may form when multiple small foci merge. A marked destruction of bone tissue, imitating a malignant process, occurs in rare cases.

The most significant in differential diagnostics with eosinophilic granuloma, in the range of the destructive benign and malignant lesions of the cranial vault, are osteomas (benign tumors), plasmacytoma, epidermoids, dermoid cysts, vascular tumors, osteosarcoma (malignant sarcoma), metastatic disease, meningiomas, as well as infectious and pathological conditions [5].

Bone eosinophilic granuloma may look like osteomyelitis, Ewing's sarcoma, or lymphoma on X-ray. Other skeletal lesions, such as neuroblastoma metastases, intraosseous hemangiomas, and fibrous dysplasia should also be considered in differential diagnostics. In adults, eosinophilic granuloma can mimic osteolytic metastases, multiple myeloma, and hyperparathyroidism.

The most common finding based on MRI data is a mild diffuse decrease in the signal according to the T1-WI data, combined with an increase in the signal according to the T2-WI. Edema is also visible in the soft tissues surrounding the lesion, as shown by an increased signal on the spin-echo inversion-recovery sequence. The focus of eosinophilic granuloma of the skull bones limits diffusion compared with the white matter of the brain [6]. The described changes are not specific and can occur in a number of conditions, including osteomyelitis, traumatic changes, and avascular necrosis [7].

The sensitivity indicated in the literature for 18F-FDG PET scanning is greater than 90%, whereas the specificity remains low and varies considerably, from 65% to 80% [8, 9]. False negative results are most commonly caused by low-grade tumors, which often show low levels of 18F-FDG fixation. False positive results can be caused by some benign diseases, including fibrous dysplasia and aneurismal bone cyst, as well as acute inflammation [10].

Treatment for eosinophilic granuloma is determined on the degree of the disease progression. Surgery, radiotherapy, and chemotherapy are all possible treatment methods, which can be used in isolation or combination. Surgery is usually indicated for isolated lesions when an appropriate cure can result in complete elimination of the lesion.

Despite the fact that eosinophilic granuloma is considered to be a benign condition, there have been reports of spontaneous regression and relapses after surgical excision in the literature [11, 12]. Because local relapses are often registered in a series with longer follow-up periods, it is recommended that subsequent follow-up studies be performed for at least 10 years [11–13].

## CONCLUSION

Differential diagnostics of a solitary osteolytic focus can be difficult. The use of an integrated approach in radiation diagnostics, which includes CT, MRI, and 18F-FDG PET/CT, enables to narrow the range of possible pathological conditions. At the same time, the specificity of existing radiological diagnostic

studies does not always enable to establish a precise diagnosis, so histological verification remains the preferred method. When identifying a solitary osteolytic focus in young patients, an eosinophilic granuloma should be considered.

## ADDITIONAL INFORMATION

**Funding source.** This study was not supported by any external sources of funding.

**Competing interests.** The authors declare that they have no competing interests.

**Author contribution.** The authors confirm contribution to the paper as follows: material collection and article writing: P.B. Gelezhe; histological examination data: D.V. Bulanov. All authors contributed significantly to the work's conception, acquisition, analysis, interpretation of data, drafting and revising, final approval of the version to be published, and agree to be accountable for all aspects of the work.

**Patient's permission.** The patient and the legal representative of the juvenile signed a voluntary informed consent to the publication of medical information in an anonymized form.

## REFERENCES

1. Lam KY. Langerhans cell histiocytosis (histiocytosis X). *Postgrad Med J*. 1997;73(861):391–394. doi: 10.1136/pgmj.73.861.391
2. Herzog KM, Tubbs RR. Langerhans cell histiocytosis. *Adv Anat Pathol*. 1998;5(6):347–358. doi: 10.1097/00125480-199811000-00001
3. Arseni C, Dănăilă L, Constantinescu A. Cranial eosinophilic granuloma. *Neurochirurgia (Stuttg)*. 1977;20(6):189–199. doi: 10.1055/s-0028-1090377
4. Ardekian L, Peled M, Rosen D, et al. Clinical and radiographic features of eosinophilic granuloma in the jaws: Review of 41 lesions treated by surgery and low-dose radiotherapy. *Oral Surg Oral Med Oral Pathol Oral Radiol Endod*. 1999;87(2):238–242. doi: 10.1016/s1079-2104(99)70279-9
5. Willatt JM, Quaghebeur G. Calvarial masses of infants and children. A radiological approach. *Clin Radiol*. 2004;59(6):474–486. doi: 10.1016/j.crad.2003.12.006
6. Ginat DT, Mangla R, Yeaney G, et al. Diffusion-Weighted imaging for differentiating benign from malignant skull lesions and correlation with cell density. *Am J Roentgenol*. 2012;198(6):W597–W601. doi: 10.2214/AJR.11.7424
7. Davies AM, Pikoulas C, Griffith J. MRI of eosinophilic granuloma. *Eur J Radiol*. 1994;18(3):205–209. doi: 10.1016/0720-048x(94)90335-2
8. Dimitrakopoulou-Strauss A, Strauss LG, Heichel T, et al. The role of quantitative 18F-FDG PET studies for the differentiation of malignant and benign bone lesions. *J Nucl Med*. 2002;43(4):510–518.
9. Culverwell AD, Scarsbrook AF, Chowdhury FU. False-positive uptake on 2-[18F]-fluoro-2-deoxy-D-glucose (FDG) positron-emission tomography/computed tomography (PET/CT) in oncological imaging. *Clin Radiol*. 2011;66(4):366–382. doi: 10.1016/j.crad.2010.12.004
10. Schulte M, Brecht-Krauss D, Heymer B, et al. Grading of tumors and tumorlike lesions of bone: evaluation by FDG PET. *J Nucl Med*. 2000;41(10):1695–1701.
11. Martinez-Lage JF, Poza M, Cartagena J, et al. Solitary eosinophilic granuloma of the pediatric skull and spine — the role of surgery. *Childs Nerv Syst*. 1991;7(8):448–451. doi: 10.1007/BF00263187
12. Oliveira M, Steinbok P, Wu J, et al. Spontaneous resolution of calvarial eosinophilic granuloma in children. *Pediatr Neurosurg*. 2003;38(5):247–252. doi: 10.1159/000069828
13. Rawlings CE, Wilkins RH. Solitary eosinophilic granuloma of the skull. *Neurosurgery*. 1984;15(2):155–161. doi: 10.1227/00006123-198408000-00001

## СПИСОК ЛИТЕРАТУРЫ

1. Lam K.Y. Langerhans cell histiocytosis (histiocytosis X) // *Postgrad Med J*. 1997. Vol. 73, N 861. P. 391–394. doi: 10.1136/pgmj.73.861.391
2. Herzog K.M., Tubbs R.R. Langerhans cell histiocytosis // *Adv Anat Pathol*. 1998. Vol. 5, N 6. P. 347–358. doi: 10.1097/00125480-199811000-00001
3. Arseni C., Dănăilă L., Constantinescu A. Cranial eosinophilic granuloma // *Neurochirurgia (Stuttg)*. 1977. Vol. 20, N 6. P. 189–199. doi: 10.1055/s-0028-1090377
4. Ardekian L., Peled M., Rosen D., et al. Clinical and radiographic features of eosinophilic granuloma in the jaws: Review of 41 lesions treated by surgery and low-dose radiotherapy // *Oral Surg Oral Med Oral Pathol Oral Radiol Endod*. 1999. Vol. 87, N 2. P. 238–242. doi: 10.1016/s1079-2104(99)70279-9
5. Willatt J.M., Quaghebeur G. Calvarial masses of infants and children. A radiological approach // *Clin Radiol*. 2004. Vol. 59, N 6. P. 474–486. doi: 10.1016/j.crad.2003.12.006

6. Ginat D.T., Mangla R., Yeane G., et al. Diffusion-Weighted imaging for differentiating benign from malignant skull lesions and correlation with cell density // *Am J Roentgenol.* 2012. Vol. 198, N 6. P. W597–W601. doi: 10.2214/AJR.11.7424
7. Davies A.M., Pikoulas C., Griffith J. MRI of eosinophilic granuloma // *Eur J Radiol.* 1994. Vol. 18, N 3. P. 205–209. doi: 10.1016/0720-048x(94)90335-2
8. Dimitrakopoulou-Strauss A., Strauss L.G., Heichel T., et al. The role of quantitative 18F-FDG PET studies for the differentiation of malignant and benign bone lesions // *J Nucl Med.* 2002. Vol. 43, N 4. P. 510–518.
9. Culverwell A.D., Scarsbrook A.F., Chowdhury F.U. False-positive uptake on 2-[18F]-fluoro-2-deoxy-D-glucose (FDG) positron-emission tomography/computed tomography (PET/CT) in oncological imaging // *Clin Radiol.* 2011. Vol. 66, N 4. P. 366–382. doi: 10.1016/j.crad.2010.12.004
10. Schulte M., Brecht-Krauss D., Heymer B., et al. Grading of tumors and tumorlike lesions of bone: evaluation by FDG PET // *J Nucl Med.* 2000. Vol. 41, N 10. P. 1695–1701.
11. Martinez-Lage J.F., Poza M., Cartagena J., et al. Solitary eosinophilic granuloma of the pediatric skull and spine — the role of surgery // *Childs Nerv Syst.* 1991. Vol. 7, N 8. P. 448–451. doi: 10.1007/BF00263187
12. Oliveira M., Steinbok P., Wu J., et al. Spontaneous resolution of calvarial eosinophilic granuloma in children // *Pediatr Neurosurg.* 2003. Vol. 38, N 5. P. 247–252. doi: 10.1159/000069828
13. Rawlings C.E., Wilkins R.H. Solitary eosinophilic granuloma of the skull // *Neurosurgery.* 1984. Vol. 15, N 2. P. 155–161. doi: 10.1227/00006123-198408000-00001

## AUTHORS' INFO

\* **Pavel B. Gelezhe**, MD;

address: 28-1, Srednyaya Kalitnikovskaya street, Moscow, 109029, Russia; tel.: +7 (495) 933-55-55;

ORCID: <https://orcid.org/0000-0003-1072-2202>;

eLibrary SPIN: 4841-3234; e-mail: gelezhe.pavel@gmail.ru

**Dmitry V. Bulanov**, MD, Cand. Sci. (Med.);

ORCID: <https://orcid.org/0000-0001-7968-6778>;

eLibrary SPIN: 4641-1505; e-mail: dbulanov@emcmos.ru

## ОБ АВТОРАХ

\* **Гележе Павел Борисович**;

адрес: Россия, 109029, Москва, ул. Средняя Калитниковская, д. 28, стр. 1; тел.: +7 (495) 933-55-55;

ORCID: <https://orcid.org/0000-0003-1072-2202>;

eLibrary SPIN: 4841-3234; e-mail: gelezhe.pavel@gmail.ru

**Буланов Дмитрий Владимирович**, к.м.н.;

ORCID: <https://orcid.org/0000-0001-7968-6778>;

eLibrary SPIN: 4641-1505; e-mail: dbulanov@emcmos.ru



DOI: <https://doi.org/10.17816/DD58392>

# Radiotheranostics: new lease of life of personalized medicine

© Pavel O. Rumyantsev

Endocrinology Research Centre, Moscow, Russian Federation

Radiotheranostics is a radionuclide therapy intended to perform molecular imaging *in vivo* (single-photon emission computed tomography [SPECT], positron emission tomography [PET]) using various radiopharmaceuticals (RP) and selectively affects pathological metabolic processes caused by a tumor. Thyrotoxicosis and thyroid cancer have been treated successfully using the theranostics paradigm since the 1950s with the use of radioactive iodine. In recent years, owing to advances in the development of nuclear medicine (an increase in the number of cyclotrons, SPECT/CT and PET/CT in medical institutions) and ultimately RP, radiotheranostics is developing very rapidly worldwide. The emergence of new radioligands based on  $^{177}\text{Lu}$ ,  $^{225}\text{Ac}$ , and other radioisotopes triggered a great number (>300) of clinical studies on radioligand therapy for prostate cancer, neuroendocrine tumors, pancreatic cancer, and other malignant neoplasms. One of the most promising fields of radiotheranostics application is the development of radioligands based on targeted anticancer drugs, which helps summarize two effects in one RP, namely, inhibition of the signaling cascades and radiation damage. Radiotheranostics is multidisciplinary in nature, technologically complex, and a priori integral (e.g., isotopes, RPs, SPECT, and PET), and requires high competence and teamwork. The development of radiotheranostics and elaboration of targeted RP are still at their infancy in Russia. The main problems are the lack of specialists in this field, such as doctors, physicists, chemists, radiopharmacists, biologists, geneticists, engineers, and programmers. The low awareness of doctors and patients about the possibilities of radiotheranostics also hinders its development and implementation in clinical practice in the country.

**Keywords:** radiotheranostics; radiopharmacy; oncology.

## To cite this article

Rumyantsev PO. Radiotheranostics: fresh impetus of personalized medicine. *Digital Diagnostics*. 2021;2(1):83–89. DOI: <https://doi.org/10.17816/DD58392>

Received: 17.01.2021

Accepted: 26.01.2021

Published: 01.02.2021

DOI: <https://doi.org/10.17816/DD58392>

## Радиотераностика: новое дыхание персонализированной медицины

© П.О. Румянцев

Национальный медицинский исследовательский центр эндокринологии, Москва, Российская Федерация

Радиотераностика — радионуклидная терапия, позволяющая с помощью различных радиофармпрепаратов (РФП), проводить молекулярную визуализацию *in vivo* (однофотонная эмиссионная компьютерная томография, позитронно-эмиссионная томография) и селективно воздействовать на патологические метаболические процессы, вызванные опухолью. Используя парадигму тераностики, с 1950-х годов прошлого столетия с помощью радиоактивного йода успешно лечатся тиреотоксикоз и рак щитовидной железы. В последние годы, благодаря успехам в развитии ядерной медицины (рост числа циклотронов, однофотонная эмиссионная компьютерная томография/компьютерная томография и позитронно-эмиссионная томография/компьютерная томография в медицинских учреждениях), и прежде всего радиофармацевтики, в мире очень бурно развивается радиотераностика. Появление новых радиолигандов на основе  $^{177}\text{Lu}$ ,  $^{225}\text{Ac}$  и других радиоизотопов стимулировало большое количество (более 300) клинических исследований по радиолигандной терапии рака простаты, нейроэндокринных опухолей, рака поджелудочной железы и других злокачественных новообразований. Одним из самых перспективных направлений радиотераностики является разработка радиолигандов на основе таргетных противоопухолевых препаратов, что позволяет суммировать в одном РФП два эффекта — ингибирование сигнальных каскадов и лучевое повреждение. Радиотераностика по природе своей мультидисциплинарна, технологически сложна, априори интегральна (изотопы, радиофармсубстанции, РФП, однофотонная эмиссионная компьютерная томография, позитронно-эмиссионная томография), требует высокой компетенции и командной работы. Развитие радиотераностики и разработка таргетных радиофармпрепаратов в нашей стране находится в зачаточном состоянии. Главной проблемой является нехватка специалистов в данной области — врачей, физиков, химиков, радиофармацевтов, биологов, генетиков, инженеров, программистов. Низкая информированность врачей и пациентов о возможностях радиотераностики также тормозит её развитие и внедрение в клиническую практику в нашей стране.

**Ключевые слова:** радиотераностика; радиофармацевтика; онкология.

### Как цитировать

Румянцев П.О. Радиотераностика: новое дыхание персонализированной медицины // *Digital Diagnostics*. 2021. Т. 2, №1. С. 83–89.  
DOI: <https://doi.org/10.17816/DD58392>

DOI: <https://doi.org/10.17816/DD58392>

# 放射性核素诊疗一体化：一种新的个性化医学

© Pavel O. Rumyantsev

Endocrinology Research Centre, Moscow, Russian Federation

放射性核素诊疗一体化允许使用各种放射性药物在体内进行分子成像（单光子发射计算机断层摄影术，正电子发射断层摄影术），并选择性地影响肿瘤引起的病理代谢过程的放射性核素治疗。自上世纪50年代以来，利用治疗诊断学的范式，在放射性碘的帮助下，成功地治疗了甲状腺毒症和甲状腺癌。近年来，由于核医学（在医疗机构回旋加速器、单光子发射计算机断层扫描/计算机断层扫描、正电子发射断层摄影术/计算机断层摄影术数量的增加）特别是放射药物的成功发展，放射性核素诊疗一体化在世界上发展非常迅速。基于 $^{177}\text{Lu}$ 、 $^{225}\text{Ac}$ 等放射性同位素的新型放射性配体的出现，刺激了大量（超过300）的前列腺癌、神经内分泌肿瘤、胰腺癌等恶性肿瘤的放射配体治疗的临床研究。基于靶向抗肿瘤药物的放射配体的开发是放射性核素诊疗一体化中最有前途的领域之一，这使得总结出一种放射药物的两种作用—信号级联抑制和辐射损伤。放射性核素诊疗一体化本质是多学科的、技术复杂的（同位素，放射性药物，单光子发射计算机断层扫描，正电子发射断层扫描）、整体的，并要求高能力和团队合作。放射性核素诊疗一体化和靶向放射药物的发展在俄罗斯尚处于起步阶段。主要的问题是领域缺乏专家：医生、物理学家、化学家、放射性药物学家、生物学家、遗传学家、工程师、程序员。医生和患者对放射性核素诊疗一体化可能性的认识不足也阻碍了其在俄罗斯临床应用的发展。

**关键词：**放射性核素诊疗一体化；放射药剂学；肿瘤学。

## 引用本文：

Rumyantsev PO. 放射性核素诊疗一体化：一种新的个性化医学. *Digital Diagnostics*. 2021;2(1):83–89. DOI: <https://doi.org/10.17816/DD58392>

收到: 17.01.2021

接受: 26.01.2021

发布时间: 01.02.2021

## BACKGROUND

Anticancer drug therapy is based on the shutdown of proteins in the cells of malignant tumors, which stimulate pathologically their autonomous growth, mitosis, and migration (metastasis). Immunotherapy mobilizes the body's own immunity to fight cancer. At the same time, traditional methods of treatment, such as surgery, chemotherapy, and radiation therapy, remain the mainstay of treatment for most types of cancer.

Radiation therapy was first used to treat cancer over one century ago. Today, about half of patients with cancer receive it in various forms. Until recently, most of the methods of radiation therapy were based on the remote delivery of a dose of radiation to destroy the tumor focus; however, radiation therapy is neither systemic nor selective of tumor cells. Despite its efficiency, external beam radiation therapy has many side effects associated with irradiation of healthy tissues surrounding the tumor. Even with the use of the most advanced external beam radiation therapy equipment, normal tissues surrounding the tumor are inadvertently damaged. At the same time, external beam radiation therapy and sealed-source radiotherapy, focusing mainly on the methods of structural imaging (such as endoscopy, ultrasonography, X-ray diagnostics, including mammography, multispiral computed tomography, and magnetic resonance imaging), cannot have a systemic antitumor effect by affecting local tumor foci.

A new class of drugs for "metabolic" diagnostics and treatment of tumors, called radiopharmaceuticals (RPs), is being actively developed in other countries. In radionuclide therapy, "smart" RPs are able to deliver the required dose of radiation directly to the cancer cells that have impaired metabolism. The number of clinical trials of new RPs, both diagnostic and therapeutic, is growing rapidly. These studies show that the selective delivery of radioactive isotopes to all tumor cells will improve fundamentally the diagnostics and treatment of cancers, which tend to grow and disseminate throughout the body. This type of treatment is called radionuclide therapy, and it is based on a pathologically high uptake of various metabolites by tumor cells, namely, minerals (i.e., iodine and calcium), hormone precursors, other biologically active substances (e.g., norepinephrine and dopamine), hormone receptors that are overexpressed on the surface of tumor cells (such as somatostatin, prostate-specific antigen, and glucagon-like peptide), and monoclonal antibodies (e.g., CD20 and CD38).

A huge number of new RPs, especially for therapeutic purposes, is currently studied in various phases of clinical trials. These are diagnostic RPs based on SPECT (such as  $^{99m}\text{Tc}$  and  $^{123}\text{I}$ ) and PET isotopes (i.e.,  $^{13}\text{N}$ ,  $^{11}\text{C}$ ,  $^{15}\text{O}$ ,  $^{18}\text{F}$ ,  $^{67}\text{Cu}$ ,  $^{68}\text{Ga}$ ,  $^{82}\text{Rb}$ , and  $^{89}\text{Zr}$ ). Radioisotope diagnostics of pathological foci by replacing the diagnostic isotope in the RP with a therapeutic one (e.g.,  $^{131}\text{I}$ ,  $^{177}\text{Lu}$ ,  $^{90}\text{Y}$ ,  $^{223}\text{Ra}$ , and  $^{225}\text{Ac}$ ) reveals the possibilities for systemic radioligand therapy, or

radiotheranostics. This new strategic algorithm has been rapidly developing worldwide.

In the near future, radiotheranostics will expand the horizons of endocrinology, oncology, cardiology, neurology, and other fields of medicine.

## FUNDAMENTAL METABOLISM

Delivering radiation directly to tumor cells is not a new approach in medicine. Radioactive iodine therapy has been used since the 1940s to treat thyroid cancer and thyrotoxicosis. Iodine is naturally actively captured and accumulated not only in normal cells of the thyroid gland, but also in cells of a malignant tumor. As a rule, cells of differentiated thyroid cancer (~95% of all cases) retain this metabolic mechanism provided by the sodium–iodine symporter functioning. Fundamental research has revealed specific breakdowns in genes that disrupt the sodium–iodine symporter functioning, which opens up new views for planning and predicting the efficiency of radioactive iodine therapy. By contrast, this motivates us to develop new targeted drugs to influence malfunctioning metabolic processes due to genetic breakdowns in various cancer diseases.

When swallowed (as a capsule or liquid), radioactive iodine is accumulated and kills cancer cells without distinction of their location. Individual targeted biodosimetry enables calculation of more effective and safe activities of radioactive iodine for systemic therapy of tumor foci.

A similar natural metabolic mechanism was later used in the development of drugs for the treatment of cancer with bone metastases, such as radium-223 dichloride (Xofigo), approved by the Food and Drug Administration (FDA) in 2013, for the treatment of metastatic prostate cancer. Metastatic foci in the bone marrow cause destruction of bone tissue. The body then tries to repair this damage by regenerating new bone with the use of osteoblasts. This is a natural defense process that requires loads of calcium. Radium, as a chemical element, is a metabolic analog of calcium, which accumulates selectively in bone metastases and destroys them.

Researchers wondered if it was possible to create new radioactive molecules specifically for other cancer diseases. They presented engineered RPs, which are made up of three basic building blocks, namely, a radioactive molecule, a target molecule (which recognizes cancer cells and attaches to them), and a linker that connects these two elements. Such compounds, as a rule, are administered into the bloodstream, and they are selectively accumulated therefrom in the pathological foci that were previously identified during radionuclide diagnostics.

RPs work best when they can penetrate cells. Irradiation of neighboring cells creates an additional therapeutic effect, but its range is limited, so the surrounding healthy tissues will not be greatly affected. Alpha emitters have much less distance run in tissues (<0.1 mm) than beta emitters (usually

up to 2 mm). When an RP adheres or penetrates a cancer cell, the radioactive isotope decays there, releasing energy that damages the DNA of this cell and its neighboring cells. Cancer cells are susceptible to radiation-related damage to the DNA. When a cell's DNA is irreparably damaged, the cell dies.

Depending on the type of radioactive radiation used (gamma, beta, and alpha), the energy affects not only the target cell, but also 10–30 surrounding cells, which enable killing more cancer cells with one RP molecule.

By the mid-2010s, the US FDA approved two new RPs targeting specific B-cell molecules for the treatment of patients with non-Hodgkin's lymphoma, one of the hematological diseases. However, these drugs were not widely used, as physicians of patients with lymphoma were untrained and were simply apprehensive about prescription of these radioactive compounds to their patients. In addition, non-radioactive anticancer drugs are competing to the new RPs, and their manufacturers were involved in informing and training doctors.

The turning point in radiotheranostics was in 2018 when the FDA approved  $^{177}\text{Lu}$ -DOTATATE (Lutathera) RP for the treatment of neuroendocrine tumors (NETs) of the digestive tract (NETTER 1 study). Currently, clinical studies of peptide-receptor radionuclide therapy with  $^{177}\text{Lu}$ -DOTATOC are being completed and are planned with  $^{177}\text{Lu}$ -DOTANOC. These peptide radioligands adhere to somatostatin receptors activated on the surface of NETs. The wider the spectrum of radioligands, the more individualized the treatment can be, based on the results of molecular imaging, namely, single-photon emission computed tomography (SPECT) or positron emission tomography (PET), at the diagnostic stage.

In the same way, according to global leading experts, the use of RPs accumulating selectively can possibly affect other solid tumors.  $^{177}\text{Lu}$ -DOTATATE was better at inhibiting the growth of NETs (randomized controlled trial phase III NETTER-1) than any drug used previously. This was a quantum leap in the development of radiotheranostics.

## FROM VISUALIZATION TO THERAPY

Currently, researchers are developing and testing new RPs for the treatment of various cancers, such as melanoma, lung cancer, colorectal cancer, pancreatic cancer, brain cancer, multiple myeloma, and lymphoma. Any tumor that has a targeted molecule (such as receptor, transporter, and antibody) on the cell surface and good blood supply represents a potential target for radiotheranostics.

PET techniques, using short-lived radionuclides, can detect tumor foci throughout the body at once. The resolution limit of modern models of PET/CT devices is up to 2–3 mm. The higher the metabolic activity of a tumor, the higher is the chance of detecting it, even at microscopic sizes. Researchers have learned to repurpose targeted diagnostic molecules

to “charge” them with a powerful radioactive isotope to not only visualize, but also treat tumor foci.

Prostate cancer was one of the first beneficiaries of this repurposing. A protein called prostate-specific membrane antigen (PSMA) is found in high amounts and is very active in prostate cancer cells. Several RPs targeting PSMA receptor overexpression are currently studied in clinical trials.

Most prostate cancers are sensitive to radiation exposure or can be resected through traumatic surgery. However, the use of these local methods of treatment for disseminated or recurrent cases of cancer is challenging, when tumor cells spread throughout the body, forming widespread metastases in different organs. Systemic anticancer therapy is the treatment of choice in these clinical situations. The combination of antitumor drug effect and systemic tumorotropic radiation exposure constitute an ideal choice.

The administration of RPs with high tropism for PSMA receptors overexpressed on tumor cells (which is established during radionuclide diagnostics using SPECT and PET) is the best method of selective radionuclide therapy, as once in the bloodstream, RP attaches to prostate cancer cells throughout the body. The advantage of “smart” molecules for imaging and therapy (radiotheranostics), using the same metabolic target, is the fact that preliminary radionuclide imaging (i.e., SPECT and PET) provides a preliminary idea of whether treatment will give result.

In addition to the well-proven radiotheranostic ligands DOTATATE (NETs) and PSMA (prostate cancer), great expectations in oncology are associated with the new ligand fibroblast-activation-protein inhibitor. This ligand has demonstrated high and theranostic (radionuclide diagnostics + therapy) efficacy in more than 30 malignant tumors.

## PERSONALIZATION OF COMBINED CANCER THERAPY

Although RPs have shown promising results in early studies, it cannot be confirmed whether they, like other types of anticancer drugs, will destroy independently all tumor foci.

The use of RPs in combination with other treatment methods is the main paradigm for a personalized combination of potentially effective methods of treatment. Many researchers are now testing RP in combination with radiation sensitizers, drugs that make cancer cells even more vulnerable to radiation. For example, clinical trials are performed for lutetium  $^{177}\text{Lu}$ -DOTATATE in combination with the radiation sensitizer triapine, which blocks the production of compounds by cells, required for DNA repair after radiation damage. Another study is testing  $^{177}\text{Lu}$ -DOTATATE with a poly (ADP-ribose) polymerase (PARP) inhibitor. These drugs, already approved for treatment of certain types of breast, ovarian, and other cancers, block the DNA repair process itself. Thus, radiation can cause DNA damage, and a PARP



inhibitor will prevent tumor cells from healing their DNA after irradiation.

Research on combined radionuclide and immunotherapy is also being conducted to improve the efficiency of treatment without increasing its toxicity. Recent studies have shown that RPs can increase the sensitivity of tumors to immunotherapy.

Many tumors are “invisible” to immune therapy because immune cells do not recognize them or do not work properly in the microenvironment around tumors. When cancer cells are destroyed by radionuclide therapy, proteins, and DNA from those cells enter the bloodstream so that immune cells can recognize them. Radionuclide therapy helps transfer tumor foci from being invisible to being targets of immunotherapeutic drugs by even partially destroying them. Immunotherapy is proved to work better if every metastasis in every tumor is exposed to radiation, as is the case with systemic radionuclide therapy.

In the future, it is reasonable to combine RPs with external beam radiation therapy, especially for large foci and/or those partially resistant to radionuclide therapy. Dosimetric and topometric planning of such combined radiation therapy ensures an effective and safe treatment plan.

## FROM DISINTEGRATION

## TO INTEGRATION AND TEAM WORK

The development of radiotheranostics and elaboration of targeted RPs are in infancy in Russia. The main problem is the lack of specialists in this field, namely, doctors, physicists, chemists, radiopharmacists, biologists, geneticists, engineers, and programmers.

Russia has no specific field of nuclear medicine, as it exists in all other developed countries. By its nature, nuclear medicine is multidisciplinary, technologically complex, and a priori integral (isotopes, RP, SPECT, PET), and requires high competence and teamwork. At the same time, the field is rapidly developing and is being re-equipped, updated with innovative targeted RPs. Molecular imaging, dosimetry, evidence base of knowledge, information, and analytical technologies for the formation of artificial intelligence in the field of radiomics and radiogenomics are being improved. In the author's opinion, the main problem is the absence of appropriate personnel and technologies. In Russia, no relevant

educational programs, specialties, or scientific schools are established. This field is being developed very rapidly that, even in the United States, there is an acute shortage of doctors and related nuclear medicine specialists.

A serious problem is the lack of contemporary and licensed (Good Manufacturing Practice) RP production in the country of both medical radioactive isotopes and cold kits for their manufacture in medical institutions (world practice). In Russia, not a single modern therapeutic RP is being developed and is not planned to be introduced.

The low awareness of Russian doctors and patients about the possibilities of radiotheranostics also hinders its development and implementation in clinical practice.

## CONCLUSION

New RPs are surprising, and they cause mistrust and disbelief in their availability, as well as in the attitudes of doctors and patients. However, only doctors, and through their patients, are able to obtain the real benefits from the introduction of technology into the clinical practice. In recent years, the great breakthrough in radionuclide diagnostics and therapy is based on the ability to integrate technologies and competencies. This cannot be done without teamwork from planning and production, from the laboratory cabinet to the patient's bed.

In 2019, in the United States, the National Cancer Institute launched the Radiopharmaceutical Development Initiative to accelerate further trials of new promising RPs. Similar programs of state support for radiopharmacy and radiotheranostics have also been launched in Europe, Australia, etc.

We should also think over such integration programs for the development of radiopharmacy and radiotheranostics, especially taking into account existing trends and potential leadership opportunities (production of isotopes, pharmaceutical substances, development of SPECT and PET technologies, radionuclide therapy departments, and personnel training) in Russia.

## ADDITIONAL INFORMATION

**Funding.** This study received no external funding.

**Conflict of interest.** The author declares no conflicts of interest.

## AUTHOR INFO

**Pavel O. Rumyantsev**, MD, Dr. Sci. (Med.);

address: Dmitry Ulyanova street 11 k 2, 117036 Moscow, Russia;

ORCID: <https://orcid.org/0000-0002-7721-634x>;

eLibrary SPIN: 7085-7976; e-mail: [pavelrum@gmail.com](mailto:pavelrum@gmail.com)

## ОБ АВТОРЕ

**Румянцев Павел Олегович**, д.м.н.;

адрес: 117036, ул. Дмитрия Ульянова, д. 11, к. 2;

ORCID: <https://orcid.org/0000-0002-7721-634x>;

eLibrary SPIN: 7085-7976; e-mail: [pavelrum@gmail.com](mailto:pavelrum@gmail.com)

